Observational Clues to the Progenitors of Type Ia Supernovae

Dan Maoz
School of Physics and Astronomy, Tel-Aviv University

Filippo Mannucci
INAF, Osservatorio Astrofisico di Arcetri

Gijs Nelemans
Department of Astrophysics/IMAPP, Radboud University Nijmegen
Institute for Astronomy, KU Leuven

Key Words .....

Abstract Type-Ia supernovae (SNe Ia) are important distance indicators, element factories, cosmic-ray accelerators, kinetic-energy sources in galaxy evolution, and endpoints of stellar binary evolution. It has long been clear that a SN Ia must be the runaway thermonuclear explosion of a degenerate carbon-oxygen stellar core, most likely a white dwarf (WD). However, the specific progenitor systems of SNe Ia, and the processes that lead to their ignition, have not been identified. Two broad classes of progenitor binary systems have long been considered: single-degenerate (SD), in which a WD gains mass from a non-degenerate star; and double-degenerate (DD), involving the merger of two WDs. New theoretical work has enriched these possibilities with some interesting updates and variants. We review the significant recent observational progress in addressing the progenitor problem. We consider clues that have emerged from the observed properties of the various proposed progenitor populations, from studies of their sites – pre- and post-explosion, from analysis of the explosions themselves, and from the measurement of event rates. The recent nearby and well-studied event, SN 2011fe, has been particularly revealing. The observational results are not yet conclusive, and sometimes prone to competing theoretical interpretations. Nevertheless, it appears that DD progenitors, long considered the underdog option, could be behind some, if not all, SNe Ia. We point to some directions that may lead to future progress.

CONTENTS

Because I have contemplated explaining what I think, not only about the location and movement of this light, but also about its substance and origin, and believing that I have found an explanation that, for lack of evident contradictions, may well be true, I have finally arrived at the belief of being capable of knowing something about this wonder, beyond the point where pure conjecture ends.
Letter by Galileo to O. Castelli regarding the *Stella Nova* of 1604

1 Introduction

1.1 Type-Ia supernovae – a brief overview

The observations of the supernovae (SNe) of 1572 and 1604, and the attempts, by Tycho, Kepler, Galileo, and others, to understand their natures and locations, were transformational events in the history of science. These attempts can be viewed as signaling the beginnings of modern astrophysics. Among the handful of historical SN events in the Galaxy recorded over the past two millenia, we now know that at least some were core-collapse (CC) SNe, involving the explosion of massive ($M \gtrsim 8M_{\odot}$) stars, while others were the thermonuclear explosions of lower-mass stars, now known as Type-Ia supernovae (SNe Ia). In modern-day surveys that search for stellar explosions, SNe Ia are often the ones most frequently discovered, owing mainly to their large optical luminosities, $\sim 10^{43}$ erg s^{-1} near the time of maximum light.

SNe Ia are classified (see review by Filippenko 1997) by a lack of hydrogen and helium signatures in their spectrum, and by kinematically broadened and blueshifted ($\sim 10^3 - 10^4$ km s^{-1}) features, mainly of silicon, iron, and calcium, around the time of maximum light. Contrary to CC SNe (e.g., Smartt 2009), SNe Ia are observed to explode both in young and in old stellar populations. The spectra and light curves of most SNe Ia are remarkably uniform. The light curves rise to maximum light within $\sim 15 - 20$ d, decline by about 3 mag in one month, and then by a further mag each month, with the more specific behavior depending on the observed photometric band. Based on the light-curve shape, optical spectroscopy, and X-ray analysis of SN Ia remnants, the observed luminosity of SNe Ia is driven by inverse-β and electron-capture radioactive decays, first of ^{56}Ni to ^{56}Co, and then of ^{56}Co to stable ^{56}Fe, with exponential timescales of 9 d and 114 d, respectively. Gamma-rays and positrons from these decays are reprocessed by the optically thick ejecta into the optical photons that dominate the luminosity (Colgate & McKee 1969). SNe Ia are a decisively optical-range phenomenon, with $\sim 85\%$ of the luminosity emitted between the U and I bands (e.g. Howell et al. 2009a).

The tight correlation between the luminosity of SNe Ia at maximum light and various measures of light-curve development speed (Phillips 1993, see Howell 2011 for a review) have made them excellent cosmological distance indicators. As such, they provided the first evidence for acceleration of the cosmic expansion (Perlmutter et al. 1999, Riess et al. 1998), and hence for the current, dark-energy-dominated cosmic mass-energy inventory. SNe Ia continue being a major cosmographic tool, with future efforts focusing on determining the evolution, on cosmological timescales, of the dark-energy equation of state (Howell et al. 2009a). The yet-unknown identity of the progenitor systems of SNe Ia, the subject of this article, is a concern for SN Ia cosmography, given that changes with cosmic time or environment, in the progenitor populations or in some details of the explosions, could, in principle, lead to systematic errors in distances deduced based on calibrations of nearby SNe Ia. For example, systematic differences have been reported in the residuals in the Hubble diagram, depending on host galaxy mass and metallicity (e.g., D'Andrea et al. 2011, Hayden et al. 2013, Pan et al. 2013). These differences could impact the measurements of cosmological parameters, as low-mass and low-metallicity galaxies dominate the production of SNe Ia at progressively higher redshifts.

Every normal SN Ia enriches the interstellar medium with roughly 0.7 M$_{\odot}$ of iron (to within a factor of a few), and a similar total amount in other elements, including mainly carbon, oxygen, neon, magnesium, silicon, sulfur, argon, and calcium. Combined with their large numbers, this means that SNe Ia play an important role in chemical evolution, and understanding such evolution requires knowing the dependences, on cosmic time and environment, of SN Ia rates and metal yields (e.g. Wiersma, Schaye & Theuns 2011).

The kinetic energy of SN Ia ejecta also affects gas dynamics and star formation in galaxies,

contributing to the ejection of matter from galaxies to the intergalactic medium, and thus SNe Ia are a factor in galaxy evolution (e.g. Davé, Oppenheimer & Finlator 2011). As is the case for other SN types, the remnants of SNe Ia are the likely sites for the acceleration of cosmic rays up to energies of $\sim 10^{15}$ eV (e.g. Drury 2012). And, as detailed further in this review, SNe Ia may or may not signal two important end points in binary stellar evolution – accretion onto, and/or the mergers of, white dwarfs (WDs). The final stages of the latter events are expected to be the main source of foreground, but also interesting signals, for space-based gravitational-wave observatories (e.g. Amaro-Seoane et al. 2013). For all of these reasons, it is important to understand the physics of all stages of the development of SNe Ia, and particularly, to identify their progenitor systems.

1.2 Basic physics of SNe Ia

Physical models of SN Ia explosions have been reviewed by Hillebrandt & Niemeyer (2000), with updates in Hillebrandt et al. (2013). Here we only skim the surface. The energetics and chemical composition of SN Ia explosions, as measured in the course of the explosions and in their remnants, have long led to the inference (Hoyle & Fowler 1960) that they involve the thermonuclear combustion of a degenerate stellar core. The absence of hydrogen and helium in the spectrum, and the occurrence of some SNe Ia in old stellar populations, indicate that this core is most likely a WD of carbon-oxygen (C/O) composition. The burning is partly into iron-group elements and partly into intermediate-mass elements, with some residual unburnt carbon and oxygen, as indicated by the stratification and composition deduced from observations. The spectral evolution of SNe Ia indicates the presence of ~ 0.6 M$_\odot$ of radioactive ^{56}Ni in a typical explosion, along with a similar amount of total mass distributed among stable iron-group elements, and among the lighter elements mentioned above, for a total ejecta mass similar to the Chandrasekhar WD mass limit, $M_{\rm Ch} = 1.44$ M$_\odot$ (e.g. Mazzali et al. 2007). This chemical makeup and stratification is also deduced from X-ray analysis of the ejecta of historical SN Ia remnants (e.g. Badenes et al. 2006) such as Tycho's SN of 1572.

Looking at energetics, the nuclear binding energy released by burning 0.6 M$_\odot$ of C and O into ^{56}Ni is 1.1×10^{51} erg. A comparable mass of C and O burning to intermediate-mass elements releases additional energy. The gravitational binding energy of a WD of mass close to $M_{\rm Ch}$ is $\sim 0.5 \times 10^{51}$ erg. The thermonuclear energy release is thus sufficient to unbind the WD, and to give the ejecta the kinetic energy indicated by the deduced ejecta mass and its observed expansion velocities, of order 10^4 km s^{-1}, i.e. $\sim 10^{51}$ erg. Furthermore, the equation of state of the degenerate electron gas in a WD is just what is needed for an unstable thermonuclear runaway, once carbon is somehow ignited. Nuclear reaction rates have steep rising dependences on temperature. A highly degenerate gas, when heated, does not expand and cool as a classical gas would. As a result, an explosive burning front can, in principle, quickly consume a WD. The carbon ignition threshold can be crossed via an increase in some combination of pressure and temperature. That increase has generally been attributed to the accumulation of accreted mass on the WD, up to the neighborhood of $M_{\rm Ch}$, with a corresponding decrease in radius. Specifically, the carbon in the core of a non-rotating C/O WD will ignite at a WD mass of $\sim 1.38 M_\odot$ (Arnett 1969, Nomoto 1982). The fact that the "bomb" is always a C/O WD with $M \sim M_{\rm Ch}$ would naturally explain the limited range of SN Ia luminosities, which has been so instrumental for cosmology.

Beyond this simplified picture, however, much about SNe Ia is still poorly understood. At the most fundamental level, it is unknown what are the initial conditions and evolutionary paths that, in practice, take a WD away from stable equilibrium and lead it to mass growth, ignition, and explosion. In other words, we do not know the identity and nature of the systems that explode as SNe Ia. This is the "SN Ia progenitor problem".

2 Progenitor models and open questions

Progenitor scenarios have traditionally focused on getting a C/O WD to ignite, by having it approach or exceed $M_{\rm Ch}$. This can be done either through accretion from a non-degenerate star in the single-degenerate (SD) model (Whelan & Iben 1973)); or by merging two WDs in a tight binary, through loss of energy and angular momentum to gravitational waves, in the double-degenerate (DD) model (Iben & Tutukov 1984, Tutukov & Yungelson 1981, Webbink 1984). See Wang & Han 2012 for a recent review.

2.1 Single-degenerate models

Accretion from a non-degenerate secondary can assume many configurations. Mass transfer can proceed through Roche-lobe overflow or through a strong wind from the companion (Li & van den Heuvel 1997). The secondary can be a main sequence star (e.g. van den Heuvel et al. 1992), a subgiant (e.g. Han & Podsiadlowski 2004), a helium star (Tutukov & Yungelson 1996, often called a "hot subdwarf", i.e. a star that has been stripped of its hydrogen envelope by binary interaction, e.g. Geier et al. 2013), or a red giant (sometimes called a "symbiotic" companion, e.g. Patat et al. 2011). For each of these cases, different configurations are possible, depending on previous common enevelope and mass transfer phases (e.g., Wang & Han 2012).

In the SD scenario, the challenge is to get an accreting WD to actually grow in mass. In a narrow range of about a factor of three in mass accretion rate, centered around $\dot{M} = 10^{-7}\ M_\odot\ {\rm yr}^{-1}$ for a 0.8 $\rm M_\odot$ WD, and around $\dot{M} = 5\times10^{-7}\ M_\odot\ {\rm yr}^{-1}$ for a 1.4 $\rm M_\odot$ WD, stable nuclear burning of hydrogen to helium on the WD surface can take place (Nomoto 1982). WDs in such an accretion mode should resemble an observed class of objects known as supersoft X-ray sources (van den Heuvel et al. 1992 – see Section 3.1.2, below). Accretion above this range likely leads to expansion of the accretor to a red-giant-like configuration, engulfment of the donor in a common envelope, and thus cessation of the growth process toward $M_{\rm Ch}$ and toward explosion as a SN Ia (Iben & Tutukov 1984). In this high-accretion-rate regime, however, Hachisu, Kato & Nomoto (1996, 1999) have proposed that self-regulation of the accretion flow occurs, keeping the mass flow that actually accumulates on the WD at the steady-burning rate. This is achieved by means of an optically-thick wind emerging from the accretor, driven by the luminosity of the nuclear burning on the WD surface. Questions, however, have been raised as to whether this does not require too much fine tuning (e.g., Piersanti et al. 2000, Shen & Bildsten 2007, Woosley & Kasen 2011), or contradictory assumptions about the spherical symmetry of the accretion flow – on the one hand an asymmetric Roche-lobe overflow, on the other hand a spherical inflow that can be regulated by the spherical outflowing wind (Hillebrandt & Niemeyer 2000). In any case, the efficiency of the accretion mode is limited to the ratio of the steady burning rate to the mass transfer rate.

Accretion at rates lower than the stable-burning range will lead to accumulation of the accreted hydrogen in a cold degenerate layer on the accretor, up to its ignition and burning in a thermonuclear-runaway "nova" eruption (Starrfield et al. 1972). Because hydrogen burning produces more energy per unit mass than required to eject that mass from the surface of a WD, most of the accreted material is expected to leave the accretor. Over the accumulation timescale, hydrogen can diffuse inward and mix with the WD's carbon and oxygen layer. As a result, during the burning, some of the original WD material is blown away, along with the ashes of the accreted material (e.g. Yaron et al. 2005). However, with increasing accretion rates and WD masses, ignition conditions are reached at lower accumulated mass and less degenerate conditions, so there may be a parameter range where mass gain is possible after all.

Recent studies of the long term evolution of WDs accreting hydrogen at different rates have had some seemingly conflicting conclusions. Idan, Shaviv & Shaviv (2013), studying accretion at a high rate ($\dot{M} = 10^{-6}\ M_\odot\ \mathrm{yr}^{-1}$, i.e. above the steady burning regime) find, rather than steady hydrogen burning, recurrent thermonuclear runaway flashes on ten-year timescales, during which most of the accreted mass is retained. However, the accumulated helium ash is ignited after several thousand hydrogen flashes, and ejects essentially all of the accreted mass At a lower accretion rate of ($\dot{M} = 10^{-7}\ M_\odot\ \mathrm{yr}^{-1}$), some mass is retained, and the WD mass grows, albeit inefficiently. Newsham, Starrfield & Timmes (2013) and Wolf et al. (2013), on the other hand, do find steady burning, and WD mass growth, but again that a hot helium layer ignites at some point, possibly ejecting much of the accumulated mass.

Alternatively, the donor may be a helium-rich star, avoiding the challenges involved in mass gain through hydrogen-rich accretion (see Wang et al. 2009a). The accumulated helium layer ignites at a larger accumulated mass, but may suffer from the same problem as described above, of a helium nova in which much of the accreted material is ejected. The efficiency of hydrogen and helium accretion is thus theoretically uncertain, leading to a large range of possibilities for WD growth (see Bours, Toonen & Nelemans 2013; Yungelson 2005)

2.2 Double-degenerate models

In the DD scenario, the more-massive WD is generally thought to tidally disrupt and accrete the lower-mass WD, initially through an accretion disk configuration, that then likely takes on a more spherical geometry (e.g., Lorén-Aguilar, Isern & García-Berro 2009; Moll et al. 2013; Pakmor et al. 2012; Raskin et al. 2012; Schwab et al. 2012; Shen et al. 2012). Accretion of carbon and oxygen at a high rate should prevent the problems of inefficient mass growth, encountered in novae, eventually leading to carbon ignition in the core. Against this picture, however, it has long been argued that the large accretion rate will lead to off-center ignition and burning of carbon in the accretor, to oxygen and neon. Further accretion and approach to $M_{\rm Ch}$ will drive electron capture on Mg and Ne, leading to gravitational instability and to an "accretion-induced collapse" to a neutron star (Nomoto & Iben 1985, Saio & Nomoto 1998, Shen et al. 2012). The collapse could manifest itself as some kind of non-SN Ia, low-luminosity, hydrogen-free, transient (Darbha et al. 2010 and Piro & Kulkarni 2013 have considered the signatures of such an event). On the other hand, rotation of the merger remnant has been considered as a way to slow down the accretion and to avoid off-center ignition (Piersanti et al. 2003, Tornambé & Piersanti 2013; see also 2.5, below).

Recent 3D hydrodynamical merger models have cast doubt on the picture of a merger remnant as an unperturbed primary-mass WD that accretes the remains of the secondary WD. Instead, complex structures with regions of high temperature and density are found, in which explosive carbon ignition may occur. Such "violent mergers" may lead to a SN Ia, even if the total mass of the merger is below $M_{\rm Ch}$ (Dan et al. 2013, Guillochon et al. 2010, Pakmor et al. 2013, Raskin et al. 2013, van Kerkwijk, Chang & Justham 2010, Zhu et al. 2013). Details depend on the WD masses (a primary WD mass $\gtrsim 0.9\ \mathrm{M}_\odot$ is likely required) and on the presence of He, which can facilitate ignition.

2.3 Collisional double-degenerate models

A special case of a WD merger configuration is the "collisional" one, whereby two WDs collide head-on, rather than spiraling in due to gravitational-wave losses. Benz, Thielemann & Hills (1989); Lorén-Aguilar, Isern & García-Berro (2010); Raskin et al. (2009, 2010); Rosswog et al. (2009) and Hawley, Athanassiadou & Timmes (2012) have invoked this scenario, generally in the context of some SNe Ia possibly arising in dense stellar environments such as globular

clusters and galactic nuclei. A different implementation of the collisional DD scenario was raised by Thompson (2011), who proposed that many binary WDs may actually be in "hierarchical triple" systems, with a third, low-mass star in orbit about the inner WD binary. The tertiary could induce Kozai (1962) - Lidov (1962) oscillations in the eccentricity of the inner binary. A high eccentricity increases gravitational wave losses, and thus decreases the time until merger, and so enlarges the population of tight WD binaries that merge (leading to an enhanced rate of SNe Ia). Rare head-on collisions would sometimes also occur among the most eccentric systems. Prodan, Murray & Thompson (2013) considered also tidal dissipation of orbital energy of the inner binary (Mazeh & Shaham 1979), further enhancing the merger rate. However, it is not clear that triple systems, with the post-common-envelope orbit ratios needed for this mechanism to operate, can be realized.

Katz & Dong (2012) discovered that one of the approximations used in previous Kozai-Lidov calculations is invalid for "mild" hierarchical triples, i.e. those in which the tertiary orbit is $\sim 3-10$ times the inner orbit. Among such cases, they found, through direct numerical integration for a range of initial tertiary orbit inclinations, a rather high probability, $\sim 5\%$, for a Kozai-Lidov-induced head-on collision between the inner WD pair. Katz & Dong (2012) argued that, if a large fraction of all intermediate-mass stars are in the appropriate triple systems, most or all SNe Ia could come from such collisions. Kushnir et al. (2013) and García-Senz et al. (2013) have performed the latest hydrodynamic thermonuclear simulations of such collisions, and obtained promising agreement with some of the phenomenology of observed SN Ia explosions. Kushnir et al. (2013), using high spatial resolution ($\sim$ 1 km) in their simulations, and avoiding some numerical artifacts that affected previous work, find that a collision between, e.g., two 0.7 $M_\odot$ WDs produces an explosion with a ^{56}Ni yield of 0.56 $M_\odot$, similar to a typical SN Ia.

However, it seems unlikely that a large fraction of all WDs are in such triples – only $\sim 10-20\%$ of stars are triples (Duchêne & Kraus 2013, Leigh & Geller 2013), and probably only a fraction of those have the required special orbit ratios. A further problem with this model is how to avoid a collision of the inner binary early on, when the components are still on the main sequence, and their geometrical cross-sections for collision are 100 times greater than when they have become WDs. Hamers et al. (2013) have used "binary population synthesis" calculations (see Section 2.6, below) to confirm that, for this reason alone, the enhancement of SN Ia rates is already minimal for initially wide inner binaries that would not interact without a tertiary component. Katz & Dong (2012) have suggested that the relative orientations of the inner and outer orbits could be "reset" by small kicks, during the mass loss phases of the stars of the inner binary, or by a passing perturbing star. Colliding WD cases could then arise from among those systems that avoided collisions while on the main-sequence.

2.4 Double detonations and rotating super-Chandrasekhar-mass models

WDs accreting helium at low rates (from either non-degenerate or helium-WD donors) can accumulate a helium layer that is sufficiently massive and degenerate such that the resulting helium ignition becomes explosive (Taam 1980). This detonation drives a shock into the underlying C/O WD, which then ignites carbon at or near the center, even in sub-$M_{\rm Ch}$ WDs (Fink et al. 2010, Livne 1990, Shen & Bildsten 2009). Originally, these "double-detonation" or "edge-lit detonation" models were considered for non-degenerate helium donors, in which the ignition masses of the helium layers were found to be ~ 0.2 $M_\odot$. Models for such explosions typically predicted strong signatures of carbon and oxygen (from the burned helium) in the SN spectra, which were inconsistent with observed spectra. However, Bildsten et al. (2007) found that, for helium WD donors, the higher mass transfer rates lead to smaller helium layers at explosion time, and better agreement with observations (e.g. Fink, Hillebrandt & Röpke

2007). Recently, Guillochon et al. (2010), Pakmor et al. (2013), and Shen & Bildsten (2013) have found that also in "violent mergers" (see Section 2.2, above) there may first be a surface He detonation, triggering the C detonation, if the merger is between a He and a C/O WD, or in mergers between two C/O WDs where there is a thin surface layer of He present.

At the other extreme, the nickel mass deduced for some very bright SN Ia explosions is suggestive of a super-Chandrasekhar-mass progenitor, with mass $\gtrsim 2M_\odot$ (e.g. Howell et al. 2006, Kamiya et al. 2012, Scalzo et al. 2012, 2010, Silverman et al. 2011, Taubenberger et al. 2011, 2013a). WD rotation has been proposed as a means of supporting such massive progenitors. On the other hand, Hillebrandt, Sim & Röpke (2007) and Hachinger et al. (2013) have argued that the explosion of a rotating super-$M_{\rm Ch}$ WD will not necessarily produce the inferred nickel mass, or other characteristics, of such bright events, and they have suggested asymmetric explosions instead (see also Moll et al. 2013). Chamel, Fantina & Davis (2013) have shown that another proposed means of supporting super-$M_{\rm Ch}$ WDs, via ultra-strong quantizing magnetic fields, is impractical, due to electron-capture reactions that would make the WD unstable.

More generally, WD rotation has been invoked in several so-called "spin-up/spin-down" scenarios. Di Stefano, Voss & Claeys (2011); Justham (2011); Yoon & Langer (2004, 2005), and Hachisu, Kato & Nomoto (2012) have argued, in the context of the SD model, that a WD that has grown in mass, even beyond $M_{\rm Ch}$, could be rotation-supported against collapse and ignition, perhaps for a long time, during which the accretion could run its course and end, and the traces of the process (or even of the donor itself) could disappear. DD mergers whose explosions are delayed by rotational support have also been proposed (Piersanti et al. 2003, Tornambé & Piersanti 2013). A WD undergoing maximal solid-body rotation is stable against carbon ignition up to a mass of 1.47 $M_\odot$, i.e., only $\approx 0.1M_\odot$ more than in the case of a non-rotating WD. In the context of SD models, where a typical WD needs to accrete ~ 1 $M_\odot$ before exploding, it would appear that this extra $0.1M_\odot$ provides not much of an opportunity for the accretion process to conclude. Yoon & Langer (2005) have therefore constructed models of differentially rotating WDs in which, for some radially increasing profiles of angular rotation speed, the maximal stable WD mass reaches $\sim 2M_\odot$. Saio & Nomoto (2004) and Piro (2008), however, have argued that "baroclinic" instabilities, and/or the shear growth of small magnetic fields, provide torques that will quickly bring a differentially rotating WD to solid-body rotation, with its limited rotational support. Hachisu et al. (2012) have countered that these instabilities might not occur, as only the necessary conditions for them, but not the sufficient ones, are satisfied. The theoretical viability of massive, rotation-supported, WDs is thus still unclear. Observationally, a spin-up/spin-down scenario could potentially "erase" many of the clues that we discuss in this article.

2.5 Alternative models

Kashi & Soker (2011) have introduced a "core-degenerate" model, in which a WD and the core of an asymptotic-giant-branch (AGB) star merge already in the common-envelope phase. After ejection of the envelope, the merged core is supported by rotation, potentially for long times, until it spins down, e.g. via magnetic dipole radiation, and only then explodes (Ilkov & Soker 2011). Wheeler (2012) has sketched a SD progenitor model consisting of a WD and an M-dwarf donor, where accretion by the WD and its growth toward $M_{\rm Ch}$ are enhanced by magnetic channeling, self-excited mass loss from the M dwarf, and magnetic inhibition of mixing of the WD surface layer, thus avoiding excessive mass loss in nova events. Single-star SN Ia progenitor models have also been occasionally attempted (Iben & Renzini 1983, Tout 2005), in which the degenerate carbon-oxygen core of an AGB star is somehow ignited after it has lost its hydrogen envelope (as it must, if the SN is to appear as a Type-Ia).

2.6 Linking theory and observations

As already noted briefly above, apart from the issue of the identity of the progenitors, and the intrinsic problems of each of the progenitor scenarios, many gaps remain in our understanding of the phases that precede each "progenitor setup" that will eventually lead to an observed SN Ia. These gaps of knowledge include the details of binary evolution, and particularly the enigmatic common-envelope phases that a pre-SN Ia binary system undergoes in almost all models (see Ivanova et al. 2013, for a review).

An important theoretical tool for obtaining observational predictions from the various scenarios, despite these obstacles, has been the calculation of binary population synthesis (BPS) models. In BPS, one begins with a large population of binaries with a chosen distribution of initial parameters (component masses, separations), and one models the various stages of their stellar and binary evolution, including transfer and loss of both mass and angular momentum, and possibly multiple common-envelope phases, with the physics of each stage parametrized in some way (e.g., Bogomazov & Tutukov 2011; Jorgensen et al. 1997; Meng & Yang 2011; Mennekens et al. 2013; Ruiter et al. 2013; Toonen, Nelemans & Portegies Zwart 2012; Wang, Li & Han 2010; Yungelson & Livio 2000 Claeys et al. 2013b). At the end of such a simulation, one can see what fraction of the initial stellar population, and from which specific progenitors, has ended up at the conditions thought to lead to a SN Ia explosion through a particular channel (e.g. DD, Chandrasekhar-mass SD, etc.). Furthermore, as discussed in Section 3.5, below, for each progenitor channel one can obtain the distribution of "delay times" between star formation and SN Ia explosion, a distribution that can be compared to observations.

Even after the conditions for a SN Ia explosion have been met, many additional questions remain as to the ensuing phases: the trigger and the locations of WD ignition; the mode in which the burning front consumes the WD (see Hillebrandt & Niemeyer 2000, and Section 3.3.4, below); uncertainties in nuclear cross sections (Parikh et al. 2013); and the transfer of radiation through the expanding ejecta (e.g. Dessart et al. 2013b, Mazzali et al. 2013, Pinto & Eastman 2000, Piro & Nakar 2012, 2013). There is thus a multitude of theoretical paths to a SN Ia explosion, some of this multiplicity arising from real physical possibilities, and some of it due to uncertainties in the often-complex physics. Among these many theoretical paths, the ones that are actually realized and seen in Nature likely encrypt observational clues to the solution of the progenitor question. With this in mind, we attempt an overview of the state of the art of observations that may provide such clues. We arrange our review according to the various possible observational approaches to the problem.

3 Evidence from the observations

A variety of observational approaches have been brought to bear on the SN Ia progenitor problem. The existing populations of potential progenitors can be studied (Sec. 3.1); pre-explosion data at the sites of nearby events may reveal the progenitors (Sec. 3.2); the observed properties of the events themselves may carry clues to the progenitors (Sec. 3.3); the remnants of presumed SNe Ia can be searched for remaining traces of the progenitor systems (Sec. 3.4); and the rates at which SNe Ia explode as a function of time and environment provide another avenue to address the problem (Sec. 3.5). We review each of these approaches in turn.

3.1 Clues from potential progenitor populations

Since a typical galaxy hosts of order 10^7 SNe Ia over a Hubble time (see Section 3.5.7), a viable type of progenitor system should be present in significant numbers and therefore observable, whether as individual objects, or through their collective emission. Thus, the

first observational approach to the progenitor problem that we consider is to look for specific potential progenitor systems, to measure their properties and numbers, and to see if those conform to expectations, given known SN Ia properties.

3.1.1 Recurrent novae The Milky Way and similar large galaxies have populations of $\sim 10^6$ "cataclysmic variables" – WDs accreting from non-degenerate donor stars through Roche-lobe overflow or through a wind, with orbital periods down to about 80 min (e.g. Warner 2003). Among the ways in which these systems reveal themselves are "nova eruptions" (see Sect. 2.1, above), which occur in the Galaxy and in M31 at rates of ~ 35 yr^{-1} and ~ 65 yr^{-1}, respectively (Darnley et al. 2006, della Valle et al. 1994). As already noted, it is thought that few, if any, novae gain more mass during accretion than the mass they lose in the eruptions, in which case such systems are not SN Ia progenitors [1].

However, members of a subclass of novae called "recurrent novae", have long been suspected as possible SN Ia progenitors (e.g. della Valle & Livio 1996; Kato & Hachisu 2012; Schaefer 2010; Starrfield, Sparks & Truran 1985). Recurrent novae are defined as novae with more than a single outburst over the past century or so. There are only 10 recurrent novae known in the Galaxy. Some of the donor stars are main-sequence, some sub-giants, and some red giants. Recurrent novae have eruptions every few decades, on an irregular basis. Because the mass needed for ignition scales inversely with both WD mass and accretion rate (Fujimoto 1982, Shen & Bildsten 2009, Truran & Livio 1986), these short recurrence times have been interpreted to indicate that the WD mass is close to $M_{\rm Ch}$, specifically $M \gtrsim 1.2M_\odot$, and that the accretion rate is relatively high, the same parameters for which mass gain may be possible. A number of observational mass estimates are indeed suggestive of large WD masses, but uncertainties are large, and there are only two double-lined eclipsing systems that have reliable mass estimates: U Sco, with a WD mass of $1.55 \pm 0.24M_\odot$ (Thoroughgood et al. 2001), and CI Aql, with $1.00 \pm 0.14M_\odot$ (Sahman et al. 2013). Observationally, little is known about the formation of massive WDs in binaries, so it is unclear if these high masses indicate that the WDs have accumulated mass. Recurrent nova eruptions may in fact be caused by instabilities in the accretion discs, leading to periodic accretion at the steady-burning rate, during which the WDs do grow in mass (Alexander et al. 2011). Then again, Hachisu & Kato (2012) point out that it is unclear if steady burning can ignite for such short accretion episodes.

Yet another view is that recurrent novae are systems in which the WD mass is decreasing with time, and which will thus never become SNe Ia (Patterson et al. 2013, Schaefer 2013, see below). As noted, there are few known recurrent novae, and even fewer that have had well-studied multiple outbursts. The debate regarding their being SN Ia progenitors has therefore focused on individual objects and on individual outbursts.

For example, after the latest outburst of U Sco in 2010 (e.g. Schaefer et al. 2010), Schaefer (2013) deduces, based on the period change, that much more material was ejected than had been previously accreted, challenging the idea of WD mass growth (e.g. Diaz et al. 2010). Whether or not the massive WD has a C/O composition (as required of a SN Ia), or an oxygen-neon one, is also debated (e.g. Kato & Hachisu 2012, Mason 2013). RS Oph is a symbiotic binary consisting of a massive WD and a red giant in a 454 d orbit (see Kato & Hachisu 2012, and references therein). Its latest outburst in 2006, from which Hachisu et al. (2006) infer a high WD mass, also revealed a shock from the interaction of the ejecta with the red-giant wind (Sokoloski et al. 2006), and radio emission suggesting the launching of a jet

[1] See, however, Zorotovic, Schreiber & Gänsicke (2011), who find that accreting WDs, on average, have higher masses than WDs with low-mass companions in post-common-envelope binaries that are destined to become semi-detached systems with stable mass transfer. This suggests either that WD masses do grow, or that the majority of cataclysmic variables form from systems with higher mass companions, that by some selection effect, harbor more massive WDs.

(Rupen, Mioduszewski & Sokoloski 2008). Patat et al. (2011) have studied the evolution of the absorption features, and find similarities with those found in the spectra of some SNe Ia (see Section 3.3.8). T Pyx is a short period system (P = 1.8 hr, Uthas, Knigge & Steeghs 2010), implying a low donor mass (if it is to fit in the Roche lobe at this period), and more typical of systems harboring classical novae, with its most recent outburst in 2011. Schaefer, Pagnotta & Shara (2010) suggested a high mass-transfer rate that would imply a high WD mass. However, Uthas, Knigge & Steeghs (2010) derive a mass ratio of 0.2, that for a realistic donor mass implies a WD mass of only 0.7 $M_\odot$. In any case, Selvelli et al. (2008) and Patterson et al. (2013) conclude that this system, again, is ejecting more mass than it accretes. T CrB is another wide symbiotic recurrent nova, with two known outbursts (see Anupama 2013), for which Luna, Sokoloski & Mukai (2008) argue a high WD mass based on the detection of hard X-ray emission. V407 Cyg is formally not a recurrent nova, as only one nova outburst (in 2010) has been observed, but the similarity of the eruption to that of RS Oph (e.g. Shore et al. 2011) implies a massive WD (Hachisu & Kato 2012, Nelson et al. 2012). On the other hand, Chomiuk et al. (2012a) use extensive radio observations to argue that the environment of V407 Cyg is not one typical of SNe Ia.

Could recurrent novae be the phase during which accreting WDs achieve a significant fraction of their growth toward $M_{\rm Ch}$ and explosion as SNe Ia? The answer is no, unless the number of recurrent novae is orders of magnitude larger than estimated. Beyond the 10 known systems, Schaefer (2010) estimates that as many as 60-100 Galactic sources that have been classified as classical novae are, in reality, recurrent novae whose repeated outbursts have been missed. Furthermore, his analysis of the Galactic spatial distribution of both types of novae suggests that their true numbers are several times larger than the numbers currently known. Thus, the Galactic population of recurrent novae could conceivably number ~ 300. However, to get a Galactic SNIa rate of at least once per 200 yr (see Section 3.5.7) and accrete at the very least $\sim 0.2 M_\odot$ at the limiting accretion rate onto a WD for a recurrent nova, of $\dot{M} < 3 \times 10^{-7}\ M_\odot\ {\rm yr}^{-1}$, over 3300 systems are needed. The recurrent nova phase can constitute $\lesssim 9\%$ of the time of the final 0.2 $M_\odot$ of WD mass growth. If we consider a more-realistic $0.4 - 0.9\ M_\odot$ mass gain required of C/O WDs (which have masses of $\sim 0.5 - 1 M_\odot$) in order to reach $M_{\rm Ch}$, then only 2-5% of that mass gain can take place during recurrent nova phases.

3.1.2 Supersoft X-ray sources In the evolutionary scenario proposed by Hachisu, Kato & Nomoto (1999), the recurrent nova phase, with accretion rates estimated at $\dot{M} \sim 1 - 3 \times 10^{-7}\ M_\odot\ {\rm yr}^{-1}$, follows a phase when a SD progenitor system is a supersoft X-ray source, growing via a larger accretion rate, $\dot{M} \sim 3 - 6 \times 10^{-7}\ M_\odot\ {\rm yr}^{-1}$. The high accretion rate (and hence temperature), compared to those of novae, lifts the degeneracy of the accreted hydrogen layer, and it burns stably to helium on the WD surface.

Observationally, "persistent" or "permanent" supersoft X-ray sources are identified, as their name implies, by their soft X-ray spectra, peaking at 30-100 eV, with typical luminosities of 10^{37-38} erg s^{-1}. Optical and X-ray followup of the best studied of these objects (e.g. Lanz et al. 2005, Rajoelimanana et al. 2013) has shown that they indeed consist of a hot WD in a close orbit with a non-degenerate donor, where hydrogen accreted from the donor, at roughly the above rates, burns more-or-less stably into helium on the WD surface (van den Heuvel et al. 1992). However, not all supersoft source spectra are easily interpreted in this way, as some show P-Cygni profiles indicative of a wind rather than a WD atmosphere (Bearda et al. 2002). Because of interstellar absorption of their soft X-ray spectrum, supersoft sources have been discovered mainly in external nearby galaxies. Only two are known in the Galaxy (MR Vel and Q And; e.g. Šimon 2003) but there are 15 in the Magellanic Clouds, and of order 10 in M31 (Orio et al. 2010). Classical and recurrent novae, discussed in Section 3.1.1 above, also have supersoft phases, but these are transient, occurring after their outbursts, and lasting of

order a month. As a result, only a minority of the supersoft sources that turn up in X-ray surveys of nearby galaxies are of the persistent kind, rather than being the transient supersoft phases of post-outburst novae (Orio et al. 2010).

Since the persistent supersoft X-ray sources in an $\sim L_*$ galaxy such as M31 again number only in the few tens of objects, the same argument, used above in the case of recurrent novae, holds as well: if supersoft sources are accreting WDs growing toward $M_{\rm Ch}$, and such SD systems are to explain the bulk of the SN Ia rate, then $< 1\%$ of the WD's growth time is spent in this phase. This is an order of magnitude less than the mean $\sim 5\%$ fraction of the time in the supersoft phase found by model calculations (Meng & Yang 2011). This paucity of supersoft sources has been pointed out by Di Stefano (2010), based on the numbers of such sources observed in six nearby galaxies, and by Gilfanov & Bogdán (2010), based on the integrated X-ray flux observed from nearby elliptical galaxies. Hachisu, Kato & Nomoto (2010) and Meng & Yang (2011) (see also Lipunov, Panchenko & Pruzhinskaya 2011) have countered that the nuclear-burning accreting WDs spend the majority of the time in a third possible phase, hidden within optically thick outflows (e.g Nielsen et al. 2013a, Wheeler & Pooley 2013, Woods & Gilfanov 2013b). We discuss this possibility in Section 3.1.3. Although proto-DD systems, at the time that only the first WD has formed, may also undergo mass transfer and a SD-like supersoft phase, its duration is much shorter than in SD progenitor systems (Nielsen et al. 2013b). As a result, fewer supersoft sources are expected in the DD scenario, by at least an order of magnitude, and consistent with their observed rarity. Considering also the delay, between the supersoft phase of proto-DD systems and the eventual WD merger and SN Ia explosion, further lowers the number of expected supersoft sources from DD progenitors.

3.1.3 Rapidly accreting WDs As noted above, Hachisu, Kato & Nomoto (1996, 1999) have proposed that the rapid accretion phase is self-regulated by an optically thick wind. The wind drives away the excess mass, effectively keeping the WD growth and the stable nuclear burning on the WD surface at the same rates as during the supersoft phase (but see Idan, Shaviv & Shaviv 2013, Section 2.1, above). The excess mass that is blown off the WD could create an optically thick photosphere that reprocesses the X-rays to UV emission. Nielsen et al. (2013a), Nomoto et al. (2007), Wheeler & Pooley (2013), and Lepo & van Kerkwijk (2013) have considered the possible appearances of such "rapidly accreting WDs", and argued that they might appear as undersized OB stars, i.e. with effective temperatures of $10^{4.5-5}K$, but with sizes of only a few $R_\odot$, dictated by the WD's Roche lobe radius. Another possibility is an appearance similar to Wolf-Rayet (WR) stars or WR planetary nebulae.

Among the objects considered possibly to be such rapidly accreting WDs are V-Sagittae-type nova-like cataclysmic variables, a class consisting of a handful of known objects (Steiner & Diaz 1998). The prototype, V Sge, is a double-lined eclipsing binary with a rich high-ionization emission-line spectrum, a period of 0.5 day, quasi-periodic high and low states lasting ~ 180 days, and supersoft X-ray emission in its low state. Hachisu & Kato (2003a) have modeled V Sge as a $1.25M_\odot$ WD accreting at a high rate from a Roche-lobe-filling $\sim 3M_\odot$ companion. Other moderately well-studied objects in the V Sge class are RX 0513.9-6950 (Hachisu & Kato 2003b) and QU Car (Kafka, Honeycutt & Williams 2012). A different type of object which could be a rapidly accreting WD is the peculiar planetary nebula LMC N66 in the Large Magellanic Cloud, whose WR-like core has undergone two optical outbursts over the past 60 years, each lasting several years, during which its luminosity was comparable to WN-type WR stars. There is no evidence yet for binarity in LMC N66, and no X-ray emission has been detected. Hamann et al. (2003) have modeled it, again, as a WD with mass inflow from a companion at rates of 10^{-6} to 10^{-5} $M_\odot$ yr^{-1} during its low and high states.

Lepo & van Kerkwijk (2013) have performed a search in the Small Magellanic Cloud for the ~ 100 rapidly accreting WD systems that are expected there, if such progenitors are

to produce the bulk of the SN Ia rate. They obtained optical spectra for about 750 sources, selected to be UV-bright at 1600 Å and to have unusual optical colors. They failed to find any object with unusual spectral signatures such as strong He II lines, or with optical variability, based on the long term OGLE monitoring database (Udalski, Kubiak & Szymanski 1997). From this, they deduce a $\lesssim 10\%$ contribution to the SN Ia progenitor population, of systems that are similar to LMC N66 or to WR stars. The color selection of targets employed by Lepo & van Kerkwijk (2013) included only a limited number of objects with colors similar to V Sge, and therefore such systems cannot yet be ruled out as SN Ia progenitors by this experiment.

Taking a more integral approach, Woods & Gilfanov (2013b) have argued that, in any scenario where the X-ray emission from nuclear-burning WDs is shielded by $T = 10^{5-6}K$ photospheres, the emerging UV radiation will still be quite hard, and capable of ionizing interstellar He atoms. In elliptical galaxies, a substantial mass of extended neutral hydrogen is often detected, as well as diffuse regions of low-ionization line emission, thought to arise through ionization of some of the gas by evolved stars. The integrated radiation from a population of rapidly accreting WDs could lead to ionization of some of the He in this gas to He^{++}, and to a detectable signal of diffuse He II λ4686 recombination line emission. Woods & Gilfanov (2013b) combine stellar spectral synthesis models with photoionization models to calculate the line emission as a function of galaxy age, gas covering fraction, and WD photospheric temperature. They predict, for an elliptical galaxy with a SD-dominated progenitor population with $T = 2 \times 10^5 K$ photospheres, a typical line equivalent width of a few tenths Å. In the absence of nuclear-burning SD systems, with ionization only by evolved stellar populations, a line flux one order of magnitude lower is expected. Woods & Gilfanov (2013a) extend these predictions to excitation of forbidden emission lines of C, N, and O by nuclear-burning WDs with photospheres in the upper part of the $T = 10^{5-6}K$ range. Johansson et al. (2013, submitted) have searched for the He II λ4686 signal in high-signal-to-noise stacks of 11,600 Sloan Digital Sky Survey (SDSS; Abazajian et al. 2009) spectra of early-type galaxies. The galaxies are selected to have weak but measurable line emission, in order to include galaxies with gas, but to exclude, based on the line diagnostics, galaxies with ongoing star formation or with active nuclei. In all four galaxy age-group stacks that they produce, they detect HeII λ4686 emission only at the level expected from ionization by the known evolved stellar populations, but not from ionization by rapidly accreting WDs. This sets a 10% upper limit on the contribution to the SN Ia rate by rapidly accreting WDs.

3.1.4 Helium-rich donors No clear-cut cases are known of systems that could be SN Ia progenitors through the helium-rich SD donor channel. However, the only known helium nova, V445 Pup, shows a pre-outburst magnitude (Ashok & Banerjee 2003) that suggests it is a WD accreting from an evolved helium star (Kato et al. 2008, Woudt et al. 2009). Modeling the nova outburst, Kato et al. (2008) find a high WD mass, but the predicted distance disagrees somewhat with the one determined from the expansion parallax of the bi-polar outflow from Woudt et al. (2009). At least one case is known of a close detached binary consisting of a C/O pre-WD and a lower-mass helium star, CD-30° 11223 (Geier et al. 2013). Its future helium accretion rate is expected to be in the right range to set off an edge-lit detonation, possibly leading to a double-detonation SN Ia (Yungelson 2008, see Sect. 2.4). The same could be true for some fraction of the so-called AM CVn systems, a class of objects in which a WD accretes helium from a very low-mass companion (see Solheim 2010 for a review), although the majority of the observed systems have evolved to too-low mass transfer rates for a double detonation.

3.1.5 Binary WDs As a test of the DD scenario, one can search our Galactic neighborhood, within a few kpc of the Sun, for short-period WD binaries whose orbits will gravitationally decay and merge within, say, a Hubble time, surpassing (or not) the Chandrasekhar

mass and perhaps thus producing SNe Ia. For the classic DD scenario to work, the Galactic SN Ia rate should match the WD merger rate (or some fraction of it involving mergers of the suitable masses). For the range of masses of WDs with a C/O composition, $0.5 - 1.0\ M_\odot$, pairs merging within a Hubble time will have separations of $a \lesssim 0.015$ AU, orbital periods of $P \lesssim 12$ hr, and circular orbital velocities $v \gtrsim 100$ km s^{-1}.

Marsh (2011) and Kaplan, Bildsten & Steinfadt (2012) present recent compilations from searches for binary WDs. In the current century, the first large survey to search systematically for such WD pairs was SPY (Geier et al. 2007, Napiwotzki et al. 2004, Nelemans et al. 2005). SPY obtained high-resolution (~ 2 km s^{-1} radial velocity [RV] resolution) VLT spectra for a sample of ~ 1000 WDs, with two epochs per target, separated by at least one day. Given the $\lesssim 12$ hr periods of close WD binaries, this essentially gives two samplings at random phases in the orbit. They searched for RV variations between epochs, that could result from the motion of an observed WD about a binary center of mass[2]. Candidate systems discovered by the survey were then followed up to obtain radial velocity curves and constraints on the binary parameters. SPY discovered ~ 100 candidate binary WDs, and among the ~ 10 systems for which parameters are measured, a handful will merge within a Hubble time. None of these future mergers have total masses $M_{\rm tot}$ that are unambiguously above $M_{\rm Ch}$, although for one system (WD 2020-425) the masses are difficult to measure and the best estimate is $M_{\rm tot} = 1.35$ M$_\odot$ (Napiwotzki et al. 2007). Then again, $M_{\rm tot} \geq M_{\rm Ch}$ may not necessarily be a pre-condition for a DD-scenario SN Ia (see Sections 2.2 and 2.4, above). Furthermore, a statistical interpretation of these results that accounts for the selection effects and efficiencies of the survey is still lacking. It is therefore yet unclear what these results imply for the merger rate of WDs in general, and for $M_{\rm tot} \geq M_{\rm Ch}$ mergers in particular.

A number of tight binaries, found by other searches, some that are not quite yet bona-fide double WD systems, may possibly become $M_{\rm tot} \geq M_{\rm Ch}$, Hubble-time-merging, WD systems (Geier et al. 2010, 2007; Maxted, Marsh & North 2000; Rodríguez-Gil et al. 2010; Tovmassian et al. 2010). Brown et al. (2011) have even discovered a binary WD system with a 13-min orbit that will merge within < 1 Myr, and Hermes et al. (2012) have detected, over a ~ 1-year baseline, the gravitational decay of its orbit. However, with component WD masses of only 0.26 and 0.50 $M_\odot$, this merger is unlikely to result in a SN Ia.

In terms of analysis of the observed binary WD population, Nelemans, Yungelson & Portegies Zwart (2001) and Toonen, Nelemans & Portegies Zwart (2012) have used BPS to simulate, under the various parametrizations for the physics of the common-envelope phase, the properties of WD binaries that would be observed, such as masses and periods. They have qualitatively compared them to the masses and periods of a compilation of known binary WD systems, as well as quantitatively with the WD space density and WD production rate, finding reasonable correspondence. The Galactic WD merger rates indicated by these BPS models, $1 - 2 \times 10^{-2}$ yr^{-1} (or $\sim 2 - 3 \times 10^{-13}$ yr$^{-1} M_\odot^{-1}$ for a Milky Way stellar mass of $6 \times 10^{10} M_\odot$), agree with other BPS studies (e.g. Han 1998; Iben, Tutukov & Yungelson 1997). This merger rate is similar to recent estimates of the SN Ia rate per unit mass in Sbc-type galaxies of Milky-Way mass, $\sim 1 \times 10^{-13}$ yr$^{-1} M_\odot^{-1}$ (Li et al. 2011b, Mannucci et al. 2005, see Section 3.5.7, below). However, only about one-third of the BPS mergers involve two C/O WDs, and an even smaller fraction have $M_{\rm tot} \geq M_{\rm Ch}$. Among known binary WDs, indeed only a handful are C/O+C/O, but this is partly due to the fact that some surveys are designed specifically to discover low-mass WD binaries (e.g. Kilic et al. 2012). The merger rates predicted by BPS thus may or may not be at the level required to explain SN Ia rates, depending on the ranges

[2]Note that a WD's luminosity can have a large range, depending on the WD effective temperature, which decreases with WD age, and on its surface area, which decreases with increasing WD mass. Therefore, in a WD binary, one of the WDs, not necessarily the least or more massive one, will often be much fainter than the other WD, and thus will remain undetected.

of $M_{\rm tot}$ assumed to lead to a SN Ia. More on this issue in Section 3.5.10, below.

Badenes et al. (2009) have been searching for close binary WDs among the spectra in the SDSS. The large number of WDs in SDSS, and the fact that SDSS spectra are always split into at least two sub-exposures, separated by at least 30 min, make this possible. With a ~ 70 km s^{-1} RV resolution possible with SDSS spectra of WDs (the resolution varies with WD type and brightness), this permits discovering candidate short-period WD binaries. The observed distribution of maximum RV differences between any two epochs, $\Delta_{\rm RVmax}$, can be compared to model distributions predicted for a range of binary population parameters (Maoz, Badenes & Bickerton 2012). Badenes & Maoz (2012) have applied the method to a sample of 4000 DA-type WDs in SDSS with the best signal-to-noise ratio. The model combinations of binary fraction and separation-distribution parameters that are consistent with the observed $\Delta_{\rm RVmax}$ distribution have a WD merger rate, per unit stellar mass[3], of $\sim 1\times10^{-13}$ yr$^{-1}M_{\odot}^{-1}$, a bit below the BPS estimates, and again quite similar to the expected SN Ia rate per unit mass in the Milky-Way. The fraction of $M_{\rm tot} \geq M_{\rm Ch}$ mergers is unconstrained by these observations – $\Delta_{\rm RVmax}$ is sensitive foremost to the WD separation, rather than to $M_{\rm tot}$. As noted above, based on known double WD systems and from BPS calculations, the fraction may be small, but $M_{\rm tot} \geq M_{\rm Ch}$ may not be required for a SN Ia.

3.1.6 Rapidly rotating massive WDs In the various spin-up/spin-down scenarios (see Section 2, above), one could expect the existence of a progenitor population of rapidly rotating, super-$M_{\rm Ch}$ WDs, with rotation periods of order seconds, either single or in post-interaction binaries. To achieve stability at significantly super-$M_{\rm Ch}$ masses, the WDs would need to have differential rotation profiles.

WD rotation is difficult to measure but, with few or no exceptions, WDs with measured rotations are observed to spin extremely slowly (see, e.g. Kawaler 2004). The typical period is ~ 1 d, and most periods range from a few hours to a few days. For example, Berger et al. (2005), using the core of the Ca II K line to measure rotational broadening in 38 DAZ-type WDs, find a projected rotation velocity $v_{\rm rot}\sin i < 30$ km s^{-1}, and typically just a fraction of this velocity. This shows that there is efficient radial angular momentum transport in WDs, at least between the core and the pre-WD envelope, or that the WDs were formed slowly spinning (Spruit 1998, Suijs et al. 2008). Charpinet, Fontaine & Brassard (2009) and Fontaine, Brassard & Charpinet (2013) have used asteroseismology to measure the inner rotation profiles of four newly formed pulsating WDs of the GW Vir class. They find slow, solid-body, rotation throughout $\sim 99\%$ of the WD mass. While still few, these cases suggest strong coupling and efficient angular-momentum transfer between the layers of the WD, which again argues against the differential WD rotation that is essential for the spin-up/spin-down scenario. Córsico et al. (2011), applying the same methods to another GW-Vir-type WD, find that the WD core may be spinning up to 4 times faster than the surface, but within the uncertainties, solid-body rotation cannot be excluded in this case.

Magnetic fields in WDs are also difficult to measure, unless the fields are strong. Some 10-30% of WDs have fields of $10^4 - 10^9$ G (Kawka et al. 2007), and $\sim 10\%$ have $10^3 - 10^4$ G (Jordan et al. 2007, Landstreet et al. 2012). Nordhaus et al. (2011), Tout et al. (2008) and García-Berro et al. (2012) have argued that strong magnetic fields in WDs are always the result of binary interactions, be it through accretion, common-envelope evolution, or mergers. In magnetic WDs, photometric variability due to spots and variable dichroic polarization open two additional avenues to measure rotation. While magnetic WDs tend to be significantly more massive than normal WDs (e.g. Kepler et al. 2013), they rotate just as slowly (Kawaler

[3]The analysis naturally gives the specific merger rate per WD, i.e. the reciprocal of the mean time until merger. This can be converted to a rate per unit stellar mass, using estimates for the stellar mass density and the WD number density in the Solar neighborhood.

2004), suggesting that WDs are unable to spin persistently, even after binary interactions. Several cases of non-variable magnetic WDs, suspected as possibly unrecognized fast rotators, have been shown to actually be very slow rotators (Beuermann & Reinsch 2002, Friedrich & Jordan 2001). However, Boshkayev et al. (2013) have proposed that soft-gamma-ray repeaters and anomalous X-ray pulsars could actually be massive, rapidly rotating, magnetic WDs.

If spin-up/spin-down is a dominant SN Ia progenitor channel, we can estimate the number of WDs in Solar-neighborhood samples that could reveal evidence of being such progenitors, again using a SN Ia rate per unit mass in Sbc spirals of Milky Way mass, 1×10^{-13} yr^{-1} $M_\odot^{-1}$. The local stellar density is 0.085 $M_\odot$ pc^{-3} (McMillan 2011). If spin-down requires a Hubble time to occur, there should be, within a distance of 100 pc, about 400 WDs with super-$M_{\rm Ch}$ masses, and rotations of order 1000 km s^{-1}. If spin-down and explosion occur on timescales of $\lesssim 10^8$ yr, only about four such nearby fast rotators are expected. Nonetheless, in the latter case, being young and hence hot and luminous, they should still be quite conspicuous (Di Stefano, Voss & Claeys 2011). Upcoming large and complete WD samples, such as those that will be discovered by *Gaia*, will further test this scenario.

3.2 Pre-explosion evidence

The most direct way to resolve the progenitor problem would be to see the progenitor system of an actual SN Ia, before it exploded. Unfortunately, and contrary to the situation for CC SNe, where a good number of progenitor stars have been identified in pre-explosion images (see review by Smartt 2009), no such progenitor has ever been convincingly detected for a SN Ia. Pre-explosion optical images for several Virgo-distance SNe Ia, at the pre-explosion sites, have set upper limits on progenitor luminosities, corresponding to supergiants evolved from stars of initial mass $\gtrsim 8$ M$_\odot$ (Graur & Maoz 2012a,b, Maoz & Mannucci 2008, Nelemans et al. 2008, Voss & Nelemans 2008; see also summary in Li et al. 2011a). Nielsen, Voss & Nelemans (2012) and Nielsen, Voss & Nelemans (2013) placed upper limits on the pre-explosion progenitor X-ray luminosities at the sites of 13 nearby SNe Ia, in several cases limits that are comparable to the luminosities of supersoft X-ray sources. Voss & Nelemans (2008) did find a possible pre-explosion X-ray source at the site of the SN Ia 2007on. However, the best-fit position of the X-ray source (based on 14 photons) is offset by 1.1 arcsec from the optical SN position, making this detection ambiguous. On the other hand, the source was not detected after the event (albeit in shallower images) and chance alignment of such a soft source, that almost certainly originates in the same galaxy as the SN, is unlikely as well (Roelofs et al. 2008).

3.2.1 The case of SN 2011fe

The strongest pre-explosion limit on the presence of a SD donor star was set in the case of SN 2011fe in the nearby (6.4 Mpc; Shappee et al. 2013) galaxy M101. Being the nearest SN Ia event in 25 years, and having been discovered very early, SN 2011fe was extremely well studied, and has permitted many tests relevant to the progenitor question (see Chomiuk 2013 and Kasen & Nugent 2013 for reviews). SN 2011fe was about as typical as a SN Ia can be, in all of its observed characteristics (Mazzali et al. 2013), making it particularly relevant for addressing the question of the progenitors of SNe Ia, as a population. As a final bonus, it had negligible Milky Way and intrinsic line-of-sight extinction (Nugent et al. 2011).

Li et al. (2011a) analyzed deep (2σ limiting Vega magnitudes $\sim 27-28$) pre-explosion *Hubble Space Telescope* (HST) images of the site of the event in four optical bands, corresponding roughly to B, V, I (all from 2002), and R (from 1998). They used adaptive-optics imaging of the SN, obtained with the Keck II telescope, to determine the SN location on the HST images to 21 mas precision. *Spitzer* images at 3.6 μm to 8 μm, and 142 ks of *Chandra* images in the 0.3-8 keV band, both from 2004, were also examined. No source was detected at the SN position. In addition, they searched about 3000 epochs of shallower, ground-based,

monitoring data of M101, from 12 years preceding the explosion. These data set optical flux limits, reaching $\sim 20-23.5$ mag, on any pre-SN variable or transient events at the SN location.

From the HST data, Li et al. (2011a) strongly rule out the presence of a red giant at the location of the SN in the decade prior to the explosion. Also excluded are any stars more massive than 3.5 $M_\odot$ that have evolved off the main sequence. Two Galactic symbiotic recurrent novae, RS Oph and T CrB, would have been detected in the data if placed, at their quiescent luminosities, at the distance of M101. The "helium nova" V445 Pup in quiescence, where the donor is a helium star, would have likewise been detected in the HST data. Conversely, main-sequence and subgiant donors with masses below 3.5 $M_\odot$ are allowed, and a system like the recurrent nova U Sco, in which the donor is a main sequence star, would be undetected in quiescence. Figure 1 shows these results.

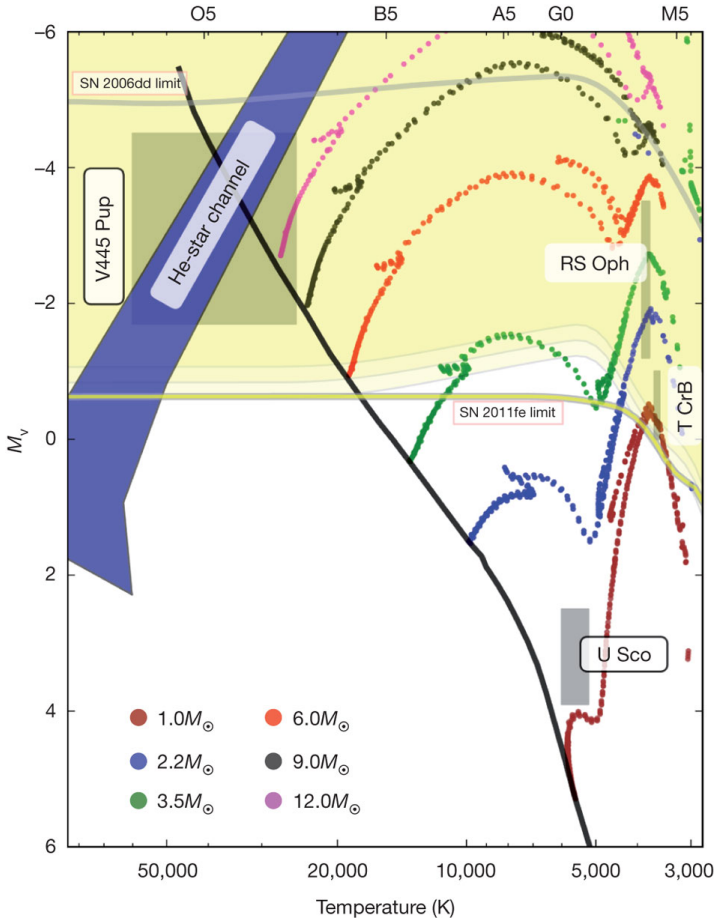

Figure 1: HR diagram (absolute V magnitude versus effective temperature) showing the 2σ upper limits (thick-yellow line) on the presence of progenitors in pre-explosion HST images of SN 2011fe in M101, from Li et al. (2011a). Also shown are theoretical evolution tracks of isolated stars with a range of masses, theoretical location of a SD He-star donor, and location on the diagram of several known recurrent novae. The data rule out red giants, and any evolved star more massive than 3.5 $M_\odot$, as well as the recurrent nova systems above the limit. Gray curve is the corresponding limit by Maoz & Mannucci (2008) for the more distant SN 2006dd.

Li et al. (2011a) found that a pre-explosion eruption at the site of SN 2011fe, with a luminosity typical of nova outbursts, could have been detected by the decade of optical monitoring

data, but there is a 37% probability that such an eruption would have been missed, given the actual cadence of those observations. Analysis of the X-ray data sets an upper limit on the pre-explosion bolometric X-ray luminosity of $(4-25)\times10^{36}$ erg s^{-1} (depending on the assumed spectrum). Nielsen, Voss & Nelemans (2012) used a deeper stack of of 800 ks *Chandra* data to set a somewhat stronger X-ray upper limit in the case of SN2012fe. A weaker limit was set by Liu et al. (2012a), based on these *Chandra* data, but Nielsen, Voss & Nelemans (2012) point out possible errors in the analysis. In any event, the X-ray data rule out the pre-explosion presence, at the location of SN 2011fe, of typical persistent supersoft X-ray sources, but allows the presence of somewhat fainter ones.

Shara et al. (2013) imaged M101 with HST, including the location of SN 2011fe, in 2010, about 1 year prior to the event, in a narrow band centered on the He II $\lambda4686$ line. The hard photon flux from a nuclear-burning accreting WD (see Section 3.1.3, should, in principle, produce a 1-30-parsec-sized (i.e. unresolved or resolved, depending on the outflow rate and the surrounding gas density) He III Stromgren sphere in the interstellar medium (ISM) of the galaxy (Rappaport et al. 1994). Graur, Maoz, & Shara (2013, in preparation) use the HST data to set a 2σ upper limit on the pre-explosion He II line luminosity at the SN position, of $L_{\rm HeII} < 3\times10^{34}$ erg s^{-1}, for an unresolved He III region. From photoionization models for a supersoft X-ray source ionizing a surrounding ISM of density $n = 10$ cm^{-3} (Rappaport et al. 1994), this implies a limit on the X-ray luminosity of $L_x < 2\times10^{37}$ erg s^{-1}. As opposed to the limits based on direct X-ray observations, detailed above, on the presence of supersoft progenitors during the decade before the explosion, the He II line emission limit is an indicator of the mean ionizing luminosity over $\sim 10^5$ yr (the He III region's recombination time) prior to the explosion.

On the other hand, there is only one known case, CAL 83, of a supersoft X-ray source that has a detected ionization nebula, while nine others that have been searched for such extended line emission have yielded only upper limits, at luminosity levels an order magnitude lower than that of CAL 83 (Remillard, Rappaport & Macri 1995). Furthermore, the X-ray luminosity of CAL 83 is $L_x = 3\times10^{37}$ erg s^{-1}, but its He II line luminosity is only $L_{\rm HeII} \approx 2\times10^{33}$ erg s^{-1}, an order of magnitude below model expectations (Gruyters et al. 2012). Contrary to the Hα and [O III] emission, which is roughly symmetrical around the source, the He II emission is concentrated on one side, within ~ 1 pc. The reasons are unclear for the discrepancy between the observed supersoft ionization nebula luminosities and model expectations, but, in any case, an He-III region similarly faint to that seen in CAL 83 would be undetected in the HST M101 data at the site of SN 2011fe. Furthermore, if the WD progenitor of SN 2011fe were in a rapidly accreting mode, the fast wind would carve-out in the ISM a rarified cavity of order 30 pc (e.g. Badenes et al. 2007). Such an extended, low-surface-brightness, emission-line region would be undetected in the HST image.

In summary, the pre-explosion data for SN 2011fe rule out SD systems with red giant and helium-star donors, bright supersoft X-ray sources, and accreting WDs that produce significant He II ISM ionization, but allow main-sequence and sub-giant SD donors, and faint supersoft sources. DD progenitors are of course not limited by these data, nor spin-up/spin-down models with long delays between the end of accretion and explosion.

3.3 Clues from during the SN events

The observed characteristics of the emission of a SN Ia explosion itself, at various wavelengths and times, contains information on the exploding system, including its progenitor aspect.

3.3.1 Early light curve and spectral evolution Among the clues to the progenitor that, in principle, can be obtained from observables obtained during a SN event itself, the early development of the light curve and the spectra can be particularly revealing. The early

light-curve evolution of a SN Ia, starting from the time of explosion, has been recently studied in a number of theory papers (Höflich & Schaefer 2009; Kasen 2010; Nakar & Sari 2010, 2012; Piro, Chang & Weinberg 2010; Piro & Nakar 2012, 2013; Rabinak, Livne & Waxman 2012; Rabinak & Waxman 2011). Briefly, the expected behavior is as follows.

Assuming that the explosion, which begins near the center of the WD, at some point expands outward as a supersonic detonation (see Section 3.3.4, below), the shock wave propagates toward the surface, heating and igniting the WD material and giving it an outward bulk velocity. The shock propagates most of the way at $\sim 10^4$ km s^{-1}, approaching the surface after ~ 1 s. The shock accelerates to relativistic velocities in the dropping density profile near the WD surface. When it emerges, it produces a ms-timescale gamma-ray flash of energy $E_\gamma \sim 10^{40-41}$ erg, constituting "shock breakout" (Nakar & Sari 2012). Following breakout, the radiation emerging from the explosion comes from the matter that is outside of a "diffusion front", advancing from the surface into the expanding ejecta below it. The radius of the diffusion front is defined by the diffusion time of photons through the outer envelope, at the time of observation. The expanding shock-heated ejecta quickly cools adiabatically. In the outer regions, where pressure is radiation dominated, the temperature decreases with growing radius R as $T \propto R^{-1}$, while in the inner matter-dominated regions, the cooling is faster, $T \propto R^{-2}$. The luminosity drops steeply for about 1 s after breakout, until the diffusion front reaches material with sub-relativistic bulk velocity. From this point on, the escaping bolometric luminosity initially falls with time as $L_{\rm bol} \sim t^{-0.4}$, while the effective temperature observed in the ejecta falls as $T_{\rm eff} \sim t^{-0.6}$.

The peak of the spectral energy distribution thus transits within minutes from gamma-rays and X-rays to the UV band. Optical-UV-band observations will, at first, be on the Rayleigh-Jeans side of this thermal spectrum, and will therefore see an optical luminosity that rises as $L_{\rm opt} \sim t^{1.5}$, peaks after ~ 1000 s at $L_{\rm opt} \sim 10^{39}$ erg s^{-1}, and then falls as the Wien peak enters the bandpass. After a time that is proportional to the initial stellar radius, (~ 1 hr in the case of a WD), the diffusion front has traversed the outer $\sim 10^{-4}$ $M_\odot$ of the WD mass, and enters the cooler, matter-dominated region of the adiabatically expanding shock-heated ejecta, and therefore there is a sharp drop-off in luminosity (Rabinak, Livne & Waxman 2012). The luminosity may drop below detection limits, initiating a "dark phase" in the light curve, lasting until photons powered by radioactive decay can diffuse to the surface. This dark phase can last up to a few days, depending on the depth of the radioactive material.

As the diffusion front enters the ejecta, the material contributing to the observed luminosity includes progressively larger amounts of ^{56}Ni from the explosion. The energy from the gamma-rays formed by the radioactive decay of ^{56}Ni diffuses through the line-blanketed ejecta and emerges in the optical. This causes the classic observed rise in the optical light curve, all the way until the peak of the bolometric light curve at ~ 18 d, which occurs roughly when the diffusion front has traversed all of the ejecta (and therefore the luminosity from all of the ^{56}Ni is observable). Beyond maximum light, the fall of the light curve is determined by the exponentially decreasing number of ^{56}Ni nuclei and their radioactive ^{56}Co daughter nuclei, the changing UV opacity of the ejecta, and the increasing fraction of gamma rays and positrons that can escape the remnant due to the falling density.

Observations of the early light curve of any type of SN can provide constraints on the progenitor in several ways. First, the time between explosion and shock breakout, presuming the epoch of the explosion can be estimated, provides a measurement of the pre-explosion radius of the exploding star. (Shock breakout has been seen, to date, in several CC SNe, see e.g. Tominaga et al. 2011). Non-detection of the post-breakout thermal emission from shock-heated material, can also set upper limits on the pre-explosion radius, as further detailed below. Second, the observed time dependence of the ^{56}Ni-powered rise indicates the amount of ^{56}Ni as a function of depth into the ejecta, and can thus constrain the ignition and combustion

scenarios, and the amount of mixing in the ejecta. Third, in any configuration of accretion onto a WD via Roche-lobe overflow from a donor star, the L1 Lagrange point, and hence the donor, will be within a few donor-star radii of the explosion. Impact of the ejecta on the donor is therefore expected within minutes to hours (for main-sequence and giant donors, respectively). The consequences of the impact should be visible for up to a few days. This third possibility is discussed in Section 3.3.2, below.

The actual gamma-ray flash of the shock breakout in a SN Ia is expected to be too dim, too brief, and at too-high photon energies, to be detected anywhere but in our Galaxy and perhaps in the Magellanic Clouds. However, the UV/optical emission from the adiabatically cooling, shock-heated, ejecta, on timescales $\lesssim 1$ hr, as well as the earliest parts of the ^{56}Ni-powered light curve, are detectable in more distant events. Among the best observations to date, in this context, have again been those of SN 2011fe, which was detected 18 days before maximum light, and quickly followed up in many wavebands. Nugent et al. (2011) found that the g-band luminosity of the event is well fit by a $L_g \propto t^2$ dependence. Such a dependence has often been used to characterize the ^{56}Ni-powered phase of the light curve, both theoretically, under some simplifying assumptions, (Arnett 1982), and observationally (e.g. Hayden et al. 2010b, who found $t^{1.8\pm0.2}$ by fitting the average light curves of SDSS-II SNe). Assuming also that this dependence can be extrapolated back in time, the actual time of explosion was determined by Nugent et al. (2011) to ± 20 min accuracy. They argued that their earliest detection of the SN, corresponding to 0.5 day after the derived explosion time, was already dominated by the ^{56}Ni-powered rise, and was therefore past the shock-heated phase of the light curve. By comparing their photometry to models by Piro, Chang & Weinberg (2010), Kasen (2010), and Rabinak & Waxman (2011), they translated the limit on the duration of the shock-heated phase to a limit on the radius of the exploding star of $R_* < 0.1\ R_\odot$. Bloom et al. (2012) used upper limits on the observed luminosity from a non-detection at the SN location obtained 8 hr earlier, i.e. just 4 hr after the presumed explosion time (see Figure 2), to argue that the light curve was past the point of the drop-off in the shock heated phase, occurring when the diffusion front reaches the shells with gas-dominated pressure. This strengthened the limit on the initial stellar radius to $R_* < 0.02\ R_\odot$. Setting aside, for a moment, the progenitor scenarios being discussed in this review (SD, DD, etc.), these limits are particularly interesting, as they constitute the most direct evidence that the exploding object in a SN Ia is, in fact, a WD.

However, Piro & Nakar (2012, 2013) and Mazzali et al. (2013) have questioned the accuracy of these conclusions. Piro & Nakar (2013) show that, in general for a SN Ia, the $L_{\rm opt} \propto t^2$ "fireball model" dependence is not expected under realistic conditions for the photospheric velocity (assumed to be constant in time in the fireball model) and for the radial distribution of ^{56}Ni in the ejecta (assumed to be uniform by Nugent et al. 2011). Piro & Nakar (2013) show that, for a range of possible conditions, the light curve is poorly approximated by a single power law, and the back-extrapolated $L_{\rm opt} \propto t^2$ dependence of the optical luminosity does not necessarily give the correct explosion time. Piro & Nakar (2012) fit the observed photospheric velocity evolution in SN 2011fe (as measured by Parrent et al. 2012) with a $v \propto t^{-0.22}$ dependence (shown to be expected theoretically in Piro & Nakar 2013) in order to constrain the explosion time, and they fit models with varying ^{56}Ni radial distributions to the observed optical light curve. They conclude that the true time of explosion is uncertain by $\sim \pm 0.5$ d, and could be ~ 1 d earlier than concluded by Nugent et al. (2011). This, in turn, weakens the upper limit on the stellar radius, obtained by Bloom et al. (2012) to $R_* < 0.1\ R_\odot$. Mazzali et al. (2013) reach a similar conclusion by estimating the explosion time from their detailed fitting of photospheric temperatures, abundances, and velocities to early-time spectra (see Section 3.3.3, below). They also favor an explosion time 0.9 d earlier than deduced by Nugent et al. (2011), and find a limit of $R_* < 0.06\ R_\odot$. These somewhat weaker limits on the stellar radius are still quite useful in ruling out most options for the exploding object in

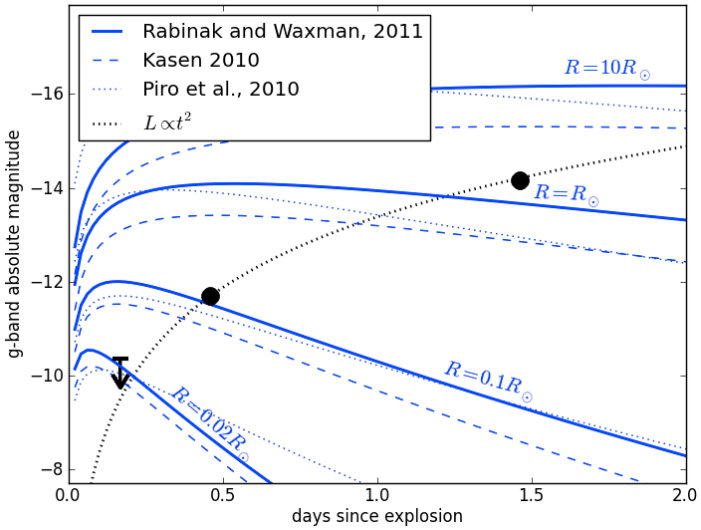

Figure 2: Early optical light curve for SN 2011fe, compared to theoretical models. The two detections are from Nugent et al. (2011), and the 5σ upper limit is from Bloom et al. (2012). Black dotted curve shows the t^2 dependence due to radioactive heating expected in the simplified "fireball" approximation. The Rabinak & Waxman (2011) and Piro, Chang & Weinberg (2010) models are for the shock-heated luminosity from an object of a given radius, as marked. Kasen (2010) models are for a shock impacting a companion (see Section 3.3.2, below), with R being the separation distance, for the case of an observer aligned with the collision axis. The data indicate a small exploding star *and* the absence of a shocked companion, but details depend on the assumed time of explosion. From Bloom et al. (2012).

SN 2012fe. Bloom et al. (2012) show that, apart from a WD, only pure carbon-oxygen stars, burning carbon stably, could have radii consistent even with these weaker limits.

The modeling of SN 2011fe by both Mazzali et al. (2013) and Piro & Nakar (2012) lead them to conclude that significant amounts of ^{56}Ni, ~ 0.1 of the total amount, existed in the outer $0.1M_\odot$ of the ejecta. Piro & Nakar (2012) find this not only for SN 2011fe, but also for SN2012cg, another SN Ia with early time data. The presence or absence of ^{56}Ni in the outer layers is relevant to understanding the explosion details, especially the possible transition from a deflagration to a detonation (see Section 3.3.4, below).

Zheng et al. (2013) have discovered a SN Ia, 2013dy, caught even earlier in its light evolution. With good light curve coverage in the first few days, they find that, indeed, a t^2 behavior fits the data poorly. Instead, they obtain a best fitting broken power law that begins with an index 0.9 and transits to an index 1.8 after about 3 days. Extrapolating this fit back in time to zero flux implies that the SN's "first light" occurred just 2.4 ± 1.2 hr before the first detection. The non-detections at earlier times again argue for upper limits of $\lesssim 0.25\ R_\odot$ on the progenitor radius.

3.3.2 Shocks from ejecta impacting companion stars and debris As already noted, in the classic SD picture, shocks from the SN ejecta hitting the companion star are unavoidable, and may be observable. Kasen (2010) has calculated the observational signatures of such events, as a function of the companion size (giants naturally produce the largest signals), and as a function of the angle between the observer, the WD, and the donor. When a giant star is between the observer and the WD, the signatures of the impact are expected in X-rays, within minutes to hours of the explosion. Emission from the shocked region in ultra-

violet/blue bands develops on a timescale of several days. Bianco et al. (2011), Hayden et al. (2010a), Tucker (2011), and Ganeshalingam, Li & Filippenko (2011) have set observational upper limits in blue optical bands in the light curves of SNe Ia with good early-time optical coverage, and have used the Kasen (2010) models to limit the presence of red-giant donors to $< 20\%$ of SN Ia progenitor systems. Foley et al. (2012a) and Brown et al. (2012b) have extended this approach using space-UV measurements to obtain such limits in several cases.

This type of limit is strongest, here again, in the case of the nearby and promptly observed SN 2011fe in M101. Nugent et al. (2011) and Bloom et al. (2012) used the same early optical observations (discussed in Section 3.3.1 above, in the context of emission from shock-heated ejecta) to exclude also shocks from ejecta hitting a companion. Brown et al. (2012a) use prompt UV observations of SN 2011fe, obtained with *Swift* starting 18 hr after the first Nugent et al. (2011) epoch, to do the same. All three studies rule out red giants donors, Brown et al. (2012a) exclude also main-sequence companions of radius $R_c \gtrsim R_\odot$, and Bloom et al. (2012) sharpen this limit to $R_c \lesssim 0.1 R_\odot$. Figure 2 shows also these limits. The conclusions, like those in Section 3.3.1 above, are sensitive to the exact time of the explosion.

This limitation has been circumvented by Olling, Mushotzky & Shaya (2013, submitted) and Olling et al. (2014, in preparation), who used the Kepler Mission to monitor continuously over several years, with 30-min exposures, 400 galaxies in the Kepler field. Among these galaxies, they discovered four SNe, two or three of them likely SNe Ia, based on their light curves. The continuous coverage reveals no signatures of companion impacts within the few days before first light, when the actual explosion must have occurred. Olling et al. again use the Kasen (2010) models to limit the presence of red giant and main-sequence companions for a range of viewing angles. An extension of the Kepler mission, particularly in sky directions that would allow ground-based followup and classification, would permit obtaining such data for many additional events, which would set strong constraints on the fraction of SNe Ia in which a SD donor star is present.

Interestingly, Nugent et al. (2011) have used the absence of impact signatures in SN 2011fe to argue also against a DD progenitor system. This argument is based on calculations by Fryer et al. (2010), who simulated DD mergers and found that a potentially large mass of debris, $0.1 - 0.7\ M_\odot$, forms an inhomogeneous envelope around the merged object, with a steeply falling density profile extending out to $\sim 1\ R_\odot$. This is based, in turn, on BPS calculations (Ruiter, Belczynski & Fryer 2009) that predict the majority of DD mergers to have masses around 2 $M_\odot$, whereas most other BPS studies predict lower masses (see also Section 3.3.4). Fryer et al. (2010) calculated the shock breakout and early-time spectral evolution in this model, and found behavior very distinct from that expected of a "bare" exploding WD, with UV emission lasting for days, and similar to the early-phases of Type II SNe. However, Fryer et al. (2010) also found that, in general, the spectra and light curves produced in the context of this model bear little resemblance to those of normal SNe Ia. The results of the calculations, if taken at face value, can therefore be considered evidence against the DD scenario, irrespective of the lack of shock signatures in the Nugent et al. (2011) data for a very typical SN Ia. However, DD merger simulations differ regarding the amount of debris at small distances at the time of explosion (Dan et al. 2012; Raskin & Kasen 2013; Shen, Guillochon & Foley 2013). As explained by Pakmor et al. (2012), one critical ingredient is the time elapsed from merger until explosion. In the violent-merger scenarios, where ignition occurs within minutes of the merger, any merger debris, moving at the escape velocity of a few thousand km s^{-1}, will be overtaken by the ejecta, and will cease to interact with it, minutes after the explosion (see, in this context, also Soker, Garcia-Berro & Althaus 2013). Also important, for the amount and location of debris, are the WD mass ratio and the assumed WD spin initial conditions (Dan et al. 2013).

3.3.3 Spectral and light curve modeling As the ejecta of a SN expands, the photosphere recedes into progressively deeper layers, revealing the chemical stratification and velocity structure of the ejecta. These in turn, may help distinguish among progenitor models. A way to reconstruct this physical structure is through calculation of synthetic spectra and light curves that match the observations.

In one such modeling approach (e.g. Hachinger et al. 2013, Mazzali et al. 2007, Stehle et al. 2005, Tanaka et al. 2011), an ejecta density profile is assumed, based on a hydrodynamical explosion model. A Monte Carlo radiative transfer calculation is used to propagate photon packets from a blackbody spectrum through the model photosphere. The element abundances and the velocity at each radius are varied in order to obtain the best fit to the set of observed spectra and photospheric velocities. Mazzali et al. (2013) have recently applied the method to the combined UV spectra from *HST* and ground-based optical spectra for SN 2011fe. A good match to the data is found using a hybrid between the density profiles from the SD one-dimensional (1D) fast-deflagration W7 model of Nomoto, Thielemann & Yokoi (1984), and from a 1D delayed-detonation model from Iwamoto et al. (1999) (more on deflagrations and detonations in Section 3.3.4, below).

Blondin et al. (2011) have carried out a more "first-principles" approach by taking a set of 44 hydrodynamical 2D $M_{\rm Ch}$ SD delayed-detonation models from Kasen, Röpke & Woosley (2009), and comparing them to observed light curves and multi-epoch spectra of 251 SNe Ia. The details of the nucleosynthesis and the resulting element distributions were calculated by means of tracer particles distributed throughout the volume, with nuclear reaction networks calculated for the conditions at each location. Finally, photon packets were again Monte-Carlo-propagated through the ejecta, to obtain synthetic light curves and spectra at the epochs corresponding to the observations. Overall good agreement is found between the data and some of the models, particularly those that satisfy the Phillips (1993) relation, but some details do not match, such as too-high model velocities in the maximum-light spectra.

Röpke et al. (2012) have extended this approach, to test example models from the two main progenitor scenarios, SD and DD, against optical spectra of SN 2011fe. One model is a $M_{\rm Ch}$ SD delayed-detonation model from Seitenzahl et al. (2013b), and the other is a violent-merger DD model from Pakmor et al. (2012), merging 1.1 $M_\odot$ and 0.9 $M_\odot$ WDs. For each model, Röpke et al. (2012) used a 3D hydrodynamics code to calculate the evolution of the density and the temperature. Nucleosynthetic abundances are again calculated via tracer particles and Monte-Carlo radiative transfer is performed. Both progenitor models produce reasonable matches to the observations but, again, both also have shortcomings in matching the details. Overall, the DD model fares somewhat better in this comparison. The differences in the predictions of the two models, and the discriminating power of the data, suggest that future applications of this approach, with a larger range of 3D models, should be very useful.

The amount and velocity distribution of unburnt carbon observed in SN Ia ejecta can be a diagnostic that distinguishes among scenarios. Folatelli et al. (2012), Parrent et al. (2011), Thomas et al. (2011), and Silverman & Filippenko (2012) analyze several samples with pre- or near-maximum spectra, and estimate that the C II λ6580 absorption feature is present in about 30% of SNe Ia. In all studies, the feature tends to appear in events with "low velocity gradients" (see Section 3.3.4, below). The implied carbon mass is $10^{-3} - 10^{-2} M_\odot$. In SN 2011fe, Nugent et al. (2011) clearly detect this line in the earliest high-resolution spectrum, along with high-velocity O I absorption. Both features almost disappeared in a spectrum obtained only 8 hours later. From their modeling of these data, Mazzali et al. (2013) deduce the existence of an almost-pure carbon outer layer of $\sim 0.01 M_\odot$. They speculate that this layer reflects the properties of the accreted material, whether hydrogen or helium that has burned to carbon. Soker, Garcia-Berro & Althaus (2013) propose, instead, that the outer-layer carbon enrichment is a byproduct of crystallization in a WD that has been rotation-supported

against collapse and has cooled, for ~ 1.4 Gyr, in a spin-up/spin-down scenario, such as core-degenerate. Zheng et al. (2013) similarly see strong C II absorption in SN 2013dy, within the first few days after explosion, weakening and becoming undetectable within a week.

3.3.4 Diversity and correlations among spectral and environmental observables Observers have long sought, and sometimes found, relations among the observed properties of SN Ia events. These include relations among the various spectral and photometric properties, and between those properties and the properties of the host galaxies as a whole, or of the specific locations of SNe Ia within a galaxy. An observed correlation, assuming it is not due to selection effects, may be merely a consequence of some basic physics of SN Ia explosions in general, rather than of a specific progenitor channel leading up to the explosion. Nevertheless, in such relations there is a potential for clues to the progenitor problem.

The width-luminosity relation: The strongest and clearest correlation seen among SN Ia properties is the so-called Phillips (1993) relation, connecting the maximum-light luminosity of an event to its light-curve evolution (as parametrized in a variety of ways), and to the observed color at maximum light (e.g. Hillebrandt et al. 2013, Kattner et al. 2012). Less-luminous SNe Ia, which have synthesized less ^{56}Ni, evolve more quickly. Less-luminous SNe Ia are also redder, due to some combination of intrinsically redder color, and reddening by dust, a combination that has proved hard to disentangle. The problem is compounded by evidence, often contradictory, that the dust involved in the effect might have properties distinct from Milky Way dust, with a low ratio of extinction to reddening, $R_V \equiv A_V/E(B-V) \approx 1.5-2$, as opposed to the typical Galactic $R_V \approx 3.1$ (see Howell 2011, but Scolnic et al. 2014 for a different view).

The Phillips relation itself may be a consequence of SN Ia physics, rather than of a particular progenitor scenario. The mass of synthesized ^{56}Ni largely determines the total energy of the explosion. The larger the ^{56}Ni mass, the higher also the peak luminosity due to the radioactive decay of ^{56}Ni. In parallel, iron-group elements also cause the bulk of the opacity, slowing the evolution of the light curve, i.e., leading to a higher light-curve "stretch" factor (e.g. Hoeflich & Khokhlov 1996, Kasen & Woosley 2007; see Kasen, Röpke & Woosley 2009 for additional factors, such as viewing angle, that can affect the relation). Nevertheless, progenitor models invoking explosions always near $M_{\rm Ch}$ must explain the diversity, of factor ~ 4, in explosion energy among "normal" SNe Ia (Branch & van den Bergh 1993, i.e. excluding under-luminous, SN1991bg-like, and over-luminous, SN1991T-like, events).

Timmes, Brown & Truran (2003) have proposed progenitor metallicity as the main driver for explosion energy. Main-sequence stars with a higher abundances of CNO produce, during helium burning, higher abundances of neutron-rich nuclei, particularly ^{22}Ne, that end up in the WD. In a WD undergoing combustion as a SN Ia, neutron richness leads to more synthesis of stable elements such as ^{54}Fe and ^{58}Ni, at the expense of ^{56}Ni, and hence to a lower luminosity. Although Timmes, Brown & Truran (2003) show that a large-enough range in progenitor metallicity could reproduce the observed range in normal SN Ia explosion energies, Piro & Bildsten (2008) and Howell et al. (2009b) have shown that the observed range of SN Ia host galaxy metallicities does not reach the extreme values required for this mechanism to have a significant effect on SN Ia explosion energy. The observed metallicity range of SN Ia host galaxies, even accounting for local extremes within a galaxy, would lead to $< 10\%$ variation in explosion energy. Piro & Bildsten (2008) further showed that pre-explosion neutron richness is not controlled solely by metallicity, but rather can be dominated by neutronization through carbon burning during the ~ 1000 yr "simmering" phase that $M_{\rm Ch}$-explosion models generally undergo before explosion. Mazzali & Podsiadlowski (2006) showed that, even if metallicity variations produce the range in peak luminosity, they will not affect light curve shape, i.e. the Phillips relation is not reproduced. Foley & Kirshner (2013) have analyzed two "twin" SNe Ia

(2011fe and 2011by) that have identical light curve shapes and optical spectra, but differ in their UV spectra and in their peak luminosity. Modeling the difference in UV spectral opacity by means of progenitor metallicity differences, the Timmes, Brown & Truran (2003) model correctly predicts the difference in peak luminosity. Metallicity effects may thus be at work, even if they do not explain the explosion energy diversity or the Phillips relation.

Another way to explain the observed diversity in explosions of $M_{\rm Ch}$ models is through the so-called "deflagration-to-detonation transition". It has long been known that the energetics and spectra of $M_{\rm Ch}$ models do not match observations, unless finely (and artificially) tuned as an initial subsonic deflagration that allows the WD to expand and, at the right time, spontaneously to evolve into a supersonic detonation (Blondin et al. 2013, Hillebrandt & Niemeyer 2000, Khokhlov 1991, Ma et al. 2013). Different progenitor metallicities and masses, and different accretion histories, could affect the number and location of ignition "kernels", and thus the transition to detonation (e.g. Blondin et al. 2011; Kasen, Röpke & Woosley 2009; Seitenzahl et al. 2013b; Umeda et al. 1999). Different transition times lead, in the final ejecta composition, to different proportions of unburnt carbon and oxygen, intermediate-mass elements, stable iron-peak elements, and light-curve-driving radioactive ^{56}Ni. This, in turn, could perhaps produce the observed diversity in SN Ia explosion energy (see, in this context, also "pulsational delayed detonation" models, e.g. Dessart et al. 2013a).

DD models can also readily produce a range in explosion energies. Ruiter et al. (2013) find, for "violent" mergers that include detonation of small helium layers on top of the C/O WDs (Pakmor et al. 2013), that the explosion energy varies with the mass of the primary WD in the binary, and can reproduce the full observed range of SN Ia luminosities by means of primary masses between 0.9 and 1.3 $M_\odot$. Combining this with a BPS calculation, they find that the relative frequency of SN Ia luminosities can also be reproduced, if the primary WD accretes a substantial amount of helium from the companion star when it is a helium giant, prior to becoming the secondary WD. In their own violent-merger simulations, Moll et al. (2013), also reproduce the range of SN Ia luminosities and the Phillips relation through a combination of primary WD mass and viewing angle of the highly asymmetric explosion. Taubenberger et al. (2013a) analyze the late-time "nebular"-epoch spectra of several "super-Chandrasekhar" SNe Ia to estimate $\sim 2M_\odot$ of ejecta, about half of it in ^{56}Ni, which they interpret as possibly arising from the merger of two massive WDs. In nebular-phase spectra of the sub-luminous SN Ia 2010lp, Taubenberger et al. (2013b) find oxygen emission lines which, they argue, supports a violent merger scenario. In their collisional DD model, Kushnir et al. (2013) also reproduce the observed range of ^{56}Ni masses via different combinations of WD masses. The typical observed ^{56}Ni mass of $0.6M_\odot$ requires collisions of WDs of at least $0.7M_\odot$ each (see also Piro, Thompson & Kochanek 2013).

Explosion energy, colors, spectral features, and velocities: A second, potentially strong, correlation between SN Ia properties that has been claimed is between luminous energy (as measured by the light curve "stretch") and the kinematic width of iron emission features, particularly [Fe III] λ4701, in late-time, nebular-phase, spectra (Mazzali et al. 1998). Blondin et al. (2012) and Silverman, Ganeshalingam & Filippenko (2013) have argued that the relation is driven only by very under-luminous events, and no correlation remains once they are excluded. Kushnir et al. (2013), however, have re-measured the velocities in the late-time spectra by fitting broadened narrow-line templates, rather than measuring the width of individual lines. With this procedure, they recover a correlation between ^{56}Ni mass and late-time velocity width. Physically, such a correlation may simply mean that more energetic explosions produce larger ejecta velocity distributions, without particular relevance for the progenitor issue.

Other correlations that have been reported between observed SN Ia parameters tend to be rather weak trends, whose details and strengths sometimes vary among different samples.

The blueshifted velocity of the Si II λ6150 and λ6355 absorptions at maximum light, $v_{\rm Si}$, tracing the photospheric expansion velocity of the ejecta, has been crossed with various other observables. Foley & Kasen (2011) found that $v_{\rm Si}$ correlates with stretch, but that this is driven solely by the least-luminous events with $\Delta_{m15,B} > 1.5$ (where $\Delta_{m15,B}$ is the decrease in B magnitudes at 15 days after maximum light, and is inversely related to stretch). Without those events, there is no significant trend between stretch and ejecta velocity. Wang et al. (2009b), Foley & Kasen (2011) and Foley, Sanders & Kirshner (2011) do find a weak trend for events with faster ejecta to have redder intrinsic colors, and Foley (2012) finds a weak anti-correlation between $v_{\rm Si}$ and host-galaxy mass. Maguire et al. (2012) show a weak trend of increasing near-UV Ca II H & K absorption velocity and stretch (but Foley 2013 argue that this is an artifact). They also find a rather significant dependence on stretch of the blueshift of the "λ_2" pseudo-emission feature at 3180 Å. The "λ_2" feature is thought to arise from a spectral interval of slightly lower relative opacity in the heavily line-blanketed near-UV region (Walker et al. 2012). Wang et al. (2013) have shown that $v_{\rm Si}$ correlates with a number of environmental parameters. High-$v_{\rm Si}$ events tend to occur at relatively small normalized galactic radii, while the lower-$v_{\rm Si}$ events ($< 12,000 {\rm km\ s^{-1}}$) occur at all radii. Furthermore, the stellar surface brightness distribution at the locations of high-$v_{\rm Si}$ events is similar to that of CC SNe, suggestive of a young progenitor population, while lower-$v_{\rm Si}$ events tend to come from regions of relatively lower surface brightness. Finally, high-$v_{\rm Si}$ events tend to be in larger-diameter and more luminous galaxies (in apparent contradiction to the inverse relation with galaxy mass observed by Foley 2012). Wang et al. (2013) interpret these results in terms of two different SN Ia progenitor populations, distinguished by age and metallicity. The observed correlations are intriguing, but the conclusion may be premature, given the limited direct evidence for a dependence on age and metallicity, and given the different phenomenology that is observed regarding metallicity (Howell et al. 2009b, see above) and regarding progenitor age (see below). We note here, in passing, that Foley et al. (2012b) find a correlation between $v_{\rm Si}$ and the probability for the presence of a blueshifted absorbing Na I D system in the SN spectrum, a result to which we return in Section 3.3.8, below.

Benetti et al. (2005) have separated SNe Ia into two classes – those with "low velocity gradients" and those with "high velocity gradients" – based on the decrease with time in the velocity of the Si II λ6355 absorptions, $\dot{v}_{\rm Si}$, with the border at 70 km s^{-1} d^{-1}. Events with high velocity gradients tend to also have high velocities at maximum light (Foley, Sanders & Kirshner 2011). Maeda et al. (2010) showed, for a sample of 20 SNe Ia, that high-velocity-gradient objects, in their late nebular phase, have nebular lines of [Fe II] λ7155 and [Ni II] λ7378 that are redshifted relative to the higher-excitation line of [Fe III] λ4701, while low-velocity-gradient objects tend to have velocities that are blueshifted. Maeda et al. (2010) interpreted this result, in the context of the deflagration-to-detonation transition, by means of a combination of an off-center-ignited explosion and a viewing angle effect. In their picture, the nebular [Fe II] and [Ni II] lines come from the ashes of the initial deflagration phase, while the [Fe III] line, which requires low density and heating by ^{56}Ni decay, traces the detonation ashes. If the explosion is ignited off-center, e.g. within the WD hemisphere on the observer's side, the deflagration-ash lines will be blueshifted with respect to the detonation-ash lines. The observer will see a low velocity gradient in the photospheric lines because of the density and the velocity structure encountered by the photosphere as it moves inward. Maeda et al. (2011) and Cartier et al. (2011) both find that the nebular line shifts also correlate with the SN colors near maximum light, strengthening the same idea of a dependence of observed properties on viewing angle.

Another spectral signature in SNe Ia, that tends to appear in early-time spectra of some events, is the "high-velocity features" (e.g. Gerardy et al. 2004, Mazzali et al. 2005), absorptions in Si II λ6355 or the Ca II NIR triplet, whose velocities are higher by several thousands of km s^{-1} than those of the normal photospheric absorptions in these and other lines. The origin

of these features is unclear. Recently, Childress et al. (2014) have studied them in a sample of 58 SNe. They find that the existence and strength of high-velocity features correlates with SN Ia stretch, and anti-correlates with $v_{\rm Si}$. In a subset of SNe with weak high-velocity features, stretch and $v_{\rm Si}$ are correlated.

SN stretch/luminosity and host-galaxy age/star-formation rate: A correlation between peak SN Ia luminosity, or light-curve stretch, and the age of the host galaxy has been noted for some time: the oldest hosts, with little star formation, tend to host faint, low-stretch, SNe Ia, while star-forming galaxies are more likely to host bright-and-slow SNe Ia (e.g. Hamuy et al. 2000, Hicken et al. 2009, Howell et al. 2009a, Lampeitl et al. 2010, Pan et al. 2013, Smith et al. 2012, Xavier et al. 2013). Rigault et al. (2013) have shown this trend at the local level in SN Ia host galaxies, using local Hα surface brightness as a star-formation tracer. While all of these studies see the same general trend, the scatter in the relation is large, and the various samples give different pictures of how the trend arises. For example, in Hamuy et al. (2000), the trend is driven both by a lack of bright SNe in early-type galaxies, and a lack of faint SNe in late-type galaxies. In Howell et al. (2009a), galaxies with luminosity-weighted ages $\lesssim 4$ Gyr are seen to host SNe Ia of all explosion energies, but galaxies with ages $\gtrsim 4$ Gyr host almost only faint SNe Ia. Conversely, in Hicken et al. (2009) and Smith et al. (2012), early-type galaxies host the full range of light-curve widths, but late-type galaxies host only SNe Ia with broad light-curve shapes. This situation likely arises from a combination of effects. First, the trend, as noted, has a large scatter to start with. Second, different samples may have different selection effects that could bias for or against the inclusion of more or less luminous SNe Ia hosted by different types of galaxies. This can become an issue particularly when SN samples are small, such that regions of the age-luminosity plane that have low SN rates are sparsely populated. The appearance of these scatter plots is likely affected by the different ways of defining light-curve parameters (this is evident from comparing the plot in Hicken et al. (2009), that uses the x_1 light-curve stretch parameter, with their plot that uses the Δ light-curve-width parameter), or by the surrogates used for the explosion energies (as in Howell et al. 2009a). Similarly, there are different ways of defining galaxy morphological type, or of considering a galaxy "age", which is a poorly-defined concept (galaxies have composite populations, and their full star-formation histories are the more relevant observable). Finally, galaxies are characterized by multiple correlations between morphology, age, size, metallicity, star-formation rate, extinction, and more (e.g., Mannucci et al. 2010), and it is not clear what is the main driver of the correlation with SN Ia luminosity. We revisit this issue when discussing SN Ia rates and the delay-time distributions for SNe Ia of different stretches, in Section 3.5, below. In the meantime, we note that this trend between explosion energy and host-population youth could well be an important clue to the progenitor question.

Synopsis of correlations: From all of the above, there are relations among the observed properties of SNe Ia, and one can try to sketch a rough trend of properties that go together (see e.g. Maguire et al. 2013). At one extreme are events that are luminous, have broad light curves, red intrinsic colors, high-velocity ejecta, large velocity gradients, redshifted and broad nebular lines, no carbon signatures, and star-forming hosts. At the other extreme are events with the opposite properties. We further discuss the possible source of such a trend in Section 4, below.

Peculiar SNe Ia: Apart from the diversity among normal SNe Ia, there is a growing "zoo" of abnormal events that may nonetheless belong to the SN Ia class, though with varying degrees of certainty. The numbers of known peculiar SNe Ia have grown as a result of recent untargeted field transient surveys with large SN number yields, fainter flux limits, and faster cadences than previous surveys. Their pecularities could shed light on the progenitor question if, e.g., the pecularities can be identified with some particular progenitor channels or with specific deviations from the progenitor parameters of normal events.

Of particular recent interest is the class of explosions, sometimes called "SNe Iax" (e.g. Foley et al. 2013), that are similar to the prototype event SN 2002cx. Although spectroscopically similar to normal SNe Ia, SNe Iax are characterized by low photospheric velocities at maximum light, of 2000-8000 km s^{-1}, hot photospheres, based on the presence of high-ionization lines, and peak luminosities that are typically several magnitudes faint for the observed light-curve width. Their light curves lack the "second IR bump"of normal events. At late times, instead of the nebular-phase broad forbidden lines seen in normal SNe Ia, the spectrum shows narrow permitted lines, indicating a high gas density, $n_e > 10^9$ cm^{-3}, even over a year after explosion (e.g. McCully et al. 2013). Their spectra always show carbon features, and sometimes helium. Only a few tens of SNe Iax are known, but accounting for their detectability, Foley et al. (2013) estimate that there are $\sim 20-50$ such events for every 100 normal SNe Ia, which would make SNe Iax the most common type of peculiar SNe Ia.

Jordan et al. (2012), Kromer et al. (2013) and Fink et al. (2013) have modeled SNe Iax as "failed deflagrations" – SN Ia explosions in which a transition from deflagration to detonation fails to occur, and furthermore the explosion fails to completely unbind the WD, leaving behind a ~ 1 $M_\odot$ bound remnant. This could explain the low ^{56}Ni yields, the low velocities, the unburnt carbon and helium in the ejecta, the high degree of mixing, and the clumps of high-density material. On the other hand, SNe Iax occur predominantly in star-forming galaxies (but there is one case, SN2008ge, occurring in a S0 galaxy, with no signs of star formation or pre-explosion massive stars at the explosion site, Foley et al. 2010b), and their locations within these galaxies track the star-formation rate similarly to the common Type-IIP CC-SNe (Lyman et al. 2013). Indeed, Valenti et al. (2009) have argued that SNe Iax are actually CC-SNe with low ejecta velocities, derived from $7-9$ $M_\odot$ or $25-30$ $M_\odot$ progenitors, with cores collapsing into black holes. On the other hand, Foley et al. (2010a) have pointed to the presence of sulfur in the spectra of some SNe Iax, as evidence for thermonuclear burning in a C/O WD, and against a CC-SN. It thus remains to be seen whether or not SNe Iax are the manifestations of incomplete pure deflagrations of $M_{\rm Ch}$ WDs.

3.3.5 Polarization and symmetry Polarization can reveal deviations from circular symmetry of a source, as projected on the sky. In the context of SNe, linear polarization arises from electron and line scattering of photons emerging from an asymmetric source. The percentage of total flux that is polarized is proportional to the projected geometrical axis ratio, and the angle of polarization shows the asymmetry's orientation on the sky. The bandpass dependence of continuum polarization, and the polarization across individual line profiles, can provide further information on asymmetry and orientation for specific emitting elements and velocities, and can show how they change with time as a SN evolves. Wang & Wheeler (2008) have reviewed spectropolarimetry of SNe, including SNe Ia. Spectropolarimetry can guide the SN Ia progenitor problem, since most SN Ia models have some built-in asymmetry, such as the presence of a donor or an accretion disk, a recently merged or collided secondary WD, rotational flattening, or an off-center ignition (e.g. Röpke et al. 2012).

As summarized by Wang & Wheeler (2008), SNe Ia tend to have low or zero continuum polarizations, typically fractions of a percent, and polarization is generally detected only pre- or near maximum light. This indicates that the expanding photospheres are slightly asymmetric on the outside, at levels of up to of order 10%, but quite round in the inner layers of the explosion. On the other hand, line polarizations of up to a few percent are sometimes seen in some line transitions, sometimes with different orientations than those of the continuum. While, again, line polarization tends to be seen at early times, there are exceptions (e.g. Zelaya et al. 2013). The line polarizations have been interpreted in terms of clumpy distributions of the ejecta of particular elements (Hole, Kasen & Nordsieck 2010; Kasen et al. 2003; Kasen, Röpke & Woosley 2009). Smith et al. (2011) have presented spectropolarimetry of the nearby

SN 2011fe. Like its other properties, its polarization behavior is typical of normal SNe Ia.

Wang, Baade & Patat (2007) have shown a correlation between Si II λ6355 polarization and Δm_{15}, suggesting that more luminous SNe Ia tend to be more symmetric, but this relation is driven by one or two objects, after excluding some outliers. Tanaka et al. (2010) have extended this result to the case of the proposed super-$M_{\rm Ch}$ event SN 2009dc. Although this SN's line polarization is somewhat above that expected from the Wang, Baade & Patat (2007) trend, the low continuum polarization argues for little asphericity. Tanaka et al. (2010) use this to argue against the explanation by Hillebrandt, Sim & Röpke (2007) that this was an off-center $M_{\rm Ch}$ explosion, and in favor of a super-$M_{\rm Ch}$ progenitor. However, asymmetry would be expected also from a super-$M_{\rm Ch}$ rotation-supported configuration. In the normal SNe 2012fr and 2011fe, Maund et al. (2013) and Soker, Garcia-Berro & Althaus (2013), respectively, have used the very low continuum polarization level ($< 0.1\%$), and the implied circular symmetry, to argue against the violent DD-merger scenario (Pakmor et al. 2012), in which an asymmetric ^{56}Ni distribution is predicted. At the other extreme of the same trend, Howell et al. (2001) and Patat et al. (2012) have used spectropolarimetry to deduce significant, co-aligned asphericity in both lines and continuum in the sub-luminous SNe Ia 199by and 2005ke, respectively, supporting fast rotation or a merger origin in these cases.

Leonard et al. (2005), Wang et al. (2006), and Patat et al. (2009) show that high Si II λ6355 line polarizations and line velocities are correlated. Maund et al. (2010) find, for a sample of normal SNe Ia, that the polarization of the Si II λ6355 line at 5 days pre-maximum is correlated with the line velocity's time gradient $\dot{v}_{\rm Si}$ for a given SN. They suggest that normal SNe Ia have a single, asymmetric distribution of intermediate mass elements, with the diversity of observed properties arising partly from orientations effects.

At the two extremes in trends in SN Ia properties, discussed in Section 3.3.4, above, it is not clear in which "family" fall SNe Ia with relatively high polarization. Based on Maund et al. (2010) it would be in the high-velocity, high-stretch family. Based on Wang, Baade & Patat (2007), it would be in the opposite family.

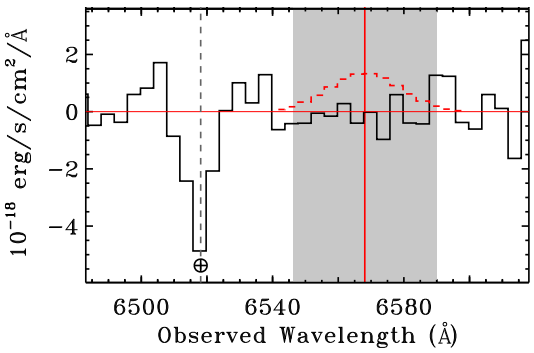

Figure 3: Nebular-phase (day 274 after maximum) Hα region of the spectrum of SN 2011fe, showing upper limits on Hα emission from any hydrogen stripped from a companion and entrained in the ejecta. The vertical red line and gray band show, respectively, the expected wavelength of Hα emission and $\pm$1000 km s^{-1} velocity width. Black solid histogram is the observed continuum-subtracted spectrum and red dashed curve is the 3σ upper limit on line emission, which implies a hydrogen mass $< 0.001 M_\odot$. Reproduced from Shappee et al. (2013).

3.3.6 Searches for emission from hydrogen In the SD scenario, almost by definition, some signs of hydrogen or helium from the non-degenerate companion should be visible at some point. Apart from the shock from the ejecta impacting a SD companion (Sec-

tion 3.3.2, above), the ejecta are expected to strip and entrain material from the companion. This stripped material, of mass $\sim 0.1 - 0.2\ M_\odot$, which is excited by energy from the radioactive decay of ^{56}Co, is then expected to become visible in the form of emission lines of width ~ 1000 km s^{-1} during the nebular phase of the explosion, when the ejecta are optically thin (Liu et al. 2012b; Marietta, Burrows & Fryxell 2000; Mattila et al. 2005). Mattila et al. (2005), Leonard (2007), and Lundqvist et al. (2013) have used high signal-to-noise nebular spectra of five SNe Ia to set upper limits on the presence of any Hα emission. These limits translate to upper limits on hydrogen mass of 0.01 to 0.03 $M_\odot$. The most stringent application of this test has been, yet again, in the case of the nearby SN 2011fe, where Shappee et al. (2013) set a limit of 0.001 $M_\odot$ on the stripped hydrogen mass (see Figure 3) These results strongly suggest that, at least in the six cases examined, there was no main-sequence or red-giant SD companion in the system at the time of explosion.

While the absence of H and He is a defining characteristic of SNe Ia, there are exceptions. Until recently, H and He in emission was reported in only two SNe Ia: SN 2002ic (Hamuy et al. 2003) and SN 2005gj (Aldering et al. 2006, Prieto et al. 2007). These events displayed a SN-Ia-like spectrum, but topped by strong variable Hα line emission, visible during most epochs, and reminiscent of a core-collapse Type-IIn spectrum. The spectra were interpreted as showing the interaction of the SN ejecta with the circumstellar medium (CSM) of an evolved SD companion (Han & Podsiadlowski 2006, Wood-Vasey & Sokoloski 2006). Another possibility that was raised was a prompt DD merger that encountered a recently ejected common envelope (Livio & Riess 2003). Chugai & Yungelson (2004) speculated that such events are examples of "SNe 1.5" (Iben & Renzini 1983), i.e. thermonuclear runaways in the CO cores of single AGB stars that have not yet lost their envelopes. Alternatively, they proposed that such "strongly CSM-interacting" SNe Ia are SD systems in which the donor is a massive red supergiant. In either case, the CSM envelope has a mass of at least several $M_\odot$. Some doubts were initially raised as to whether these rare events were, in fact, true SNe Ia. Benetti et al. (2006) argued that these explosions are actually a subclass of Type-Ic core-collapse SNe, in which the ejecta are encountering the collapsed star's previously ejected envelope, in a variant of what is thought to be the case for Type IIn SNe. Trundle et al. (2008) pointed out the resemblance of the absorption features in such events to those of the class of "luminous blue variables", which are thought to be the progenitors of type Ib/c SNe.

The most recent and well-studied object of this type is PTF11kx (Dilday et al. 2012, Silverman et al. 2013a), further discussed below (Section 3.3.8) in the context also of SNe Ia that have intervening Na I D absorption. In PTF11kx, the Hα emission is somewhat weaker and develops somewhat later than in the above two cases of CSM-interacting SNe Ia, and the light curve is more similar to those of normal SNe Ia. From analysis of the evolving spectra, Dilday et al. (2012) deduce the progenitor was a SD system with a red-giant donor and multiple shells of equatorially distributed circumstellar material, swept up by ejecta from pre-explosion nova eruptions, similar to those in the symbiotic recurrent nova RS Ophiuchi, in which a WD accretes through a wind from a red giant (see Section 3.1.1, above). Soker et al. (2013), however, have estimated that the circumstellar mass in PTF11kx is at least $\sim 0.1 - 0.6\ M_\odot$, which is higher than the CSM expected in SD models. Instead, they advocate a variant of the Livio & Riess (2003) picture (ejecta from a DD merger encountering the previously ejected common envelope). In the context of the Soker (2013) core-degenerate scenario, they propose that during the common envelope phase, the WD disrupts and accretes the less-dense AGB core (rather than vice versa), resulting in a prompt (rather than long-delayed) explosion.

Silverman et al. (2013b) have compiled a sample of 16 such strongly CSM-interacting events, some by re-classifying old events (one of them, SN 2008J, was concurrently studied by Taddia et al. 2012) and some from new discoveries from the PTF survey. They show that such events tend to have higher peak luminosities and slower light-curve evolution than normal SNe Ia,

and that their hosts are always galaxies with ongoing star formation. Dilday et al. (2012) estimate that the fraction of strongly CSM-interacting SNe Ia among all SNe Ia could be 0.1% (based on the discovery rate in the PTF survey) to 1% (based on the SDSS-II survey), but potentially higher, if cases with weaker H signatures have been overlooked, or if some cases with stronger signatures have been misclassified as type-IIn SNe.

For the two prototype CSM-interacting cases, SN 2002ic and SN 2005gj, late-time (2.2–3.8 yr and 0.4–1.4 yr post-explosion, respectively) mid-IR *Spitzer* photometry analyzed by Fox & Filippenko (2013) shows variable emission by warm (500-800 K) dust at these late times. In the case of SN 2005gj, the dust luminosity increases monotonically by a factor ~ 2 over the observed period. The inferred dust masses are of order $M_{\rm d} \sim 10^{-2} M_{\odot}$, at distances of $r \sim 10^{17}$ cm. It is unclear if this is newly formed dust condensing in the SN ejecta, pre-existing CSM dust that is being heated by UV and X-ray radiation from CSM interaction (see Section 3.3.7), or light echoes by dust that is far from, and unrelated to a CSM (Patat 2005, see Section 3.3.9). In any event, similar late-time IR emission, implying similar dust parameters, is seen in many Type-IIn SNe studied by Fox et al. (2013).

Thus, in several respects, CSM-interacting SNe Ia bear a strong resemblance to Type-IIn SNe, in which ejecta impact a large mass of CSM, of order 1 $M_{\odot}$, thus converting kinetic energy to optical-band energy that accrues significantly to the radioactively powered part of the light curve. This suggests that CSM-interacting SNe Ia are a rare subclass in which the ejecta interact with the CSM of a relatively massive star, rather than the CSM of a donor star in a traditional SD scenario. The presence of a massive star would explain why all such events identified to date have occurred in star-forming galaxies (Silverman et al. 2013b).

Returning to SN 2002cx-like events ("SNe Iax", see Section 3.3.4, above), Liu et al. (2013a) predict that if such events are indeed failed pure deflagrations in $M_{\rm Ch}$ SD systems, the low kinetic energy of the explosion means that only small amounts of HI, $\lesssim 0.01$ $M_{\odot}$, are expected to be seen in the nebular-phase spectra of such objects.

3.3.7 Radio and X-ray emission from CSM interactions Interaction of SN ejecta with a pre-explosion CSM or ISM is expected to produce radio synchrotron emission, from shock-accelerated electrons in an amplified magnetic field, and X-ray emission through inverse Compton upscattering, by those electrons, of the optical emission of the SN. The CSM could be from previous mass loss from a donor star, or from losses from the accretion flow onto the WD. The physics and signatures of such interaction have been computed by Chevalier (1982, 1998) and Chevalier & Fransson (2006); see Chomiuk et al. (2012b) and Margutti et al. (2012), for recent generalizations. Briefly, mass conservation dictates that a CSM produced by a constant pre-explosion mass-loss rate, $\dot{M}$, driving a wind of constant velocity, v_w, will have a radial density profile $\rho_{\rm csm}(r) = (\dot{M}/4\pi v_w)\ r^{-2}$. As the SN shock advances through the CSM with speed v_s, it accelerates particles to relativistic energies, and amplifies the ambient magnetic field. From the post-shock energy density, $\rho_{\rm csm} v_s^2$, the fractions in relativistic electrons and in magnetic fields are usually parametrized as ϵ_e and ϵ_B, respectively. Post-shock, the electrons assume a power-law energy distribution, $N(E) \propto E^{-p}$, above a minimum energy $E_{\rm min}$ which, in turn, depends on p, v_s, and ϵ_e.

The electrons gyrate along magnetic field lines, emitting a synchrotron spectrum with specific luminosity $L_\nu \propto \nu^{5/2}$, shaped by synchrotron self-absorption, up to a frequency, ν_S (generally in cm-wave radio bands), and an optically thin synchrotron spectrum, $L_\nu \propto \nu^{-(p-1)/2}$, at higher frequencies. As the shock advances through progressively less-dense gas, the peak emission shifts to lower frequencies. Measurements at a fixed frequency will therefore first see an intensity rising with time, t, when that frequency is in the self-absorbed part of the spectrum, up to a maximum, followed by a declining signal when observing at optically thin frequencies. In those Type Ib/c SNe in which synchrotron emission has been detected, the

electron energy distribution has an index $p \approx 3$, producing an optically-thin synchrotron power-law index of ≈ -1 (Chevalier & Fransson 2006, Soderberg et al. 2012). For these SNe, $\epsilon_e \approx 0.1$, and ϵ_B values in the range 0.01 to 0.1 have been inferred. The shock velocity, v_s, which is set by the density profiles of the CSM and of the ejecta, has a weak time dependence. In broad terms, the optically thin synchrotron luminosity then behaves as

$$L_\nu \propto v_s^3 \; E_{\rm min} \; \nu^{-1} \; t^{-1} \; \epsilon_e \; \epsilon_B \; \dot{M}^2 \; v_w^{-2}. \tag{1}$$

Given an estimate of v_s, a radio measurement of L_ν (or an upper limit on it) can therefore constrain the product $\epsilon_e \epsilon_B \dot{M}^2 / v_w^2$. A value of $\epsilon_e = 0.1$ is generally assumed. Values of ϵ_B, as noted, span one order of magnitude, and stellar wind velocities, v_w, are generally in the range of tens to a few hundred km s^{-1}. Thus some useful information can be derived regarding the interesting parameter $\dot{M}$. In the case of a uniform ISM ($\rho_{\rm csm}(r) = $ const.), L_ν grows slowly with time roughly as $t^{0.35}$ (Chomiuk et al. 2012b) and the observations will constrain the product $\rho_{\rm csm} \; \epsilon_B^{0.9}$.

In X-rays, the inverse-Compton emission for an electron population with $p = 3$ is

$$L_\nu \propto v_s \; E_{\rm min} \; \nu^{-1} \; t^{-1} \; \epsilon_e \; \dot{M} \; v_w^{-1} \; L_{\rm SN}(t), \tag{2}$$

where $L_{\rm SN}(t)$ is the bolometric optical-UV luminosity from the SN photosphere (Chevalier & Fransson 2006, Horesh et al. 2012, Margutti et al. 2012). The inverse-Compton emission, in contrast to the synchrotron emission, does not depend on the uncertain ϵ_B parameter. In the case of a shock expanding into a constant-density ISM, rather than a CSM, the ratio of the inverse-Compton luminosity to the optical-UV luminosity is roughly constant with time.

No radio or X-ray emission from a SN Ia has ever been detected. In X-rays, Hughes et al. (2007) set upper limits on flux from four SNe Ia, including two strongly CSM-interacting cases, SN2002ic, and SN2005gj (see Section 3.3.6, above). Russell & Immler (2012) set X-ray flux upper limits on 53 individual SNe Ia, and on their stacked images, and concluded that winds from evolved donor stars can be excluded. In the radio, Panagia et al. (2006) obtained VLA observations at wavelengths of 0.7 to 20 cm of 27 nearby SNe Ia at 46 epochs, roughly $\sim 10 - 100$ d after explosion, and used them to set limits on CSM interaction in each case. Hancock, Gaensler & Murphy (2011) performed a stacking analysis of these data, to obtain deeper limits. Assuming typical values for the other parameters involved, they set a limit of $\dot{M} \lesssim 10^{-7} \; M_\odot$ yr^{-1}. In radio, for SN 2006X, which showed variable Na I D lines (see Section 3.3.8, below), VLA non-detection constrains any CSM at $r \sim 10^{17}$ cm to arise from a wind with $\dot{M} \lesssim 3 \times 10^{-7} \; M_\odot$ yr^{-1}, assuming $v_w = 100$ km s^{-1} (Patat et al. 2007). This suggests a limit on the mass in the region of $M \lesssim \dot{M} \; r \; / \; v_w = 10^{-4} \; M_\odot$.

In the case of the nearby and well-studied SN 2011fe, Horesh et al. (2012) obtained radio data from 0.3 to 20 cm, using the CARMA, EVLA, and WSRT telescopes, as early as 1.3 d after the explosion time deduced by Nugent et al. (2011) (see Section 3.3.1, above). *Swift* and *Chandra* observations were secured at 1.2 d and 4 d, respectively. Comparing the upper limits on radio and X-ray flux to the expected light curves, Horesh et al. (2012) set a limit of $\dot{M} \lesssim 10^{-8} \; M_\odot$ yr^{-1}, assuming $v_s = 4 \times 10^4$ km s^{-1}, $v_w = 100$ km s^{-1}, $\epsilon_e = 0.1$, and also assuming $\epsilon_B = 0.1$ in the radio case. This excludes the presence of a circumstellar wind from a giant donor. Margutti et al. (2012) used additional *Swift* and *Chandra* epochs, including stacks of epochs that are not far from maximum optical light (which corresponds also to inverse-Compton X-ray maximum light) to obtain deeper and later-time X-ray limits. They use them to refine the mass-loss limit to $\dot{M} \lesssim 2 \times 10^{-9} \; M_\odot$ yr^{-1}. These stronger limits are used to argue, beyond giant donors, also against any stable hydrogen-burning Roche-lobe overflow scenario (i.e. with $\dot{M} > 3 \times 10^{-7} \; M_\odot$ yr^{-1}; see Section 3.1.2) in which more than 1% of the accreted material is lost, e.g. through the outer Lagrange points (i.e. other than L1).

A uniform-density CSM is constrained by Margutti et al. (2012) to have a particle density < 150 cm^{-3}. These constraints are shown in Figure 4. Finally, deeper limits have been set also in the radio by Chomiuk et al. (2012b), using additional EVLA epochs between 2 and 19 days past explosion, mostly about 5 times deeper than those of Horesh et al. (2012). Using also a higher assumed $v_s = 0.35c$, they interpret their radio flux limits as a stringent limit on CSM mass loss, $\dot{M} \lesssim 6 \times 10^{-10}\ M_\odot$ yr^{-1}, during the last 100–1000 yr leading up to the explosion. With this limit, a 1% mass loss through outer Lagrange points can be excluded even for recurrent novae, unless the wind speed v_w is particularly high, with a correspondingly rarified CSM. A uniform ISM density $n_{\rm ism} \gtrsim 6$ cm^{-1} can be excluded (for $\epsilon_B = 0.1$), or $n_{\rm ism} \gtrsim 44$ cm^{-1} can be excluded (for $\epsilon_B = 0.01$), at radii $r \sim 10^{15} - 10^{16}$ cm from the explosion. Figure 5 shows these limits. We note that all of the above limits are slightly weakened if the explosion was in fact earlier than deduced by Nugent et al. (2011), by $\sim 0.5 - 1.5$ d (Mazzali et al. 2013, Piro & Nakar 2012; see Section 3.3.1, above).

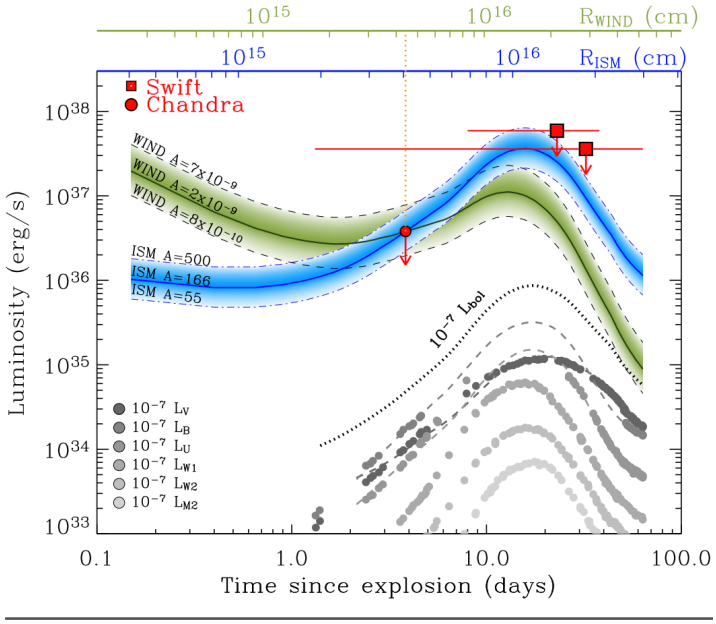

Figure 4: X-ray 3σ upper limits (points) from *Swift* and *Chandra* on the luminosity of SN 2011fe, compared to the expected X-ray evolution from inverse Comptonization of the UV-optical light curve (shown by gray filled circles for the various UV-optical bands, and with a black dotted line for the estimated bolometric light curve.) Green band is for comptonization by a CSM wind, with $\dot{M}$ values as marked in units of $M_\odot$ yr^{-1}, for a wind speed of 100 km s^{-1}. Blue band is for comptonization by a uniform-density ISM, with densities in units of cm^{-3}, as marked. The data constrain the progenitor system's mass loss through a wind to $\dot{M} \lesssim 2 \times 10^{-9}\ M_\odot$ yr^{-1}, and a uniform-density CSM to have $\lesssim 150$ cm^{-3}. Reproduced from Margutti et al. (2012).

In summary, sensitive X-ray and radio observations of a good number of SNe Ia have so far failed to detect a CSM, including in several SNe Ia that show ejecta-CSM interactions and variable Na I D absorptions. The limits make giant SD donors unlikely. For SN 2011fe, these data show a particularly "clean" environment around a SN Ia, and argue against most of the traditional SD scenarios.

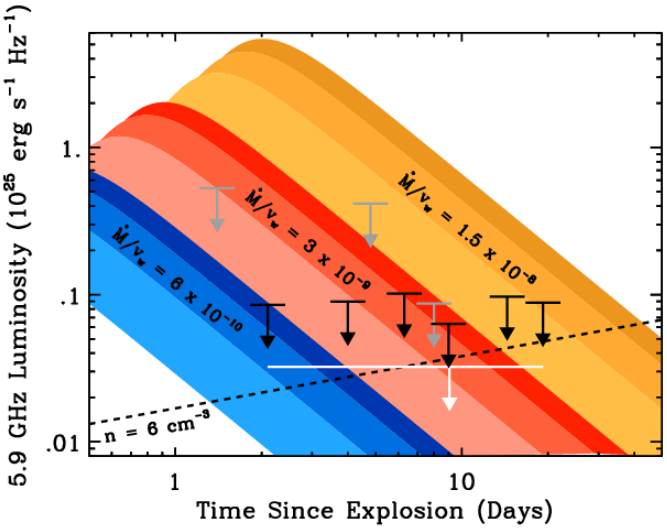

Figure 5: EVLA 3σ upper limits (black arrows) on the 5.9 GHz radio luminosity of SN 2011fe, compared to expectations from synchrotron emission due to interaction of its ejecta with a CSM. Also shown (gray arrows) are upper limits from Horesh et al. (2012), scaled to 5.9 GHz, and a time-stacked limit (white arrow). Colored swaths are the light curves expected from interaction with a wind, for the marked values of $M_\odot$ yr$^{-1}/v$, in units of $M_\odot$ yr^{-1}/100 km s^{-1}, with shades corresponding to ϵ_B in the range $0.01 - 0.1$, and $\epsilon_e = 0.1$. The dashed black line is the expected evolution for a uniform-density ISM of density $n = 6$ cm^{-3}. The mass loss limit of $\dot{M} \lesssim 6 \times 10^{-10}\ M_\odot$ yr^{-1} argues against any Roche-lobe-overflow SD scenario with $\gtrsim 1\%$ mass loss in the system. Reproduced from Chomiuk et al. (2012b).

3.3.8 Intervening absorption In the SD scenario, SN Ia spectra may be expected to show variable narrow blueshifted absorption lines from a circumstellar wind from the companion, from accretion overflows, or from pre-explosion nova-like outbursts (e.g. Patat et al. 2007). As detailed below, absorptions interpreted as such signatures have been detected in a few SNe Ia. For the DD scenario, in turn, as already discussed in Section 3.3.2 above, DD merger simulations differ on the amount and radius of merger-related debris at the time of explosion. Furthermore, Shen, Guillochon & Foley (2013) have simulated a CSM that is shaped prior to DD mergers that involve a CO primary WD and a He WD secondary (a combination raised in the context of sub-Chandrasekhar, or double-detonation, DD models, e.g. Pakmor et al. 2013, Shen & Bildsten 2013). A thin hydrogen layer, expected on the He WD's surface, accretes onto the CO WD and leads to nova-like eruptions on timescales of $\sim 10^2 - 10^3$ yr prior to the SN Ia explosion. In the ISM densities present in spiral galaxies, these pre-SN-Ia eruptions can shape the CSM so as to produce circumstellar absorptions, similar to SD model expectations and to those sometimes observed in SNe Ia. Raskin & Kasen (2013) likewise use simulations to show that, under some circumstances, tidal debris from DD mergers could produce observable absorptions in SN Ia spectra.

In terms of the observations, variable, blue-shifted ($\sim 10 - 100$ km s^{-1}) absorption in the Na I D doublet ($\lambda\lambda 5890, 5896$) has been detected in the high-resolution, multi-epoch spectra of three SNe Ia (SN 2006X, Patat et al. 2007; SN 2007le, Simon et al. 2009; and the CSM-interacting case PTF11kx, Dilday et al. 2012, see Section 3.3.6, above). In the case of PTF11kx, the absorption is also seen in narrow lines of Fe II, Ti II, and He I. A fourth variable Na I D case was found in low-resolution, but high-signal-to-noise, spectra of SN 1999cl

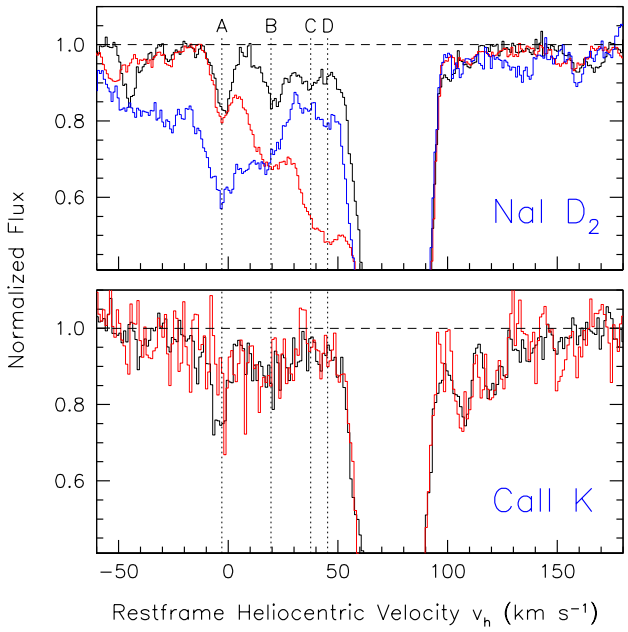

Figure 6: Spectra of SN 2006X, showing time evolution of the Na I D_2 absorption feature (top panel) between days −2 (black), +14 (red), and +61 (blue). Individual variable absorption components are labeled A-D. For comparison, the non-variable absorptions in the Ca II K line (bottom panel, only first two epochs) are also shown. The growing absorption strength is thought to be due to recombining Na II ions in a CSM, ionized earlier by UV photons from the explosion. The strongly saturated Na I and Ca II absorptions come from unrelated interstellar gas clouds in the disk of the host galaxy. ¿From Patat et al. (2007).

by Blondin et al. (2009). Because of the low resolution, in this case one cannot determine whether the absorption is blueshifted or otherwise. However, Blondin et al. (2009) noted that absorption variations of the observed magnitude exist for only two out of 31 SNe Ia with data that could have revealed them (SN 1999cl, and SN 2006X, whose variations Blondin et al. could "rediscover" at low resolution). Sternberg et al. (2013) give statistics for the detection of variable Na I D at high spectral resolution, of 3/17 (or 2/16, if excluding the unusual PTF11kx). In all four known cases, the Na I D absorption generally grows in strength on a timescale of about 10 d. In the three high-resolution cases, it is seen that the growth is in individual blueshifted velocity components, and that the absorption in the Ca II H&K lines ($\lambda\lambda 3968, 3933$) does not change in strength during the same period. Figure 6 shows SN 2006X, as an example. At least three of the cases of SNe Ia with time-variable NaI D absorption belong to the subclass of SNe Ia with "high velocity gradients" (Benetti et al. 2005) (see Section 3.3.4, above). In all four cases the hosts are late-type spirals.

Using order-of-magnitude arguments (Patat et al. 2007) and detailed photoionization mod-

eling (Simon et al. 2009), the growing Na I D absorption has been interpreted as due to recombining Na II ions in circumstellar material of density $n_{\rm csm} \sim 10^7$ cm^{-1}, at distances of $r \sim 10^{16} - 10^{17}$ cm from the explosion, with a total mass of 10^{-5} to 10^{-2} $M_\odot$. Estimates of the UV spectrum and light curve of a SN Ia, based on model templates and extrapolations of the few SNe Ia with UV data, suggest that the SN flux can ionize Na I atoms (ionization potential 5.1 eV) out to such distances, but not Ca II ions (ionization potential 11.9 eV) for which the required ionizing photons are orders of magnitude rarer in the SN spectrum. The short recombination timescale of 10 d further requires a high electron density, which implies a significant hydrogen ionization fraction, and hence limits the distance to the absorbing clouds. In SN 2006X, part of the Na I D absorption actually weakens again 2 months after maximum light, which Patat et al. (2007) interpret as the SN ejecta reaching and reionizing some components of the CSM (the corresponding weakening expected also in the Ca II absorption, due to such a process, could not be tested at that epoch because of low signal-to-noise ratio).

The absorbing gas may be a clumpy wind from a red-giant donor, or an equatorial outflow from pre-explosion recurrent nova eruptions during the decades preceding the SN Ia explosion. The asymmetric nature of such outflows could introduce a viewing angle dependence that would explain the apparent rarity of SNe Ia with variable Na I D. An alternative explanation, invoking variable line-of-sight absorption by ISM material far from the SN (Chugai 2008), explains the non-variability of the Ca II lines through abundance effects, by means of differing fractions of Ca and Na locked in dust grains in intervening clouds. Patat et al. (2011) have noted the similarities of these variable absorptions with post-outburst features in the recurrent nova RS Ophiuchi (see Section 3.1.1, above). On the other hand, U Sco did not show any variable absorption during its outburst in 2010 (Kafka & Williams 2011). In the well-studied normal SN Ia 2011fe, despite the high signal-to-noise of the available spectra, Patat et al. (2013) find no evidence for variable intervening absorption that could be associated with the CSM of the progenitor system.

Sternberg et al. (2011) compared the incidence of narrow blueshifted and redshifted Na I D absorptions in the single-epoch high-resolution spectra of 35 SNe Ia. They assigned a zero velocity to the strongest Na I D absorption, associating it with the host galaxy's ISM, and then identified additional absorption lines. They found 12 cases with blueshifted absorptions, 5 with redshifted absorption, 5 with either single or symmetric blue/red Na I D absorption, and 13 cases with no detected Na I D absorption (most of them in early-type galaxies). Sternberg et al. (2011) interpreted the 12-over-5 excess of blueshifted vs. redshifted absorptions as signatures of the CSM, and concluded that $> 20 - 25\%$ of SNe Ia in spirals derive from SD progenitors (although, as noted, such absorptions may also arise in a DD scenario; Shen, Guillochon & Foley 2013).

Foley et al. (2012b) have analyzed a somewhat-modified sample of 23 SNe Ia with high-resolution spectra, finding 10 cases with blueshifts and 5 with redshifts. They further find an association between ejecta velocity, as measured by Si II λ6355 near maximum, and the presence of blueshifted Na I D; SNe Ia with ejecta velocities $v_{\rm Si} \gtrsim 12,000$ km^{-1} s^{-1} are more likely to display blueshifted Na I D absorption. Foley et al. (2012b) point out that the run of ejecta velocities and their possible association with the presence of a CSM outflow suggest asymmetric progenitors and explosions, such that higher velocity ejecta are aligned with higher density CSM. Alternatively, the result could imply a variety of progenitor systems, such that progenitors with denser or closer CSMs tend to produce more energetic explosions. However, as already discussed, explosion energy and host galaxy type are correlated, which could provide an indirect link between explosion energy and ISM (rather than CSM) absorption.

Maguire et al. (2013) have re-analyzed spectra for 16 of the Sternberg et al. (2011) events, together with new data for 16 additional SN Ia, while defining differently the zero absorption velocity. In this combined sample, the excess of blueshifted over redshifted Na I D absorptions

is 11 versus 4, again suggesting $\sim 20\%$ CSM-related absorption. Maguire et al. (2013) confirm the tendency for $v_{\rm Si} \gtrsim 12,000$ km^{-1} s^{-1} to have blueshifted Na I D, and also find a correlation between $B-V$ color at maximum and the equivalent width of the Na I D absorption (see also Förster et al. 2013).

Phillips et al. (2013) have studied a sample of 32 SNe Ia at high spectral resolution. They find that a quarter of the objects show anomalously large Na I D absorption, relative to the dust extinction implied by the SN colors. The same extinction is indicated by the SN colors and by the diffuse interstellar band at 5780 Å, suggesting that the dust, despite its usual low values of R_V, is in the host's ISM, rather than in the CSM of the progenitor. However, all of the objects with excess Na I-absorption have Na I D blueshifts, hinting that the Na is indeed in the CSM, which was perhaps pre-enriched with this element (Phillips et al. 2013 outline several scenarios for this). On the other hand, three SNe Ia in their sample having variable Na I D, and which are therefore strong candidates for having a CSM, do not show unusually strong Na I D lines.

3.3.9 Circumstellar dust and light echoes Spectra of light echoing off interstellar dust clouds has permitted spectacular classification of several historical Galactic SNe, centuries after their explosions, including two SNe Ia, SNR 0509-67.5 (Rest et al. 2008a) and Tycho's SN (Krause et al. 2008, Rest et al. 2008b). In principle, however, monitoring of SN light echoes at much earlier times, whether by spatially resolving the echo or by inferring its integrated effect on spectra and light curves, can provide a three-dimensional mapping of the CSM and the ISM around the SN (Patat 2005, Patat et al. 2006; see Rest, Sinnott & Welch 2012 for a review). To date, there have been only four clear detections of SN Ia light echoes: SN 1991T (Schmidt et al. 1994, Sparks et al. 1999); SN 1998bu (Cappellaro et al. 2001, Garnavich et al. 2001); SN 1995E (Quinn et al. 2006); and SN 2006X (Crotts & Yourdon 2008, Wang et al. 2008). In each of these cases, the optical light curve's decline flattened abruptly after a few hundred days, and the late-time spectra showed features from earlier phases. The late-time spectra could be modeled well as luminosity weighted averages of the past spectral evolution of the SNe. Finally, HST imaging showed the actual resolved light-echo rings expanding around the SN site. In several of these cases, polarimetry provided further constraints on the scattering geometry. Modeling of these data showed, in all cases, that the scattering dust is at distances of a few tens to a few hundred pc, generally in front of the SNe. Wang et al. (2008) raised the possibility that there exists an additional inner circumstellar echo component, but analysis of the same data by Crotts & Yourdon (2008) argues against this option. The presently known cases of light echoes most likely probe dusty regions far from the event, with no direct bearing on the progenitor problem.

As noted above (Section 3.3.6), signatures of possibly circumstellar dust have been seen in several CSM-interacting SNe Ia (Fox & Filippenko 2013). In three normal SNe Ia (including SN 2011fe), Johansson, Amanullah & Goobar (2013) have used *Herschel* far-IR non-detections to set upper limits on the circumstellar dust mass, of $\lesssim 10^{-2} - 10^{-1} M_{\odot}$.

3.4 Post-explosion evidence in SN remnants

3.4.1 Searches for surviving companions The donor star, in a SD scenario, will survive the explosion, and is likely to be identifiable by virtue of its anomalous velocity, rotation, composition, temperature, or luminosity (e.g., Canal, Méndez & Ruiz-Lapuente 2001; Liu et al. 2013b; Marietta, Burrows & Fryxell 2000; Pan, Ricker & Taam 2013; Ruiz-Lapuente 1997; Shappee, Kochanek & Stanek 2013; Wang, Li & Han 2010).

Searches for a surviving donor star in Tycho's SN of 1572 (as noted, a SN Ia confirmed with a light echo spectrum, Krause et al. 2008, Rest et al. 2008b), based on chemical abundances, radial velocities, proper motions, and rotation velocities, have not been able to reach a con-

sensus (Fuhrmann 2005, González Hernández et al. 2009, Ihara et al. 2007, Kerzendorf et al. 2009, Ruiz-Lapuente et al. 2004). The individual studies have pointed out distinct preferred candidates and argued against those of the other studies. Most recently, Kerzendorf et al. (2012), based on Keck spectra and on proper motions from HST imaging, have concluded that there are no good candidates for SD survivors of any type (giant, sub-giant, or main-sequence) in this remnant. Conversely, based largely on the same data, Bedin et al. (2013) continue to advocate a star labeled Tycho-G as the likely surviving SD-scenario donor star. While the two groups broadly agree regarding the measured abundances, proper motion, and radial velocity of Tycho-G, they differ regarding the degree that these parameters are unusual or indicative of a donor-star origin for the star.

SN 1006 is widely considered a likely SN Ia, based on its 500 pc height above the Galactic plane, its symmetry, and the absence of a neutron star (Stephenson & Green 2002). However, the total iron mass in its remnant is apparently very low for a SN Ia, $\sim 0.06\ M_\odot$, based on X-ray emission lines of Fe-L (Vink et al. 2003) and Fe-K (Yamaguchi et al. 2008), and based on UV and optical absorption lines of cold Fe II along multiple lines of sight to background sources (Winkler et al. 2005, Wu et al. 1993). On the other hand, the strong X-ray emission seen in Si, S, Ar, C, and O, seems consistent with expectations from the layered outer parts of a dynamically young SN Ia remnant, in which the reverse shock has yet to reach and heat the inner, iron-rich, regions (Badenes et al. 2007). Those regions might nonetheless be photoionized by the X-ray emission from the reverse shock (Hamilton & Sarazin 1984), and hence invisible to the UV-optical low-ionization-Fe absorption studies. Be that as it may, Kerzendorf et al. (2013b) and González Hernández et al. (2012), for this SN remnant, agree on the absence of any apparent surviving companions with luminosities greater than $L_V \sim 0.5\ L_{\odot,V}$. Thus, if SN1006 was a SN Ia, all evolved SD donors are ruled out. Normal main-sequence donors are still allowed, unless their luminosities are significantly increased by the interaction with the ejecta, as predicted by the models for the post-explosion appearance of donor stars, cited above.

SNR 0509-67.5 in the Large Magellanic Cloud (LMC) is the remnant of an over-luminous SN Ia from *circa* 1600 (Badenes et al. 2008), confirmed as such with a light-echo spectrum by Rest et al. (2008a). Fortuitously, the remnant is far from the center of the LMC, in a region with low stellar density, and it has been imaged to great depth with HST. Schaefer & Pagnotta (2012) have shown (Figure 7) that there are no stars, down to V-band luminosities as low as $L_V = 0.04 L_{\odot,V}$, in the area around the remnant's geometrical center that could be populated by a runaway donor star. This luminosity corresponds to late-K-type main sequence stars of mass $\sim 0.5 M_\odot$, and essentially rules out all traditional SD companions. Some diffuse emission seen in the center of the remnant is an unrelated background galaxy (Pagnotta, Walker, & Schaefer, in prep.).

Another LMC remnant, SNR 0519-67.5, is projected on a denser stellar region, and therefore provides weaker limits on a surviving companion. A light echo found by Rest et al. (2005) indicates an explosion that is 600 ± 200 years old, and Rest, Sinnott & Welch (2012) indicate that the echo's spectrum confirms a SN Ia classification (but the spectrum is still unpublished). In this case, Edwards, Pagnotta & Schaefer (2012) again using HST imaging, are able to rule out the presence of surviving post-main-sequence donor stars, but 27 main-sequence stars, that are close enough to the explosion center, cannot be excluded as surviving companions. However, as already noted, the interaction with the ejecta would likely brighten such stars significantly, and hence the main sequence donor option is also in doubt.

Kepler's SN of 1604 is thought to have been a SN Ia, but this has not been established beyond doubt (see further discussion in Section 3.4.2, below). Kerzendorf et al. (2013a) have obtained spectroscopy for the 24 stars with $L > 10 L_\odot$ in the central 38 arcsec of the remnant, none of which show any signatures expected of a former donor star. There are also no potential

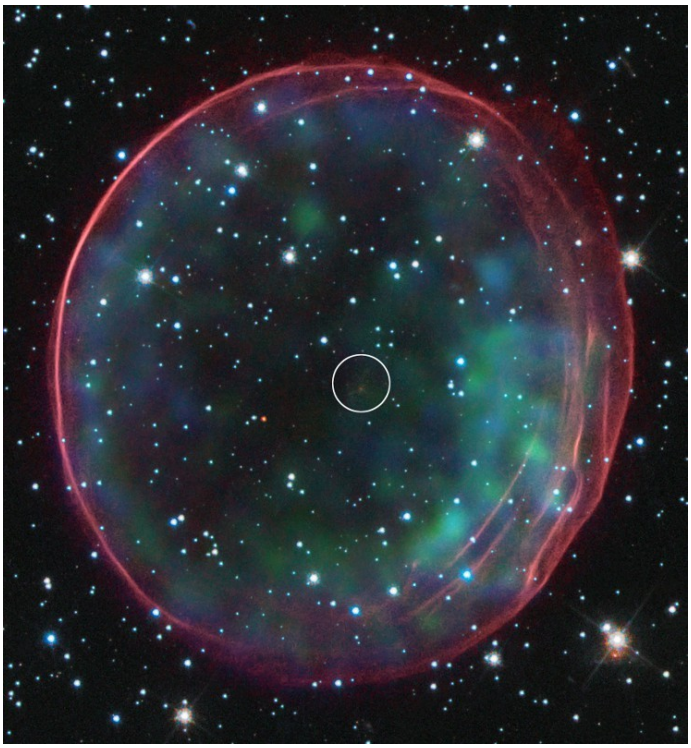

Figure 7: Composite HST/*Chandra* image, in B, V, I, Hα, and X-rays, of the $\sim$ 400-year-old SN Ia remnant 0509-67.5 in the LMC. The central 1.4-arcsec radius circle is the 3σ-confidence region that could host a surviving donor star, considering uncertainties in the geometrical center and in the remnant age, and assuming the maximum plausible proper motion. As argued by Schaefer & Pagnotta (2012), the non-detection of any potential surviving stars within this region, down to $L_V = 0.04\ L_{\odot,V}$, essentially rules out the possibility of a surviving SD companion. Credit: NASA/ESA/Hubble Heritage Team (STScI/AURA).

red giant, AGB (as has been proposed from hydrodynamical models, see below), or post-AGB surviving donor stars in this region.

The SD scenario can perhaps circumvent the above constraints via the spin-up/spin-down ideas (Di Stefano, Voss & Claeys 2011; Hachisu, Kato & Nomoto 2012; Justham 2011; see Section 2.4), if the delay between the end of accretion and the explosion is long enough for the donor star to evolve to a dim, undetectable, WD itself. However, as discussed above in Sections 2 and 3.1.6, the viability of fast WD rotation in general, and differential rotation in particular, faces theoretical and observational challenges.

3.4.2 Searches for CSM interaction in remnants Another approach to search for clues of the progenitor systems in SN remnants is through hydrodynamical models for specific remnants, thought to have been SN Ia events. The modeling elements in such analyses have included combinations of a pre-explosion environment, possibly shaped by outflows from the system, evolution of the temperature, density, and ionization of the ejecta and the CSM, and attempts to reproduce, the observed geometry, dynamics, and X-ray spectrum of a remnant (e.g., Badenes et al. 2006, 2008; Kosenko, Blinnikov & Vink 2011; Kosenko et al. 2008; Patnaude et al. 2012; Sorokina et al. 2004; see Vink 2012 for a recent review).

Badenes et al. (2007) have modeled the X-ray emission in seven young SN Ia remnants to test for the presence of large ($3 - 30$ pc) wind-blown cavities in the ISM, with densities $n_{\rm csm} \lesssim 10^{-3}$ cm^{-3}, centered on the explosion sites. They show that such swept-out cavities

are expected in the context of the optically thick, $\sim$ 1000 km s^{-1}, outflows from rapidly accreting WDs in the wind-regulated accretion picture (Hachisu, Kato & Nomoto 1996, see Section 3.1.3). In all of the seven cases examined, the observations do not support this scenario. In fact, Badenes et al. (2007) find that line fluxes and energy centroids in the X-ray spectra, and the observed radii of the forward shocks, at the known ages of the remnants, are always as expected for ejecta advancing through a uniform-density ISM of $n_{\rm csm} \approx 1$ cm^{-3}. The fast pre-explosion outflows, leading to rarified CSMs, would have resulted in larger forward-shock radii and weaker lines, by factors of a few. This result shows that, if these SNe had SD progenitors, the growth of the WDs proceeded in some way other than wind-regulated accretion, or that such growth ceased long before the explosion, as in spin-up/spin-down models. A CSM with a $\rho \propto r^{-2}$ radial density profile is expected from any constant-velocity outflow, fast or slow, be it from an evolved donor star or from the accreting WD itself. Badenes et al. (2007) found that such density profiles also gave poor correspondence with the data, but only a limited range of these $\rho \propto r^{-2}$ models was studied. Support for a uniform-density CSM comes also from modeling by Raymond et al. (2007) of the Hα filaments in the remnant of SN 1006, as seen in HST imaging. They conclude that $n_{\rm csm} \approx 0.25-0.4$ cm^{-3}, with variations of only $\sim 20\%$ on pc scales.

An exception to the absence of cavities in SN Ia remnants could be RCW 86, a proposed remnant for the SN of 185 C.E. (Vink et al. 2006), possibly a SN Ia, based on the large observed mass of Fe and the absence of a neutron star. Vink, Kaastra & Bleeker (1997), Badenes et al. (2007), and most recently Williams et al. (2011) do find evidence for a 12-pc-radius central cavity in this case. On the other hand, this remnant, which is in an OB association, has traditionally been considered a CC SN (e.g. Ghavamian et al. 2001).

Among potential SN Ia remnants, the remnant of Kepler's SN of 1604 has been studied perhaps in the most detail, but has also led to some confusing results. It was once thought to have been a CC SN, based on the asymmetrically bright, dense, and nitrogen-rich shell of material in the remnant's northern side. More recently, however, it is generally assumed to have been a SN Ia, based on its high altitude above the Galactic plane (at least 350 pc, but possibly $>$ 800 pc, given persistent incompatible estimates of its distance, see Patnaude et al. 2012), its high iron and low oxygen content, and the lack of a detected neutron star (Reynolds et al. 2007). Chiotellis, Schure & Vink (2012) modeled the remnant assuming a SN Ia explosion in a SD configuration with an AGB-star donor of initial mass $4-5$ $M_\odot$. The binary system likely had a high velocity of 250 km s^{-1} away from the Galactic disk (Borkowski, Sarazin & Blondin 1994), a velocity which may be difficult to explain for a runaway binary (Vink 2012). In this picture, the northern shell arises from the forward shock encountering a pre-explosion CSM of mass ~ 1 $M_\odot$, with the CSM previously shaped by its movement through the ISM at the said high velocity (Borkowski, Blondin & Sarazin 1992; Vink 2008). Burkey et al. (2013) find further evidence for an AGB progenitor by using *Spitzer* 24 μm data to distinguish shocked CSM from shocked ejecta emission. They identify an equatorial CSM component that they associate with an edge-on disk-like outflow from an AGB donor.

However, as noted in Section 3.4.1, above, there is no surviving AGB star in the remnant within the central 38$''$ (Kerzendorf et al. 2013a). A post-AGB star or young WD that is only a few hundred years old would have a luminosity of $\sim 10^4$ $L_\odot$ (Bloecker 1995), but the brightest star, even within a conservative 60 arcsec radius of the geometrical center, has a V-band luminosity of only 330 $L_\odot$ (Kerzendorf et al. 2013a). Furthermore, Patnaude et al. (2012), modeling the south side of the remnant, report that a simple $\rho \propto r^{-2}$ wind-shaped CSM, as favored by Chiotellis, Schure & Vink (2012), cannot simultaneously fit the observed dynamics and the X-ray spectrum. To fit all the data, Patnaude et al. (2012) find that a 0.1 pc low-density central cavity needs to be included in the CSM model. Alternatively, a model that also works is one with no wind-shaped CSM at all, but rather with a remnant

that expands into a more-or-less uniform-density ISM. A north-south gradient in this ISM (a gradient which has some support from direct 160 μm emission maps of the region by Blair et al. 2007) could explain the northern bow shock. Each of these solutions (small central cavity or uniform ISM) corresponds to a different and incompatible distance to the object, which in turn implies a sub-energetic or super-energetic SN Ia event (if, indeed, Kepler's SN was a SN Ia). With its multiple puzzles and contradictions, Kepler's SN remnant probably does not illuminate much the SN Ia progenitor issue at this point in time, but it could if its type and distance became known.

Borkowski, Hendrick & Reynolds (2006) have modeled two remnants in the Large Magellanic Cloud with strong Fe-L line emission in their interiors, which they conclude requires a large interior density, as would be expected from a slow pre-explosion wind. While distinct from the fast accretion-driven winds of the Hachisu, Kato & Nomoto (1996) scenario, this result may be considered as evidence for the presence of pre-explosion SD companions. On the other hand, without good X-ray spectra and well-determined ages, the typing of these two remnants as SNe Ia is not secure.

Another interesting constraint comes from the existence of "Balmer-dominated shocks" primarily in remnants thought to be of SN Ia origin (see Vink 2012). Optical spectra of such regions show pure Balmer-line emission with a narrow core and a broad base. The narrow emission is understood to arise by collisional excitation, by electrons and protons, of cold neutral hydrogen just being overrun by the forward shock. The broad component is due to hot post-shock protons, that undergo charge transfer with atoms, to become hydrogen atoms at excited levels, or subsequent collisional excitation of those hydrogen atoms (Chevalier, Kirshner & Raymond 1980; Heng 2010). Core-collapse remnants generally do not show Balmer-dominated shocks, which is reasonable given that their SN explosions are bright in the UV and therefore can photoionize a large surrounding region. Conversely, Ghavamian et al. (2003) have pointed out that the existence of Balmer-dominated shocks, and hence neutral hydrogen, at radii of < 30 pc in SN Ia remnants (and often below 5 or 10 pc, see Vink 2012) limits the pre-explosion photoionizing flux of the progenitors during the $t \sim 10^5/n$ years prior to the explosion (corresponding to the recombination time at ambient densities of $n/(1\ \mathrm{cm}^{-3})$. Supersoft X-rays sources in particular, with their UV/X-ray luminosities of up to $\sim 10^{38}$ erg s^{-1}, would have carved out ionized Stromgren spheres of radius ~ 30 pc around the remnants (Rappaport et al. 1994), in conflict with the observed Balmer-dominated emission at smaller radii.

3.5 SN Ia rates and the delay-time distribution

SN Ia rates and their dependence on environment and on cosmic time can provide further clues to the progenitor problem. In essence, finding the dependence of the SN rate on the age distribution of the host stellar population can reveal the age distribution of the actual SN Ia progenitors. Different progenitor scenarios involve different timescales that control the production rate of SN Ia events, and will thus predict different SN Ia age distributions. For a detailed review on surveying for SNe for rate purposes, the derivation of SN Ia rates, and their application to the progenitor question, see Maoz & Mannucci (2012).

A fundamental function for progenitor-question purposes is the distribution of times between star formation and SN Ia explosion, usually called the delay-time distribution (DTD). The DTD is the hypothetical SN rate versus time that would follow a brief burst of star formation, with the burst having one unit of total mass in formed stars. It is the "impulse response" that embodies the physical information of the system, free of nuisances – in the present context – the diverse star-formation histories (SFHs) of the galaxies hosting the SNe. Determining the DTD observationally has increasingly become the objective of SN Ia rate

measurements.

3.5.1 THEORETICAL EXPECTATIONS As noted in Section 2, theoretical forms for the DTD can be derived from binary population synthesis (BPS) calculations, obtained by numerically evolving simulated populations of binaries with chosen distributions of initial parameters, or alternatively by following analytic approximations (e.g. Greggio 2005). The DTDs for each progenitor channel can be compared to observationally derived DTDs.

The DD model naturally gives rise to a broad range of delay times (Yungelson & Livio 2000). With some simplifying assumptions, this DTD form can be seen to result from the strong dependence of the merger time on the post-common-envelope separation of the WD pair (Greggio 2005, Totani et al. 2008). Suppose the post-common-envelope separation, a, is distributed as a power law, $dN/da \propto a^{\alpha}$, over the range of separations that will merge over a Hubble time. Suppose further that the time until merger depends on the separation to some power, $t \propto a^{\gamma}$. Then the form of the DTD will be given by $dN/dt \propto t^{\beta}$ with $\beta = -1 + (\alpha + 1)/\gamma$. For the angular momentum loss due to gravitational waves, $\gamma = 4$. The post-common-envelope distribution of WD separations is generally found by BPS simulations to be similar in form to the input distribution of main-sequence binaries, which is about flat in log separation, i.e., a power law with $\alpha \approx -1$ (Toonen, Nelemans & Portegies Zwart 2012; Yungelson 2013). A $\sim t^{-1}$ DTD is thus expected even if the separation distribution is not exactly flat in log a, as long as the value of γ is sufficiently large. The "collisional DD" model of Katz & Dong (2012) (see Section 2.3), with $\gamma = 5/2$ would give a similar DTD.

The $\sim t^{-1}$ DTD behavior breaks down at short delays. A "bottleneck" in the process is the production rate of WDs that can serve as SN Ia progenitors. The production rate is zero for at least $30 - 40$ Myr, until main sequence stars with masses below $\sim$8 $M_{\odot}$ evolve into the first WDs to emerge from the stellar population. The WD production rate then rises to a maximum, and falls as $\sim t^{-1/2}$ (e.g. Pritchet, Howell & Sullivan 2008), up to a cutoff time, t_c, corresponding to the main-sequence lifetime of the least massive stars whose descendant WDs contribute to a DD-channel SN Ia. Since this main-sequence mass is usually considered to be $2 - 3$ $M_{\odot}$, t_c is generally ~ 1 Gyr. The DTD will be the convolution of the WD production rate and the merger rate dependences, resulting in a broken power law, t^{β}, with indices $\beta \sim -1/2$ at $t < t_c$ and $\beta \sim -1$ at $t > t_c$. More realistically, the supply of WDs that will eventually merge is more complex, given that two WDs are required, and that the time until they are "ready" to evolve solely via gravitational decay depends on the initial binary parameters of their progenitors, which determine the ensuing interactions among the pair. BPS simulations indeed show a complex behavior (that varies among models, according to the different physical recipes assumed), for the pre-t_c DTD shape. However, as expected, the DD models generally do show the generic t^{-1} behavior after ~ 1 Gyr. This can be seen in Fig. 8, which includes a compilation by Nelemans, Toonen & Bours (2013) of some recent BPS theoretical DTDs for the DD channel.

For the standard SD model, the defining property is that the accretion rate onto the WD needs to be in a rather narrow range, near $\dot{M} \sim 3 \times 10^{-7}$ $M_{\odot}$ yr^{-1} (see Section 2, above). Such a rate is realized only by main-sequence, or slightly evolved sub-giant, donor stars that can transfer of the order of 1 $M_{\odot}$ to the WD on a thermal (i.e. Kelvin-Helmholtz) timescale, $t_{\rm th}$, of the donor star (van den Heuvel et al. 1992). A donor star, upon losing mass, will contract adiabatically on a dynamical timescale. Thermal equilibrium is regained on a thermal timescale, causing re-expansion and a renewed mass supply on that timescale (e.g. Pols & Marinus 1994). The accretion rate is thus

$$\dot{M} \sim \frac{1\ M_{\odot}}{t_{\rm th}} \sim \frac{1\ M_{\odot}}{GM^2/RL} \sim 3 \times 10^{-7} M_{\odot}\ {\rm yr}^{-1} \left(\frac{M}{2\ M_{\odot}}\right)^3 , \quad (3)$$

assuming that stellar main-sequence radius scales with mass, as $R \propto M$, and luminosity as

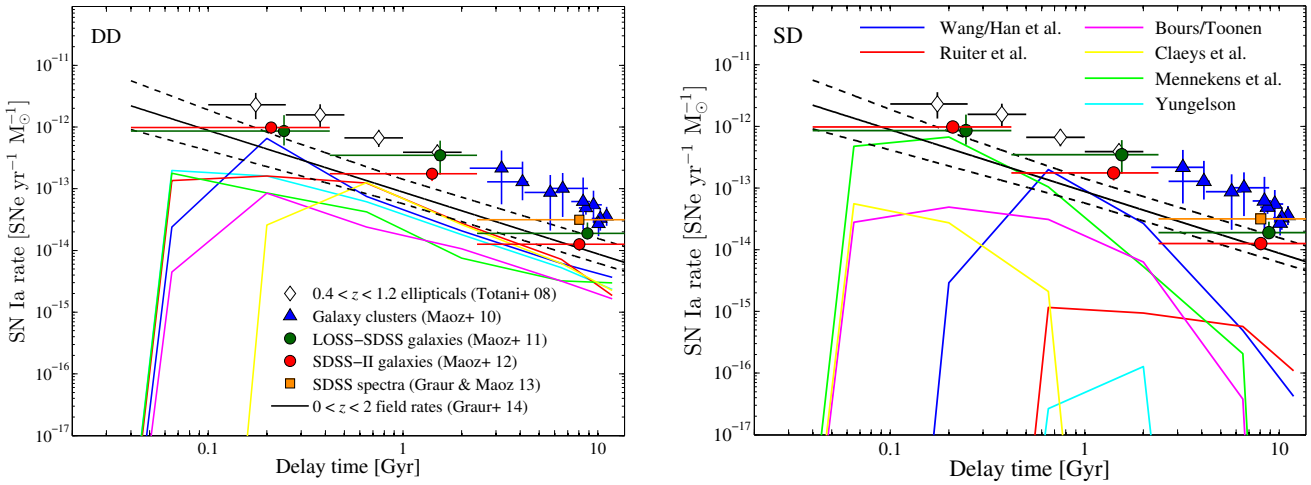

Figure 8: Observed versus theoretical delay-time distributions. In both panels, points and the straight black lines are some of the observationally derived DTDs discussed here. Colored curves are theoretical DTDs adapted from the compilation of BPS predictions for DD models (left panel) and for SD models (right panel) by Nelemans, Toonen & Bours (2013), who adjusted all models to have the same physical input parameters. All DTDs, observed and theoretical, are shown with a consistently assumed definition (SNe per year per formed stellar mass) and a consistent IMF. The Toonen, Nelemans & Portegies Zwart (2012) curve shown here corrects a misprint in the plot shown in Nelemans, Toonen & Bours (2013).

$L \propto M^4$. There is therefore a limited range of donor masses, 2−3 M$_\odot$, that can supply material at the rate required for stable hydrogen burning on the WD surface. This is confirmed by detailed calculations (e.g. Han & Podsiadlowski 2004, Langer et al. 2000). Since these systems explode during, or shortly after, the main sequence, in many models the DTD is concentrated between a few-hundred Myr and 1–2 Gyr, dropping off sharply before and after (Yungelson 2005). Fig. 8 illustrates this for a set of BPS theoretical DTDs for the SD channel.

Similar exponential cutoffs are seen in analytic approximations of SD model DTDs (e.g., Greggio 2005). A limiting factor of such predictions is that the binary evolution calculations involve many uncertain assumptions, and therefore the theoretical DTD predictions vary among different groups. This is apparent, in Fig. 8, in particular for the SD channel.

Hachisu, Kato & Nomoto (1996) have suggested that an optically thick wind, driven from the accreting WD, can stabilize the mass transfer in binaries where a low-mass giant fills its Roche lobe. The long evolutionary time of the low-mass donor can produce a SD model with long delay times. Hachisu, Kato & Nomoto (2008b) have proposed that this same optically thick wind can strip mass from donors in the traditional main-sequence model, and thereby raise the mass range for donor stars up to 8 M$_\odot$, thereby extending the SD model also to short delay times. Studies using these extended parameter ranges to calculate the DTD based on BPS (Bours, Toonen & Nelemans 2013; Meng & Yang 2010; Mennekens et al. 2010; Wang, Li & Han 2010) have typically found DTDs that are indeed broader and (depending on how massive the donors that are allowed) extend to short delay times, but find very few systems with giant donors. The reason is that the required period range for such systems, of a few hundreds of days, is sparsely populated in BPS models by post-common-envelope binaries (see Yungelson & Livio 2000). There are known examples of symbiotic binaries (e.g. T CrB, RS Oph) and post-AGB-star binaries (see van Winckel et al. 2009) observed in that period

range, but their statistical fraction is unclear. Hachisu, Kato & Nomoto (1999) have proposed that many wide systems can evolve into this period range by interaction of the binary with the slow wind of the giant, although the efficiency of this process is debated. Combining all of these effects, Hachisu, Kato & Nomoto (2008a) have suggested that a combination of SD main-sequence and red-giant channels could together give a $\sim t^{-1}$-shaped DTD.

The helium SD channel is expected to contribute at short delay times ($\lesssim 10^8$yr), due to the fact that the helium donors evolve from rather massive main-sequence stars with little delay (and the WDs need to have formed even earlier, e.g. Wang et al. 2009a).

3.5.2 Observed DTD from SN rates vs. color and Hubble type The first observational indications for the existence of a range of SN Ia delay times (i.e. a DTD) was found by Mannucci et al. (2005) and Mannucci, Della Valle & Panagia (2006) who, analyzing a local SN sample (Cappellaro, Evans & Turatto 1999), demonstrated that the SN Ia rate per unit stellar mass changes with host-galaxy color and Hubble type – parameters that trace the star-formation rate (SFR). Nonetheless, early-type galaxies with no current star formation were seen to have a non-zero SN Ia rate (as was already well known). A similar SN Ia rate dependence on host color and specific SFR was found by Sullivan et al. (2006) for the Supernova Legacy Survey (SNLS) sample of SNe Ia, and more recently by Li et al. (2011b) for the Lick Observatory SN survey (LOSS) sample (Leaman et al. 2011, Li et al. 2011c), , and by Smith et al. (2012) for the SDSS-II SN sample (Frieman et al. 2008, Sako et al. 2008).

Early interpretations of these results argued for the co-existence of two SN Ia populations: a "prompt" population, with rates proportional to the CC SN rates (Mannucci et al. 2005) or to the star-formation rate (Sullivan et al. 2006), that explodes within $\sim 100-500$ Myr; and a delayed channel, proportional to the stellar mass, that produces SNe Ia on timescales of order 5 Gyr. In the similar "$A+B$" formulation (Scannapieco & Bildsten 2005), the SN Ia rate in a galaxy is proportional to the stellar mass (through the A parameter) and to the galaxy's star-formation rate (through B). In retrospect, however, the "prompt-plus-delayed" interpretation is, in essence, a DTD with two coarse time bins, and these two "channels" appear to represent the two sides of a broad DTD. More quantitative information on the DTD can be obtained by comparing the rates with the stellar age distribution of each galaxy type, and indicates that, indeed, to reproduce the SN rate vs. host-color relations, a broad DTD is required, with delays below 0.5 Gyr to trace the SFR, and an extended tail to $\gtrsim 5$ Gyr delay times, to produce SNe Ia in galaxies with low current SFR. Mannucci, Della Valle & Panagia (2006) and Mannucci (2008) showed this using several SD models, while Maoz & Mannucci (2012) showed that a $\sim t^{-1}$ DTD can do so as well. While The '$A+B$' parametrization is still sometimes used to analyze SN Ia rates, it is a poor physical metric. For example, the A component depends on the mean stellar age of the monitored population, with younger stellar systems producing more SNe for any declining DTD.

3.5.3 DTD from rates in galaxy clusters and in field ellipticals Measuring the SN rate in galaxy clusters as a function of redshift is probably the most direct way to recover the DTD. Optical spectroscopy and multiwavelength photometry of cluster galaxies has shown that most of their stars were formed within short episodes (~ 100 Myr) at high redshift ($z \sim 3$; Jimenez et al. 2007, Rettura et al. 2011), a good approximation to the δ-function burst defining the DTD. Thus, an almost-direct measurement of the DTD is provided by the observed SN Ia rate per unit stellar mass in galaxy clusters, as a function of the time since the cluster's star-formation epoch (i.e. the cosmic epoch at the observed cluster redshift minus the stellar formation epoch). Cluster SN Ia rates have been measured over the past decade in the redshift range $0 < z < 1.5$, corresponding to DTD delays of $2-10$ Gyr (Barbary et al. 2012; Dawson et al. 2009; Dilday et al. 2010a; Gal-Yam et al. 2008; Gal-Yam, Maoz & Sharon 2002; Germany et al. 2004; Graham et al. 2008; Mannucci et al. 2008; Maoz &

Gal-Yam 2004; Maoz, Sharon & Gal-Yam 2010; Sand et al. 2012, 2008; Sharon et al. 2007). These measurements are still limited by significant Poisson errors due to small SN numbers.

Maoz, Sharon & Gal-Yam (2010) derive a DTD based on most of these galaxy-cluster SN Ia rate measurements, which is shown in Figure 8. They find consistency with a $\sim t^{-1}$ form at $t > 2$ Gyr, and show that the $\sim t^{-1}$ conclusion is not critically dependent on uncertainties in the input parameters involved, such as the precise redshift of star formation in clusters, whether it was a brief or extended burst, or the contribution of ongoing low-level star formation in clusters, as long as these are at the levels, redshifts, and cluster locations allowed by direct measurements of star-formation tracers in clusters.

A related approach to DTD recovery was taken by Totani et al. (2008), using field elliptical galaxies instead of galaxy clusters. Comparing SN Ia rates in early-type galaxies of different luminosity-weighted ages, seen at $z = 0.4 - 1.2$ as part of the Subaru/XMM-Newton Deep Survey, they were the first to show observationally that the DTD is consistent with a t^{-1} form. This observed DTD is also shown in Fig. 8. Like the elliptical galaxies in clusters, field ellipticals are dominated by old stellar populations created in a short burst at early times, allowing for a direct derivation of the DTD. However, in general, the concept of a "typical age" for a host galaxy, interpreted as a SN Ia progenitor age, is a risky zeroeth-order approximation to the full SFH of a galaxy (see Mannucci 2009 and Maoz & Mannucci 2012). The SN rate of a galaxy with a wide distribution of ages is likely to be dominated by the youngest stellar population, even when those young stars are present only at low levels that may escape detection (Mannucci 2008). As opposed to ellipticals in the central regions of clusters, which appear to be very quiescent, non-cluster ellipticals often host non-negligible amounts of late-time star formation (e.g. Zhu, Blanton & Moustakas 2010).

In a possible instance of this, Della Valle et al. (2005) found that radio-loud early-type galaxies have higher SN Ia rates than otherwise-similar radio-quiet galaxies. A possible confirmation of the effect was found by Graham et al. (2010). Mannucci, Della Valle & Panagia (2006) proposed that quiescent early-type galaxies sometimes acquire new gas in a minor merger, and that this material leads to both radio activity (through accretion onto the central black hole) and star formation which, in turn, produces prompt SNe Ia. Greggio, Renzini & Daddi (2008) have pointed to the absence of the expected CC-SNe in the same radio galaxies, or in early-type galaxies in general (e.g., Hakobyan et al. 2008.) On the other hand, CC SNe have been found in some early-type galaxies showing clear signs of ongoing star formation, based on UV data (Suh et al. 2011). The observed rate trend in radio galaxies still lacks confirmation and, furthermore, the constraints on the DTD would be quite model-dependent, while other explanations have also been proposed (Capetti 2002; Livio, Riess & Sparks 2002).

Other applications of the "rate vs. age" approach have been made by Aubourg et al. (2008); Cooper, Newman & Yan (2009); Raskin et al. (2009); Schawinski (2009) and Thomson & Chary (2011). They confirm the wide distribution of delays and, in particular, the existence of "prompt" SNe Ia, though with a wide range defining the age of that population. Uncertainties are again dominated by assumptions regarding the parent stellar populations.

3.5.4 DTD FROM IRON ABUNDANCES IN GALAXY CLUSTERS Constraints on the DTD can also come from considering element abundances in galaxy clusters. As reviewed in Maoz, Sharon & Gal-Yam (2010), X-ray observations of the intracluster medium (ICM) and optical observations of the stellar populations determine the ratio of iron-to-stellar masses. As iron is a main product of SN Ia explosions (with a mean of $\sim 0.7 M_{\odot}$ per event), and nothing escapes the deep cluster potential, this ratio sets the time-integrated number of SNe Ia in clusters, per formed stellar mass (after estimating and subtracting the iron contributions by CC SNe). This integral constraint, minus an integral over the DTD at delays $t > 2$ Gyr from direct cluster rate measurements, can provide an indirect estimate of the DTD at delays

$0 < t < 2$ Gyr. Although the DTD value thus obtained in this early bin tends to be somewhat high, it is consistent with the $\sim t^{-1}$ form found directly from the SN Ia rates at lower redshifts. Uncertainties on the mass of the iron in the stellar and ICM components, and on the contribution of CC-SNe to iron production, propagate into this estimate (Loewenstein 2013). The combined constraint on the DTD power-law index is $\beta = -1.2 \pm 0.3$.

The time evolution of iron abundance in clusters can, in principle, also be used to measure the shape of the DTD. Calura, Matteucci & Tozzi (2007) have shown that a broad DTD that is peaked at short delays, when combined with assumptions about the winds that transfer iron from the galaxies to the ICM, can reproduce the observed evolution of iron abundance in the ICM between $z = 0.2$ and $z = 1.2$

3.5.5 DTD FROM VOLUMETRIC RATE EVOLUTION Another observational approach to recovering the DTD has been to compare the volumetric SN rate from field surveys, as a function of redshift, to the cosmic SFH. An advantage of this approach is the averaging-out, over large cosmic volumes, of the uncertainties in SN rates and SFHs based on few galaxies. Furthermore, field surveys are not biased in favor of SNe in particular types of galaxies, as opposed to galaxy-targeted surveys. On the other hand, uncertainties in the cosmic SFH have remained a limiting factor in deriving a DTD (e.g. Graur et al. 2013). As the DTD is the SN "response" to a short burst of star formation, the volumetric SN rate versus cosmic time, $R_{Ia}(t)$, will be the convolution of the DTD with the SFH (i.e. the star formation rate per unit comoving volume versus cosmic time, $\dot{\rho}(t)$),

$$R_{Ia}(t) \propto \int_0^t \dot{\rho}(t-\tau)\Psi(\tau)d\tau. \quad (4)$$

Starting with Ruiz-Lapuente & Canal (1998) and Sadat et al. (1998), the volumetric rate evolution has been compared to cosmic SFH. Numerous volumetric rate measurements, progressively more accurate and at higher-redshift, have accumulated over the past decade (see Graur et al. 2013 for a recent compilation). Early on, Dahlen, Strolger & Riess (2008); Dahlen et al. (2004); Strolger et al. (2004) and Strolger, Dahlen & Riess (2010) argued for a DTD that is peaked at a delay of ~ 3 Gyr, with little power at either shorter or longer delays. This conclusion was based on their measurements of the SN Ia rate at $z > 1$ with HST. However, this conclusion was contested based both on re-analysis of the same data (Blanc & Greggio 2008; Greggio, Renzini & Daddi 2008; Horiuchi & Beacom 2010; Kuznetsova & Connolly 2007; Mannucci, Della Valle & Panagia 2007), and on additional $z > 1$ SN Ia rates (Poznanski et al. 2007). The main problems pointed out were the small number of SNe, and hence the large statistical errors in the rates, compounded by systematic uncertainties due to the necessary assumptions regarding SFHs and dust extinction. Mannucci, Della Valle & Panagia (2006) further pointed out that such a narrow DTD does not reproduce the dependence of local SN Ia rates on galaxy colors (see Section 3.5.2, above).

Graur et al. (2011) discovered a larger sample of 37 likely SNe Ia at $1 < z < 2$ by monitoring the Subaru Deep Field. Additional new high-z SN Ia rate measurements have emerged also from the recent CLASH (Graur et al. 2013) and CANDELS (Rodney et al. 2013) surveys with HST, with the highest-redshift SNIa in the latter survey at $z = 2.15 \pm 0.1$. Several authors (Graur & Maoz 2013, Graur et al. 2011, 2013, Kistler et al. 2013, Perrett et al. 2012, Rodney et al. 2013) have analyzed some or all of these new high-z SN rate measurements, together with precise new rates at lower redshifts from SDSS-II (Dilday et al. 2010b) and SNLS (Perrett et al. 2012). They all find that a DTD with a power-law form, $\sim t^{-1}$, when convolved with a wide range of plausible SFHs, gives an excellent fit to the observed SN rates. For example, the best-fit power-law index found by Graur et al. (2013) is $\beta = -1.00 \pm 0.06$ (random error, due to the uncertainties in the SN rates), ± 0.10 (systematic error, due to the range of possible SFHs). This power law is shown in Figure 8. The precise $z < 1$ rate

measurements are particularly constraining for the DTD. Graur et al. (2013) show that the rates are incompatible with the functional forms of DTDs from SD-model BPS calculations, which have cutoffs at delays beyond several Gyrs. Rodney et al. (2013) find that, assuming the DTD is a t^{-1} power law beyond 500 Myr, 30-65% of SNe Ia must have delays shorter than 500 Myr, consistent with a t^{-1} power law that extends all the way down to 40 Myr delays.

3.5.6 DTD FROM STAR-FORMATION HISTORIES OF INDIVIDUAL GALAXIES The convolution in Eq. 4 between SFH and the DTD, giving the SN Ia rate versus time, applies not only to a cosmological volume but also to individual galaxies. Brandt et al. (2010) and Maoz et al. (2011) introduced similar methods for recovering the DTD from SN Ia samples for which the monitored galaxies have individual estimated SFHs, based on spectral synthesis. In essence, the SFH of every individual galaxy is convolved with a trial universal DTD, and the resulting current SN Ia rate is compared to the number of SNe the galaxy hosted in the survey (generally none, sometimes one, rarely more). Maoz et al. (2011) applied the method to a subsample of the galaxies in LOSS, and the SNe that they hosted with spectral-synthesis-based SFH reconstructions by Tojeiro et al. (2009), based on spectra from the SDSS. The limited time-resolution of these SFH reconstructions dictate that the recovered DTD has only three coarse time bins, with a prompt SN Ia component, that explodes within $\tau < 420$ Myr of star formation, an intermediate component, at $0.42 < \tau < 2.4$ Gyr, and a delayed component that explodes after $\tau > 2.4$ Gyr. Brandt et al. (2010) applied their method to a sample of SNe Ia from the SDSS-II survey. Maoz, Mannucci & Brandt (2012) applied the Maoz et al. (2011) algorithm to an SDSS-II sample that is larger and more complete than the Brandt et al. (2010) sample, and corrects several oversights in the previous analysis. Finally, in Graur & Maoz (2013) the method was applied to a sample of SNe Ia discovered in archival SDSS-I galaxy spectra (the galaxies happened to host a SN within the spectroscopic aperture during the observations), again using the spectral-synthesis-based SFHs of the galaxies. All of these three-time-bin DTD reconstructions give similar monotonically decreasing DTDs, consistent with $\sim t^{-1}$. For example, Maoz, Mannucci & Brandt (2012) find $\beta = -1.07 \pm 0.07$. These DTD reconstructions are included in Fig. 8.

Brandt et al. (2010) used the "stretch parameter" of the SN light curves, to divide their SN Ia sample into a "high-stretch" subsample and a "low-stretch" one, and derived the DTD for each subsample. They found that luminous, high-stretch, SNe Ia have most of their DTD signal at short delays, while low-stretch SNe Ia have a DTD that peaks in the longest-delay bin. However, this trend largely disappears in the analysis of the more-complete SDSS-II SN Ia sample by Maoz, Mannucci & Brandt (2012). Perrett et al. (2012) similarly fail to see any strong stretch dependence in their DTD analysis of volumetric SN Ia rates. While such a dependence is expected based on the observed trends between light curve stretch and mean host galaxy stellar age (see Section 3.3.4), apparently the DTD analyses still lack the precision needed to reveal it.

3.5.7 DTD, DOWNSIZING, AND THE RATE-MASS RELATION Indirect evidence for a broad DTD comes also from an observed dependence of SN Ia rate per unit mass on galaxy mass. Li et al. (2011c) first noted that the SN Ia rate per unit mass in the LOSS sample decreases for more massive galaxies of a given type. The rate-size relation has been confirmed by Smith et al. (2012) for SDSS-II SNe Ia, and by Graur & Maoz (2013) for the SNe Ia discovered in archival SDSS spectra. Kistler et al. (2013) showed that this "rate-size relation" can be explained by a combined effect of "downsizing" in galaxy formation – more massive galaxies are formed, on average, earlier and on shorter timescales (e.g. Gallazzi et al. 2005) – combined with a $\sim t^{-1}$ DTD. Downsizing produces different mean ages and therefore SNe in more massive galaxies come from the low-rate, long-delay tail of the DTD. Graur & Maoz (2013) have independently confirmed that downsizing plus a $\sim t^{-1}$ DTD explain the effect for their sample as well. Kistler

et al. (2013) investigated also the possible effect of metallicity on the rate-mass relation. Less massive galaxies have lower metallicities (Mannucci et al. 2010, Tremonti et al. 2004). Stellar evolution at low metallicity can produce more massive WDs, and the SN Ia rates could be affected if such WDs are easier to bring to $M_{\rm Ch}$ via accretion. However, for their model's assumed influence of metallicity on WD mass and SN Ia production, Kistler et al. (2013) find only a weak effect of metallicity on the rate-mass relation.

We note in passing that the rate-mass relation permits a reliable estimate of the Milky Way's SN Ia rate. For Sbc spirals of Milky Way mass ($(6.4 \pm 0.6) \times 10^{10} M_{\odot}$; McMillan 2011), the specific SN Ia rate is $(1.12 \pm 0.35) \times 10^{-13}$ yr^{-1} $M_{\odot}^{-1}$ (Li et al. 2011c), so if the Milky Way is not atypical, the Galactic SN Ia rate is $(7.2 \pm 2.3) \times 10^{-3}$ yr^{-1}. The mean time between Galactic SNe Ia is thus 100-200 yr.

3.5.8 Element abundances in stars The different timescales of production of CC SNe and SNe Ia, coupled with the different chemical yields of the two populations of SNe, produce diverse abundance ratios in galaxies having different SFHs (see Nomoto, Kobayashi & Tominaga 2013 for a review). If a galaxy forms most of its stars in a single, brief episode of star formation, the Fe-peak-element yields from most SNe Ia will not be incorporated into subsequent generations of stars, while α elements, such as O, Mg, Si, and Ca from core-collapse SNe, with their much smaller delay time, will do so. As a consequence, the distribution of [α/Fe] (typically [O/Fe] vs. [Fe/H]) is sensitive to the DTD (De Donder & Vanbeveren 2004, Matteucci 2001, Matteucci & Greggio 1986, Tinsley 1979). Matteucci et al. (2006) find that DTDs with $\sim 10 - 30\%$ of the explosions occurring at < 100 Myr, are consistent with the abundance ratios of stars in the solar neighborhood, but is it not clear if such a fraction of short delays is required by the data.

Mennekens et al. (2013) have used BPS calculations combined with a Galactic chemical evolution model to investigate which combinations of progenitor scenarios, binary evolution parameters, star-formation histories, and initial mass functions, can simultaneously match the observed DTD and the distribution of [Fe/H] in solar-neighborhood G-dwarfs. Their main conclusion is that reproducing the observed [Fe/H] distribution requires a high DTD normalization (i.e. models with efficient SN Ia production), as indicated independently by SN-Ia-rate-based DTD estimates (see Section 3.5.10, below), *and* a significant early contribution to the DTD. This can be achieved with a combination of SD and DD progenitors, with binary parameters tuned to boost their SN Ia production efficiency. Recent applications of chemical evolution modeling by Kobayashi & Nomoto (2009), Matteucci et al. (2009), and Tsujimoto & Shigeyama (2012) take the inverse approach, and use the DTD from SN Ia rate measurements to constrain chemical evolution. With improved stellar abundance data, chemical mapping could provide stronger constraints on the early-time DTD.

Seitenzahl et al. (2013a) have recently used the [Mn/Fe] abundance ratios in solar-neighborhood stars to constrain the explosion scenario directly (i.e. not via the DTD). They find that manganese is produced efficiently only in the high-density conditions of near-$M_{\rm Ch}$ SN Ia explosions – sub-$M_{\rm Ch}$ SNe Ia and CC-SNe have yields that make [Mn/Fe] ratios about 3 times below Solar. Consequently, the observed distribution of stellar [Mn/Fe] requires that roughly 50% of SNe Ia come from near-$M_{\rm Ch}$ explosions, be they from SD, DD, or other, progenitors.

3.5.9 DTD from SN remnants An unconventional observational DTD reconstruction has been carried out by Maoz & Badenes (2010), by applying the Maoz et al. (2011) algorithm to a sample of SN remnants in the Magellanic Clouds (Badenes, Maoz & Draine 2010), and treating this as an effective SN sample, one from a survey in which the SNe are detectable for ~ 10 kyr (the visibility time of a SN remnant). The advantage of this approach is that the nearness of these galaxies permits derivation of detailed and accurate stellar age distributions of the individual galactic regions that host the SNe. The stellar age distributions are found

by comparing the densities of the resolved stars in color-magnitude diagrams to model stellar isochrones (Harris & Zaritsky 2004, 2009). The small number of remnants, with the attendant large statistical errors, allows only the coarsest DTD resolution, with two SN Ia time bins. Nevertheless, Maoz & Badenes (2010) find a significant detection of a prompt (this time $35 < \tau < 330$ Myr) SN Ia component, and an upper limit on the DTD level at longer delays that is consistent with the long-delay DTD levels measured with other methods. Larger samples can be produced in the future via ongoing and proposed deep radio surveys for the SN remnant populations in additional nearby galaxies, such as M33 and M31, and by using their spatially specific stellar age distributions, again based on the resolved stellar populations.

3.5.10 Normalization of the DTD Figure 8 compiles a number of the observational DTDs described above. Despite the consistent $\sim t^{-1}$ DTD shape, obtained by numerous different methods and samples, there is a clear tension among the normalizations of the DTD, i.e., among the Hubble-time-integrated ("total") numbers of SN Ia formed by a stellar generation. The DTDs based on volumetric SN Ia rates (which are not biased toward bright galaxies and contain a significant number of SNe in dwarf galaxies, Childress et al. 2013, Leaman et al. 2011) typically indicate a time-integrated SN Ia production efficiency of about 1 SN Ia per 1000 $M_\odot$ formed [for an assumed "diet-Salpeter" initial mass function (IMF), Bell et al. (2003)]. Galaxy-targeted SN surveys seem to find values about 2 times higher than this. Finally, DTDs based on galaxy clusters are higher yet, perhaps by another factor of $2-3$. In fact, there have been previous indications for higher rates in cluster ellipticals than in field ellipticals (Dilday et al. 2010a, Mannucci et al. 2008). The highest observed DTDs are a factor $3-10$ higher than the lowest ones. While the range in normalizations appears real, more work is required to confirm that some or all of it is not due to systematic errors, such as incorrect global or individual galaxy SFHs for particular galaxy types, surveys, or redshifts.

The lower-normalization DTDs are within reach of some of the DD-scenario DTDs from some recent BPS models (Mennekens, Vanbeveren & De Greve 2012; Ruiter et al. 2013; Toonen, Nelemans & Portegies Zwart 2012). For example, Toonen, Nelemans & Portegies Zwart (2012) find a time-integrated number of SNe Ia in their models of $2-3.3\times10^{-4}\ M_\odot^{-1}$, i.e., an order of magnitude lower than observed. However, this comes from considering as SNe Ia progenitors only CO-CO WD mergers with total masses above $M_{\rm Ch}$. Considering *all* CO-CO WD mergers, they find a time-integrated rate of $\sim 0.8\times10^{-3}\ M_\odot^{-1}$, and this assumes 50% binarity of the initial stellar population. A higher binary fraction would give a correspondingly higher result, one quite similar to some of the observed DTD normalizations above, as apparent in Fig. 8.

As also seen in Fig. 8, the BPS predictions for SD models tend to be much lower than DD predictions, both at short delays (although there is a large diversity among models), and certainly beyond the cutoffs that SD models generically have at delays of a few Gyr. Their normalizations thus miss the observed ones by at least an order of magnitude, and often by many.

A higher SN Ia number per formed stellar mass observed in the most massive galaxies could perhaps be related to the recently noted dependence of IMF on galaxy mass (Cappellari et al. 2012, Conroy & van Dokkum 2012, Geha et al. 2013), or to the well know excess of metals in clusters, compared to expectations from SN yields and the present-day stellar population (e.g. Loewenstein 2013; Maoz, Sharon & Gal-Yam 2010). On the other hand, it is unclear how the IMF variations, which are seen in the sub-solar-mass region of the IMF, could affect the production of SNe Ia whose progenitors are WDs descended from super-solar-mass stars, on the side of the IMF where variations have not been claimed.

As already noted in Section 2, above, head-on collisions of WDs in dense environments such as globular clusters and galactic centers have been proposed as a way of boosting SN Ia pro-

duction, which would raise the DTD normalization. Apart from collisions between unbound cluster WDs, dynamical encounters between binaries and other cluster stars will harden the binaries (Shara & Hurley 2002); such an effect has been used to explain the large enhancement in the number of low-mass X-ray binaries observed in globular clusters (Sarazin et al. 2003). Rosswog et al. (2009) showed that, even if such an enhancement of WD collisions occurs, the small fraction of all WDs that are in globular clusters means that this could explain only of order 1% of all SN Ia events. Observationally, the lack of globular clusters at the locations of SNe Ia observed with HST (Voss & Nelemans 2012, Washabaugh & Bregman 2013), rules out globulars as a significant overall rate-enhancement mechanism for SNe Ia.

3.5.11 Summary of the observed DTD In summary, SN Ia rate measurements quite consistently indicate a $\sim t^{-1}$ DTD. The coarse time resolution of many studies, the systematic uncertainties discussed above, and the sparse information below ~ 1 Gyr, presently allow more structured shapes, but the overall behavior of the DTD appears to be similar to that generic to the DD model. Long delay times are possible in SD models with red-giant donors, but BPS models generally produce very few of them. On the other hand, there is observational room for a SD contribution at delays $\lesssim$ 1Gyr, where the DTDs are not well-constrained. As a result, the DTD data presently cannot rule out comparable SD and DD contributions. However, in terms of total numbers, BPS predictions for SD models are generally lower than DD predictions, which themselves barely reach some of the observed DTDs.

4 Summary

4.1 The emerging picture

The SN Ia progenitor question is far from resolved, despite the major efforts to address it (e.g., there are over 400 papers in NASA-ADS over the last six years with the words "Type-Ia supernova progenitor" in their abstracts). Nevertheless, this large body of work has provided a wealth of relevant information. Progress has been made in the observational domain, but also in theoretical work where, e.g., recent 3D hydrodynamical simulations of mergers have revived the possibility that double-detonation merger scenarios could produce normal SNe Ia. To summarize some of the main observational results that have emerged:

- Censii in the Milky Way and nearby galaxies of the potential progenitor populations of SNe Ia in the standard SD model – accreting WDs growing in mass toward $M_{\rm Ch}$ – show that they cannot be recurrent novae or supersoft X-ray sources for more than a small fraction of their growth time. A hidden population of rapidly accreting WDs is also limited to be no more than a minority of the progenitors, based on the apparent absence of their expected ionizing radiation. A population of differentially spun-up super-$M_{\rm Ch}$ WDs, waiting to spin down and explode, may be out there, but has theoretical problems and seems at odds with the very slow spins observed generically in WDs. As for close double WD binaries that could be DD-model progenitors, BPS calculations and surveys for such systems both indicate that their total merger rate is of the same order of magnitude as the SN Ia rate. The traditional $M_{\rm tot} > M_{\rm Ch}$, CO+CO, mergers are probably too rare, by a factor of at least a few, but if lower-mass WD mergers, or even CO+He WD mergers, lead to a normal SN Ia, then their numbers are likely sufficient. Which ones, if any, actually lead to SNe Ia, and how, is still unclear.
- SN 2011fe, the best-ever studied SN Ia, and a very typical event to boot, has provided a wealth of progenitor constraints, essentially all of them based on null results. This event's immediate environment was remarkably "clean". There are strong limits on a

pre-explosion companion star, on any signatures of ejecta interaction with a donor star or with a CSM, on any X-ray upscattering or optical absorption signatures by a CSM, and on any hydrogen that was stripped from a companion and entrained by the ejecta. All of these are consistent with a DD origin, and challenge the SD picture for this event, unless spin-up is invoked.

- Variable Na I absorption, which could come from a CSM, has been seen, but only in three normal SNe Ia and one CSM-interacting SN Ia. The 2/31 or 2/16 discovery statistics in well-defined samples suggest a $\sim 5-15\%$ occurrence fraction. Statistical studies using single-epoch high-resolution spectra deduce, based on an excess of systems with blueshifted versus redshifted Na I absorption, a $\sim 20\%$ fraction of progenitors with a CSM, but these estimates still suffer from small numbers and systematics in defining samples and zero reference velocities. While a CSM producing the variable Na absorption is expected in the SD scenario, some DD merger models also predict such CSM absorptions.
- No normal SN Ia has shown signs of any entrained hydrogen from a companion, sometimes to stringent limits. However, a rare subclass constituting $\sim 0.1-1\%$ (maybe somewhat more) of SNe Ia, do show prominent variable hydrogen emission, and other signs of CSM interaction, such as kinetic energy input to the light curves. On the other hand, the implied CSM masses may be of order a solar mass, and it is presently unclear how such CSM masses fit into any of the traditional progenitor pictures.
- Among SN remnants known or suspected to have been SNe Ia, none have thus far revealed any obvious surviving SD-scenario donors, in several cases with strict upper limits. Hydrodynamic models of remnants having detailed X-ray observations almost always indicate ejecta expanding through a uniform-density medium, rather than through a low-density cavity from a pre-explosion SD-scenario wind.
- Derivations of the SN Ia delay-time distribution from a variety of SN Ia rate measurements and techniques, in different environments and redshifts, are all consistent with a t^{-1} dependence at delays $\gtrsim 1$ Gyr (although DTDs from different samples may be showing somewhat different normalizations of this distribution). Such a dependence is typically found for DD models, while most BPS SD models predict few or no SNe Ia at long delays. A SD contribution to the DTD at short delays is not yet constrained.
- From the diversity and correlations among observed spectral properties of SNe Ia and of their host galaxies, a rough general trend has emerged. At one extreme are events with high luminosities and slow light-curve evolution, occurring in star-forming galaxies, with high-velocity spectral features, no signs of unburnt carbon, higher symmetry indicators, and a relatively high chance of showing intervening absorption. At the other extreme are events with the opposite properties. As some of the former properties can be plausibly associated with SD-model explosions, it is tempting to suggest the existence of two "families" of progenitors, SD progenitors that produce the first type of events and DD progenitors that make the second type of SNe Ia. There are some problems with this picture. First, as reviewed in Section 3.3.4, the observed trends are weak, with large scatter, and sometimes with conflicting claims on the sense of the relations, and on selection effects. Some combination of progenitor properties, e.g., age, metallicity, and others, may explain the trend, rather than two separate families. Second, if two very diverse progenitor channels, e.g. a $M_{\rm Ch}$ SD channel and a double-detonation sub-$M_{\rm Ch}$ DD channel, were operating in parallel with comparable numbers, it would be remarkable that observed SN Ia properties are so uniform and continuous, the very features of SNe Ia that have made them so useful for cosmology.

From a recent-historical point of view, it is noteworthy that there has been something of a paradigm shift. The DD scenario has traditionally been the underdog, with review articles (e.g. Livio 2000) often concluding that the SD model will eventually be confirmed. The main argument against the DD scenario has been theoretical – that a DD merger would never lead to anything akin to a SN Ia explosion. This theoretical objection is no longer very strong, as some merger simulations now seem to successfully produce SNe Ia. And, for several SN Ia events and remnants, the observations suggest that, among the various models, only DD progenitors are not ruled out. Thus, not only can the DD model no longer be rejected offhand, but rather it could turn out to be the main, or even the only, scenario behind SNe Ia.

4.2 Future outlook

Future observational data, and progress on the theoretical issues, will undoubtedly provide new clues to the progenitor problem. Apart from obvious breakthroughs, such as the direct detection of a progenitor, or the explosion of a previously known candidate progenitor, there are several developments that, in the near or far future, could significantly advance the field.

On the theoretical side, one open issue is still how exactly does the accretion onto a WD proceed in an SD model, and what are the parameter ranges (mass transfer rate, composition, rotation, accretion history) that lead a C/O WD to grow in mass. Ignition in DD mergers is another unsolved problem. Detailed 3D hydrodynamical models, including nucleosynthesis, exploring the run of merger-model parameter space, are now being published. However, the finding that rather subtle effects may be important, such as residual hydrogen or helium on the WD, or residual carbon in the centers of oxygen-neon WDs, suggest that robust results will require higher-resolution calculations that take the previous stellar evolution into account in detail.

Progress is within reach also in the area of progenitor populations and the theoretical DTD. A recent detailed comparison of four different BPS codes (Toonen et al. 2013, submitted) shows that their outputs differ not because of numerical accuracy or treatment, but because of different physical assumptions. One clear conclusion, in particular for the DD and He-accreting SD models, is that the phase where one of the two stars is a helium star needs more detailed investigation. In parallel, comparison of the BPS predictions with observed local populations of binaries could calibrate out many of the uncertainties in BPS codes.

Turning to observations, the understanding of potential progenitor populations has advanced thanks to wide-field spectroscopic surveys, such as SDSS, that led to large and homogeneous samples of observed binaries. However, proper understanding of selection effects is still a challenge. The launch of *Gaia* will mark the next big improvement, with the discovery of large samples of WD binaries, for which distances and proper motions are also known.

The DTD has proved to be a powerful tool for testing models. A better knowledge of the parent stellar populations, and site-specific measurements of SN Ia rate vs. the stellar age distributions at the SN locations, can improve the accuracy of observational DTDs. The multivariate distribution of delay times, explosion energies, host metallicities, and more, (as opposed to the single-variable DTD), can provide physical links between these parameters, which will provide sharper discrimination among models.

SN 2011fe was a watershed event, not only because of its nearness but also because of the wealth of pre-explosion data and the very early and multi-wavelength coverage. With the rising prominence of time-domain, multi-messenger surveys, it is likely that similar or even better data will soon be available for additional SNe Ia.

Gamma-ray observations of SNe Ia by future MeV-range missions should provide excellent diagnostics not available at other energies. Horiuchi & Beacom (2010) have simulated the gamma-ray spectra and light curves of SNe Ia, out to Virgo distances, that could be obtained

by the proposed ACT mission, showing that various SD models would have distinct signatures in such gamma-ray data. Summa et al. (2013) have done this exercise for the proposed GRIPS and ASTRO-H missions. They show that the same two SD and DD models, compared by Röpke et al. (2012) to the optical data for SN 2011fe (see Section 3.3.3, above), could be distinguished by gamma-ray data from these missions.

In the more distant future, a space-based gravitational wave interferometer will be able to detect signals individually from several thousand Galactic double WD systems with orbital periods below 10 min, i.e. that are within ~ 1 Myr of merging (Amaro-Seoane et al. 2013). This will directly probe the WD merger rate. Together with the millions of longer-period binaries that are detectable as a foreground, this will provide quantitative information about the binary WD population and on its relevance as SN Ia progenitors. The gravitational signal of an actual merger will be detectable only for a Galactic (or perhaps Magellanic Cloud) event.

Indeed, we are arguably overdue for the privilege that Tycho, Kepler, and Galileo enjoyed, of a Galactic SN Ia. Of course, we may well have to wait a few more centuries for this occasion, but when it comes, it will surely be another transformational event, this time for the understanding of the workings of SNe Ia.

Acknowledgements: We thank R. Aloisio, C. Badenes, R. Foley, O. Graur, E. Nakar, P. Tozzi, and J. Vink for valuable discussions and input. DM acknowledges support by a grant from the ISF, and by I-Core Program grant 1829/12 of the PDC and the ISF.

References

Abazajian KN, Adelman-McCarthy JK, Agüeros MA, Allam SS, Allende Prieto C, et al. 2009. *ApJS* 182:543–558

Aldering G, Antilogus P, Bailey S, Baltay C, Bauer A, et al. 2006. *ApJ* 650:510–527

Alexander RD, Wynn GA, King AR, Pringle JE. 2011. *MNRAS* 418:2576–2583

Amaro-Seoane P, Aoudia S, Babak S, Binétruy P, Berti E, et al. 2013. *GW Notes, Vol. 6, p. 4-110* 6:4–110

Anupama GC. 2013. In *IAU Symposium*, eds. R Di Stefano, M Orio, M Moe, vol. 281 of *IAU Symposium*

Arnett WD. 1969. *Ap&SS* 5:180–212

Arnett WD. 1982. *ApJ* 253:785–797

Ashok NM, Banerjee DPK. 2003. *A&A* 409:1007–1015

Aubourg É, Tojeiro R, Jimenez R, Heavens A, Strauss MA, Spergel DN. 2008. *A&A* 492:631–636

Badenes C, Borkowski KJ, Hughes JP, Hwang U, Bravo E. 2006. *ApJ* 645:1373–1391

Badenes C, Hughes JP, Bravo E, Langer N. 2007. *ApJ* 662:472–486

Badenes C, Hughes JP, Cassam-Chenaï G, Bravo E. 2008. *ApJ* 680:1149–1157

Badenes C, Maoz D. 2012. *ApJL* 749:L11

Badenes C, Maoz D, Draine BT. 2010. *MNRAS* 407:1301–1313

Badenes C, Mullally F, Thompson SE, Lupton RH. 2009. *ApJ* 707:971–978

Barbary K, Aldering G, Amanullah R, Brodwin M, Connolly N, et al. 2012. *ApJ* 745:32

Bearda H, Hartmann W, Ebisawa K, Heise J, Kaastra J, et al. 2002. *A&A* 385:511–516

Bedin LR, Ruiz-Lapuente P, Gonzalez Hernandez JI, Canal R, Filippenko AV, et al. 2013. *ArXiv e-prints*

Benetti S, Cappellaro E, Mazzali PA, Turatto M, Altavilla G, et al. 2005. *ApJ* 623:1011–1016

Benetti S, Cappellaro E, Turatto M, Taubenberger S, Harutyunyan A, Valenti S. 2006. *ApJL* 653:L129–L132

Benz W, Thielemann FK, Hills JG. 1989. *ApJ* 342:986–998

Berger L, Koester D, Napiwotzki R, Reid IN, Zuckerman B. 2005. *A&A* 444:565–571

Beuermann K, Reinsch K. 2002. *A&A* 381:487–490

Bianco FB, Howell DA, Sullivan M, Conley A, Kasen D, et al. 2011. *ApJ* 741:20

Bildsten L, Shen KJ, Weinberg NN, Nelemans G. 2007. *ApJL* 662:L95–L98

Blair WP, Ghavamian P, Long KS, Williams BJ, Borkowski KJ, et al. 2007. *ApJ* 662:998–1013

Blanc G, Greggio L. 2008. *New Astronomy* 13:606–618

Blondin S, Dessart L, Hillier DJ, Khokhlov AM. 2013. *MNRAS* 429:2127–2142

Blondin S, Kasen D, Röpke FK, Kirshner RP, Mandel KS. 2011. *MNRAS* 417:1280–1302

Blondin S, Matheson T, Kirshner RP, Mandel KS, Berlind P, et al. 2012. *AJ* 143:126

Blondin S, Prieto JL, Patat F, Challis P, Hicken M, et al. 2009. *ApJ* 693:207–215

Bloom JS, Kasen D, Shen KJ, Nugent PE, Butler NR, et al. 2012. *ApJL* 744:L17

Bogomazov AI, Tutukov AV. 2011. *Astronomy Reports* 55:497–504

Borkowski KJ, Blondin JM, Sarazin CL. 1992. *ApJ* 400:222–237

Borkowski KJ, Hendrick SP, Reynolds SP. 2006. *ApJ* 652:1259–1267

Borkowski KJ, Sarazin CL, Blondin JM. 1994. *ApJ* 429:710–725

Boshkayev K, Izzo L, Rueda Hernandez JA, Ruffini R. 2013. *A&A* 555:A151

Bours MCP, Toonen S, Nelemans G. 2013. *A&A* 552:A24

Branch D, van den Bergh S. 1993. *AJ* 105:2231–2235

Brandt TD, Tojeiro R, Aubourg É, Heavens A, Jimenez R, Strauss MA. 2010. *AJ* 140:804–816

Brown PJ, Dawson KS, de Pasquale M, Gronwall C, Holland S, et al. 2012a. *ApJ* 753:22

Brown PJ, Dawson KS, Harris DW, Olmstead M, Milne P, Roming PWA. 2012b. *ApJ* 749:18

Brown WR, Kilic M, Hermes JJ, Allende Prieto C, Kenyon SJ, Winget DE. 2011. *ApJL* 737:L23

Burkey MT, Reynolds SP, Borkowski KJ, Blondin JM. 2013. *ApJ* 764:63

Calura F, Matteucci F, Tozzi P. 2007. *MNRAS* 378:L11–L15

Canal R, Méndez J, Ruiz-Lapuente P. 2001. *ApJL* 550:L53–L56

Capetti A. 2002. *ApJL* 574:L25–L27

Cappellari M, McDermid RM, Alatalo K, Blitz L, Bois M, et al. 2012. *Nature* 484:485–488

Cappellaro E, Evans R, Turatto M. 1999. *A&A* 351:459–466

Cappellaro E, Patat F, Mazzali PA, Benetti S, Danziger JI, et al. 2001. *ApJL* 549:L215–L218

Cartier R, Förster F, Coppi P, Hamuy M, Maeda K, et al. 2011. *A&A* 534:L15

Chamel N, Fantina AF, Davis PJ. 2013. *Phys. Rev. D* 88:081301

Charpinet S, Fontaine G, Brassard P. 2009. *Nature* 461:501–503

Chevalier RA. 1982. *ApJ* 258:790–797

Chevalier RA. 1998. *ApJ* 499:810

Chevalier RA, Fransson C. 2006. *ApJ* 651:381–391

Chevalier RA, Kirshner RP, Raymond JC. 1980. *ApJ* 235:186–195

Childress M, Aldering G, Antilogus P, Aragon C, Bailey S, et al. 2013. *ApJ* 770:107

Childress MJ, Filippenko AV, Ganeshalingam M, Schmidt BP. 2014. *MNRAS* 437:338–350

Chiotellis A, Schure KM, Vink J. 2012. *A&A* 537:A139

Chomiuk L. 2013. *PASA* 30:46

Chomiuk L, Krauss MI, Rupen MP, Nelson T, Roy N, et al. 2012a. *ApJ* 761:173

Chomiuk L, Soderberg AM, Moe M, Chevalier RA, Rupen MP, et al. 2012b. *ApJ* 750:164

Chugai NN. 2008. *Astronomy Letters* 34:389–396

Chugai NN, Yungelson LR. 2004. *Astronomy Letters* 30:65–72

Colgate SA, McKee C. 1969. *ApJ* 157:623

Conroy C, van Dokkum P. 2012. *ApJ* 747:69

Cooper MC, Newman JA, Yan R. 2009. *ApJ* 704:687–704

Córsico AH, Althaus LG, Kawaler SD, Miller Bertolami MM, García-Berro E, Kepler SO. 2011. *MNRAS* 418:2519–2526

Crotts APS, Yourdon D. 2008. *ApJ* 689:1186–1190

Dahlen T, Strolger LG, Riess AG. 2008. *ApJ* 681:462–469

Dahlen T, Strolger LG, Riess AG, Mobasher B, Chary RR, et al. 2004. *ApJ* 613:189–199

Dan M, Rosswog S, Brueggen M, Podsiadlowski P. 2013. *ArXiv e-prints*

Dan M, Rosswog S, Guillochon J, Ramirez-Ruiz E. 2012. *MNRAS* 422:2417–2428

D'Andrea CB, Gupta RR, Sako M, Morris M, Nichol RC, et al. 2011. *ApJ* 743:172

Darbha S, Metzger BD, Quataert E, Kasen D, Nugent P, Thomas R. 2010. *MNRAS* 409:846–854

Darnley MJ, Bode MF, Kerins E, Newsam AM, An J, et al. 2006. *MNRAS* 369:257–271

Davé R, Oppenheimer BD, Finlator K. 2011. *MNRAS* 415:11–31

Dawson KS, Aldering G, Amanullah R, Barbary K, Barrientos LF, et al. 2009. *AJ* 138:1271–1283

De Donder E, Vanbeveren D. 2004. *New A. Rev.* 48:861–975

della Valle M, Livio M. 1996. *ApJ* 473:240

Della Valle M, Panagia N, Padovani P, Cappellaro E, Mannucci F, Turatto M. 2005. *ApJ* 629:750–756

della Valle M, Rosino L, Bianchini A, Livio M. 1994. *A&A* 287:403–409

Dessart L, Blondin S, Hillier DJ, Khokhlov A. 2013a. *ArXiv e-prints*

Dessart L, Hillier DJ, Blondin S, Khokhlov A. 2013b. *ArXiv e-prints*

Di Stefano R. 2010. *ApJ* 712:728–733

Di Stefano R, Voss R, Claeys JSW. 2011. *ApJL* 738:L1+

Diaz MP, Williams RE, Luna GJ, Moraes M, Takeda L. 2010. *AJ* 140:1860–1867

Dilday B, Bassett B, Becker A, Bender R, Castander F, et al. 2010a. *ApJ* 715:1021–1035

Dilday B, Howell DA, Cenko SB, Silverman JM, Nugent PE, et al. 2012. *Science* 337:942–

Dilday B, Smith M, Bassett B, Becker A, Bender R, et al. 2010b. *ApJ* 713:1026–1036

Drury LO. 2012. *Astroparticle Physics* 39:52–60

Duchêne G, Kraus A. 2013. *ARA&A* 51:269–310

Edwards ZI, Pagnotta A, Schaefer BE. 2012. *ApJL* 747:L19

Filippenko AV. 1997. *ARA&A* 35:309–355

Fink M, Hillebrandt W, Röpke FK. 2007. *A&A* 476:1133–1143

Fink M, Kromer M, Seitenzahl IR, Ciaraldi-Schoolmann F, Roepke FK, et al. 2013. *ArXiv e-prints*

Fink M, Röpke FK, Hillebrandt W, Seitenzahl IR, Sim SA, Kromer M. 2010. *A&A* 514:A53

Folatelli G, Phillips MM, Morrell N, Tanaka M, Maeda K, et al. 2012. *ApJ* 745:74

Foley RJ. 2012. *ApJ* 748:127

Foley RJ. 2013. *MNRAS* 435:273–288

Foley RJ, Brown PJ, Rest A, Challis PJ, Kirshner RP, Wood-Vasey WM. 2010a. *ApJL* 708:L61–L65

Foley RJ, Challis PJ, Chornock R, Ganeshalingam M, Li W, et al. 2013. *ApJ* 767:57

Foley RJ, Challis PJ, Filippenko AV, Ganeshalingam M, Landsman W, et al. 2012a. *ApJ* 744:38

Foley RJ, Kasen D. 2011. *ApJ* 729:55

Foley RJ, Kirshner RP. 2013. *ApJL* 769:L1

Foley RJ, Rest A, Stritzinger M, Pignata G, Anderson JP, et al. 2010b. *AJ* 140:1321–1328

Foley RJ, Sanders NE, Kirshner RP. 2011. *ApJ* 742:89

Foley RJ, Simon JD, Burns CR, Gal-Yam A, Hamuy M, et al. 2012b. *ApJ* 752:101

Fontaine G, Brassard P, Charpinet S. 2013. In *European Physical Journal Web of Conferences*, vol. 43 of *European Physical Journal Web of Conferences*

Förster F, González-Gaitán S, Folatelli G, Morrell N. 2013. *ApJ* 772:19

Fox OD, Filippenko AV. 2013. *ApJL* 772:L6

Fox OD, Filippenko AV, Skrutskie MF, Silverman JM, Ganeshalingam M, et al. 2013. *AJ* 146:2

Friedrich S, Jordan S. 2001. *A&A* 367:577–581

Frieman JA, Bassett B, Becker A, Choi C, Cinabro D, et al. 2008. *AJ* 135:338–347

Fryer CL, Ruiter AJ, Belczynski K, Brown PJ, Bufano F, et al. 2010. *ApJ* 725:296–308

Fuhrmann K. 2005. *MNRAS* 359:L35–L36

Fujimoto MY. 1982. *ApJ* 257:767

Gal-Yam A, Maoz D, Guhathakurta P, Filippenko AV. 2008. *ApJ* 680:550–567

Gal-Yam A, Maoz D, Sharon K. 2002. *MNRAS* 332:37–48

Gallazzi A, Charlot S, Brinchmann J, White SDM, Tremonti CA. 2005. *MNRAS* 362:41–58

Ganeshalingam M, Li W, Filippenko AV. 2011. *MNRAS* 416:2607–2622

García-Berro E, Lorén-Aguilar P, Aznar-Siguán G, Torres S, Camacho J, et al. 2012. *ApJ* 749:25

García-Senz D, Cabezón RM, Arcones A, Relaño A, Thielemann FK. 2013. *MNRAS*

Garnavich PM, Kirshner RP, Challis P, Jha S, Branch D, et al. 2001. In *American Astronomical Society Meeting Abstracts*, vol. 33 of *Bulletin of the American Astronomical Society*

Geha M, Brown TM, Tumlinson J, Kalirai JS, Simon JD, et al. 2013. *ApJ* 771:29

Geier S, Heber U, Kupfer T, Napiwotzki R. 2010. *A&A* 515:A37

Geier S, Marsh TR, Wang B, Dunlap B, Barlow BN, et al. 2013. *A&A* 554:A54

Geier S, Nesslinger S, Heber U, Przybilla N, Napiwotzki R, Kudritzki RP. 2007. *A&A* 464:299–307

Gerardy CL, Höflich P, Fesen RA, Marion GH, Nomoto K, et al. 2004. *ApJ* 607:391–405

Germany LM, Reiss DJ, Schmidt BP, Stubbs CW, Suntzeff NB. 2004. *A&A* 415:863–878

Ghavamian P, Rakowski CE, Hughes JP, Williams TB. 2003. *ApJ* 590:833–845

Ghavamian P, Raymond J, Smith RC, Hartigan P. 2001. *ApJ* 547:995–1009

Gilfanov M, Bogdán Á. 2010. *Nature* 463:924–925

González Hernández JI, Ruiz-Lapuente P, Filippenko AV, Foley RJ, Gal-Yam A, Simon JD. 2009. *ApJ* 691:1–15

González Hernández JI, Ruiz-Lapuente P, Tabernero HM, Montes D, Canal R, et al. 2012. *Nature* 489:533–536

Graham ML, Pritchet CJ, Sullivan M, Gwyn SDJ, Neill JD, et al. 2008. *AJ* 135:1343–1349

Graham ML, Pritchet CJ, Sullivan M, Howell DA, Gwyn SDJ, et al. 2010. *AJ* 139:594–605

Graur O, Maoz D. 2012a. *The Astronomer's Telegram* 4226:1

Graur O, Maoz D. 2012b. *The Astronomer's Telegram* 4535:1

Graur O, Maoz D. 2013. *MNRAS* 430:1746–1763

Graur O, Poznanski D, Maoz D, Yasuda N, Totani T, et al. 2011. *MNRAS* 417:916–940

Graur O, Rodney SA, Maoz D, Riess AG, Jha SW, et al. 2013. *ArXiv e-prints*

Greggio L. 2005. *A&A* 441:1055–1078

Greggio L, Renzini A, Daddi E. 2008. *MNRAS* 388:829–837

Gruyters P, Exter K, Roberts TP, Rappaport S. 2012. *A&A* 544:A86

Guillochon J, Dan M, Ramirez-Ruiz E, Rosswog S. 2010. *ApJL* 709:L64–L69

Hachinger S, Mazzali PA, Sullivan M, Ellis RS, Maguire K, et al. 2013. *MNRAS* 429:2228–2248

Hachisu I, Kato M. 2003a. *ApJ* 598:527–544

Hachisu I, Kato M. 2003b. *ApJ* 590:445–459

Hachisu I, Kato M. 2012. *Baltic Astronomy* 21:68–75

Hachisu I, Kato M, Kiyota S, Kubotera K, Maehara H, et al. 2006. *ApJL* 651:L141–L144

Hachisu I, Kato M, Nomoto K. 1996. *ApJL* 470:L97

Hachisu I, Kato M, Nomoto K. 1999. *ApJ* 522:487–503

Hachisu I, Kato M, Nomoto K. 2008a. *ApJL* 683:L127–L130

Hachisu I, Kato M, Nomoto K. 2008b. *ApJ* 679:1390–1404

Hachisu I, Kato M, Nomoto K. 2010. *ApJL* 724:L212–L216

Hachisu I, Kato M, Nomoto K. 2012. *ApJL* 756:L4

Hachisu I, Kato M, Saio H, Nomoto K. 2012. *ApJ* 744:69

Hakobyan AA, Petrosian AR, McLean B, Kunth D, Allen RJ, et al. 2008. *A&A* 488:523–531

Hamann WR, Peña M, Gräfener G, Ruiz MT. 2003. *A&A* 409:969–982

Hamers AS, Pols OR, Claeys JSW, Nelemans G. 2013. *MNRAS* 430:2262–2280

Hamilton AJS, Sarazin CL. 1984. *ApJ* 287:282–294

Hamuy M, Phillips MM, Suntzeff NB, Maza J, González LE, et al. 2003. *Nature* 424:651–654

Hamuy M, Trager SC, Pinto PA, Phillips MM, Schommer RA, et al. 2000. *AJ* 120:1479–1486

Han Z. 1998. *MNRAS* 296:1019–1040

Han Z, Podsiadlowski P. 2004. *MNRAS* 350:1301–1309

Han Z, Podsiadlowski P. 2006. *MNRAS* 368:1095–1100

Hancock PJ, Gaensler BM, Murphy T. 2011. *ApJL* 735:L35

Harris J, Zaritsky D. 2004. *AJ* 127:1531–1544

Harris J, Zaritsky D. 2009. *AJ* 138:1243–1260

Hawley WP, Athanassiadou T, Timmes FX. 2012. *ApJ* 759:39

Hayden BT, Garnavich PM, Kasen D, Dilday B, Frieman JA, et al. 2010a. *ApJ* 722:1691–1698

Hayden BT, Garnavich PM, Kessler R, Frieman JA, Jha SW, et al. 2010b. *ApJ* 712:350–366

Hayden BT, Gupta RR, Garnavich PM, Mannucci F, Nichol RC, Sako M. 2013. *ApJ* 764:191

Heng K. 2010. *PASA* 27:23–44

Hermes JJ, Kilic M, Brown WR, Winget DE, Allende Prieto C, et al. 2012. *ApJL* 757:L21

Hicken M, Challis P, Jha S, Kirshner RP, Matheson T, et al. 2009. *ApJ* 700:331–357

Hillebrandt W, Kromer M, Röpke FK, Ruiter AJ. 2013. *Frontiers of Physics* 8:116–143

Hillebrandt W, Niemeyer JC. 2000. *ARA&A* 38:191–230

Hillebrandt W, Sim SA, Röpke FK. 2007. *A&A* 465:L17–L20

Hoeflich P, Khokhlov A. 1996. *ApJ* 457:500

Höflich P, Schaefer BE. 2009. *ApJ* 705:483–495

Hole KT, Kasen D, Nordsieck KH. 2010. *ApJ* 720:1500–1512

Horesh A, Kulkarni SR, Fox DB, Carpenter J, Kasliwal MM, et al. 2012. *ApJ* 746:21

Horiuchi S, Beacom JF. 2010. *ApJ* 723:329–341

Howell DA. 2011. *Nature Communications* 2

Howell DA, Conley A, Della Valle M, Nugent PE, Perlmutter S, et al. 2009a. *ArXiv e-prints (0903.1086)*

Howell DA, Höflich P, Wang L, Wheeler JC. 2001. *ApJ* 556:302–321

Howell DA, Sullivan M, Brown EF, Conley A, LeBorgne D, et al. 2009b. *ApJ* 691:661–671

Howell DA, Sullivan M, Nugent PE, Ellis RS, Conley AJ, et al. 2006. *Nature* 443:308–311

Hoyle F, Fowler WA. 1960. *ApJ* 132:565

Hughes JP, Chugai N, Chevalier R, Lundqvist P, Schlegel E. 2007. *ApJ* 670:1260–1274

Iben Jr. I, Renzini A. 1983. *ARA&A* 21:271–342

Iben Jr. I, Tutukov AV. 1984. *ApJS* 54:335–372

Iben Jr. I, Tutukov AV, Yungelson LR. 1997. *ApJ* 475:291

Idan I, Shaviv N, Shaviv G. 2013. *MNRAS* 433:2884–2892

Ihara Y, Ozaki J, Doi M, Shigeyama T, Kashikawa N, et al. 2007. *PASJ* 59:811–826

Ilkov M, Soker N. 2011. *MNRAS* :1798

Ivanova N, Justham S, Chen X, De Marco O, Fryer CL, et al. 2013. *A&A Rev.* 21:59

Iwamoto K, Brachwitz F, Nomoto K, Kishimoto N, Umeda H, et al. 1999. *ApJS* 125:439–462

Jimenez R, Bernardi M, Haiman Z, Panter B, Heavens AF. 2007. *ApJ* 669:947–951

Johansson J, Amanullah R, Goobar A. 2013. *MNRAS* 431:L43–L47

Jordan IV GC, Perets HB, Fisher RT, van Rossum DR. 2012. *ApJL* 761:L23

Jordan S, Aznar Cuadrado R, Napiwotzki R, Schmid HM, Solanki SK. 2007. *A&A* 462:1097–1101

Jorgensen HE, Lipunov VM, Panchenko IE, Postnov KA, Prokhorov ME. 1997. *ApJ* 486:110–+

Justham S. 2011. *ApJL* 730:L34+

Kafka S, Honeycutt RK, Williams R. 2012. *MNRAS* 425:1585–1590

Kafka S, Williams R. 2011. *A&A* 526:A83

Kamiya Y, Tanaka M, Nomoto K, Blinnikov SI, Sorokina EI, Suzuki T. 2012. *ApJ* 756:191

Kaplan DL, Bildsten L, Steinfadt JDR. 2012. *ApJ* 758:64

Kasen D. 2010. *ApJ* 708:1025–1031

Kasen D, Nugent P. 2013. *Annual Review of Nuclear and Particle Science* 63:153–174

Kasen D, Nugent P, Wang L, Howell DA, Wheeler JC, et al. 2003. *ApJ* 593:788–808

Kasen D, Röpke FK, Woosley SE. 2009. *Nature* 460:869–872

Kasen D, Woosley SE. 2007. *ApJ* 656:661–665

Kashi A, Soker N. 2011. *MNRAS* 417:1466–1479

Kato M, Hachisu I. 2012. *Bulletin of the Astronomical Society of India* 40:393

Kato M, Hachisu I, Kiyota S, Saio H. 2008. *ApJ* 684:1366–1373

Kattner S, Leonard DC, Burns CR, Phillips MM, Folatelli G, et al. 2012. *PASP* 124:114–127

Katz B, Dong S. 2012. *ArXiv e-prints*

Kawaler SD. 2004. In *Stellar Rotation*, eds. A Maeder, P Eenens, vol. 215 of *IAU Symposium*

Kawka A, Vennes S, Schmidt GD, Wickramasinghe DT, Koch R. 2007. *ApJ* 654:499–520

Kepler SO, Pelisoli I, Jordan S, Kleinman SJ, Koester D, et al. 2013. *MNRAS* 429:2934–2944

Kerzendorf WE, Childress M, Scharwachter TJ, Schmidt BPK. 2013a. *submitted*

Kerzendorf WE, Schmidt BP, Asplund M, Nomoto K, Podsiadlowski P, et al. 2009. *ApJ* 701:1665–1672

Kerzendorf WE, Schmidt BP, Laird JB, Podsiadlowski P, Bessell MS. 2012. *ApJ* 759:7

Kerzendorf WE, Yong D, Schmidt BP, Simon JD, Jeffery CS, et al. 2013b. *ApJ* 774:99

Khokhlov AM. 1991. *A&A* 245:114–128

Kilic M, Brown WR, Allende Prieto C, Kenyon SJ, Heinke CO, et al. 2012. *ApJ* 751:141

Kistler MD, Stanek KZ, Kochanek CS, Prieto JL, Thompson TA. 2013. *ApJ* 770:88

Kobayashi C, Nomoto K. 2009. *ApJ* 707:1466–1484

Kosenko D, Blinnikov SI, Vink J. 2011. *A&A* 532:A114

Kosenko D, Vink J, Blinnikov S, Rasmussen A. 2008. *A&A* 490:223–230

Kozai Y. 1962. *AJ* 67:591

Krause O, Tanaka M, Usuda T, Hattori T, Goto M, et al. 2008. *Nature* 456:617–619

Kromer M, Pakmor R, Taubenberger S, Pignata G, Fink M, et al. 2013. *ApJL* 778:L18

Kushnir D, Katz B, Dong S, Livne E, Fernández R. 2013. *ArXiv e-prints*

Kuznetsova NV, Connolly BM. 2007. *ApJ* 659:530–540

Lampeitl H, Smith M, Nichol RC, Bassett B, Cinabro D, et al. 2010. *ApJ* 722:566–576

Landstreet JD, Bagnulo S, Valyavin GG, Fossati L, Jordan S, et al. 2012. *A&A* 545:A30

Langer N, Deutschmann A, Wellstein S, Höflich P. 2000. *A&A* 362:1046–1064

Lanz T, Telis GA, Audard M, Paerels F, Rasmussen AP, Hubeny I. 2005. *ApJ* 619:517–526

Leaman J, Li W, Chornock R, Filippenko AV. 2011. *MNRAS* 412:1419–1440

Leigh NWC, Geller AM. 2013. *MNRAS* 432:2474–2479

Leonard DC. 2007. *ApJ* 670:1275–1282

Leonard DC, Li W, Filippenko AV, Foley RJ, Chornock R. 2005. *ApJ* 632:450–475

Lepo K, van Kerkwijk M. 2013. *ApJ* 771:13

Li W, Bloom JS, Podsiadlowski P, Miller AA, Cenko SB, et al. 2011a. *Nature* 480:348–350

Li W, Chornock R, Leaman J, Filippenko AV, Poznanski D, et al. 2011b. *MNRAS* 412:1473–1507

Li W, Leaman J, Chornock R, Filippenko AV, Poznanski D, et al. 2011c. *MNRAS* 412:1441–1472

Li XD, van den Heuvel EPJ. 1997. *A&A* 322:L9–L12

Lidov ML. 1962. *Planet. Space Sci.* 9:719–759

Lipunov VM, Panchenko IE, Pruzhinskaya MV. 2011. *New Astron.* 16:250–252

Liu J, Di Stefano R, Wang T, Moe M. 2012a. *ApJ* 749:141

Liu ZW, Kromer M, Fink M, Pakmor R, Röpke FK, et al. 2013a. *ApJ* 778:121

Liu ZW, Pakmor R, Röpke FK, Edelmann P, Hillebrandt W, et al. 2013b. *A&A* 554:A109

Liu ZW, Pakmor R, Röpke FK, Edelmann P, Wang B, et al. 2012b. *A&A* 548:A2

Livio M. 2000. In *Type Ia Supernovae, Theory and Cosmology*, eds. JC Niemeyer, JW Truran

Livio M, Riess A, Sparks W. 2002. *ApJL* 571:L99–L102

Livio M, Riess AG. 2003. *ApJL* 594:L93–L94

Livne E. 1990. *ApJL* 354:L53–L55

Loewenstein M. 2013. *ApJ* 773:52

Lorén-Aguilar P, Isern J, García-Berro E. 2009. *A&A* 500:1193–1205

Lorén-Aguilar P, Isern J, García-Berro E. 2010. *MNRAS* 406:2749–2763

Luna GJM, Sokoloski JL, Mukai K. 2008. In *RS Ophiuchi (2006) and the Recurrent Nova Phenomenon*, eds. A Evans, MF Bode, TJ O'Brien, MJ Darnley, vol. 401 of *Astronomical Society of the Pacific Conference Series*

Lundqvist P, Mattila S, Sollerman J, Kozma C, Baron E, et al. 2013. *MNRAS* 435:329–345

Lyman JD, James PA, Perets HB, Anderson JP, Gal-Yam A, et al. 2013. *MNRAS* 434:527–541

Ma H, Woosley SE, Malone CM, Almgren A, Bell J. 2013. *ApJ* 771:58

Maeda K, Benetti S, Stritzinger M, Röpke FK, Folatelli G, et al. 2010. *Nature* 466:82–85

Maeda K, Leloudas G, Taubenberger S, Stritzinger M, Sollerman J, et al. 2011. *MNRAS* 413:3075–3094

Maguire K, Sullivan M, Ellis RS, Nugent PE, Howell DA, et al. 2012. *MNRAS* 426:2359–2379

Maguire K, Sullivan M, Patat F, Gal-Yam A, Hook IM, et al. 2013. *MNRAS* 436:222–240

Mannucci F. 2008. *Chinese Journal of Astronomy and Astrophysics Supplement* 8:143–154

Mannucci F. 2009. In *American Institute of Physics Conference Series*, eds. G Giobbi, A Tornambe, G Raimondo, M Limongi, LA Antonelli, N Menci, E Brocato, vol. 1111 of *American Institute of Physics Conference Series*

Mannucci F, Cresci G, Maiolino R, Marconi A, Gnerucci A. 2010. *MNRAS* 408:2115–2127

Mannucci F, Della Valle M, Panagia N. 2006. *MNRAS* 370:773–783

Mannucci F, Della Valle M, Panagia N. 2007. *MNRAS* 377:1229–1235

Mannucci F, Della Valle M, Panagia N, Cappellaro E, Cresci G, et al. 2005. *A&A* 433:807–814

Mannucci F, Maoz D, Sharon K, Botticella MT, Della Valle M, et al. 2008. *MNRAS* 383:1121–1130

Maoz D, Badenes C. 2010. *MNRAS* 407:1314–1327

Maoz D, Badenes C, Bickerton SJ. 2012. *ApJ* 751:143

Maoz D, Gal-Yam A. 2004. *MNRAS* 347:951–956

Maoz D, Mannucci F. 2008. *MNRAS* 388:421–428

Maoz D, Mannucci F. 2012. *PASA* 29:447–465

Maoz D, Mannucci F, Brandt TD. 2012. *MNRAS* 426:3282–3294

Maoz D, Mannucci F, Li W, Filippenko AV, Della Valle M, Panagia N. 2011. *MNRAS* 412:1508–1521

Maoz D, Sharon K, Gal-Yam A. 2010. *ApJ* 722:1879–1894

Margutti R, Soderberg AM, Chomiuk L, Chevalier R, Hurley K, et al. 2012. *ApJ* 751:134

Marietta E, Burrows A, Fryxell B. 2000. *ApJS* 128:615–650

Marsh TR. 2011. *Classical and Quantum Gravity* 28:094019

Mason E. 2013. *A&A* 556:C2

Matteucci F. 2001. *The chemical evolution of the Galaxy*, vol. 253 of *Astrophysics and Space Science Library*. Kluwer

Matteucci F, Greggio L. 1986. *A&A* 154:279–287

Matteucci F, Panagia N, Pipino A, Mannucci F, Recchi S, Della Valle M. 2006. *MNRAS* 372:265–275

Matteucci F, Spitoni E, Recchi S, Valiante R. 2009. *A&A* 501:531–538

Mattila S, Lundqvist P, Sollerman J, Kozma C, Baron E, et al. 2005. *A&A* 443:649–662

Maund JR, Höflich P, Patat F, Wheeler JC, Zelaya P, et al. 2010. *ApJL* 725:L167–L171

Maund JR, Spyromilio J, Höflich PA, Wheeler JC, Baade D, et al. 2013. *MNRAS* 433:L20–L24

Maxted PFL, Marsh TR, North RC. 2000. *MNRAS* 317:L41–L44

Mazeh T, Shaham J. 1979. *A&A* 77:145–151

Mazzali P, Sullivan M, Hachinger S, Ellis R, Nugent PE, et al. 2013. *ArXiv e-prints*

Mazzali PA, Benetti S, Altavilla G, Blanc G, Cappellaro E, et al. 2005. *ApJL* 623:L37–L40

Mazzali PA, Cappellaro E, Danziger IJ, Turatto M, Benetti S. 1998. *ApJL* 499:L49

Mazzali PA, Podsiadlowski P. 2006. *MNRAS* 369:L19–L22

Mazzali PA, Röpke FK, Benetti S, Hillebrandt W. 2007. *Science* 315:825–

McCully C, Jha SW, Foley RJ, Chornock R, Holtzman JA, et al. 2013. *ArXiv e-prints*

McMillan PJ. 2011. *MNRAS* 414:2446–2457

Meng X, Yang W. 2010. *ApJ* 710:1310–1323

Meng XC, Yang WM. 2011. *Research in Astronomy and Astrophysics* 11:965–973

Mennekens N, Vanbeveren D, De Greve JP. 2012. *ArXiv e-prints*

Mennekens N, Vanbeveren D, De Greve JP, De Donder E. 2010. *A&A* 515:A89

Mennekens N, Vanbeveren D, De Greve JP, De Donder E. 2013. In *IAU Symposium*, eds. R Di Stefano, M Orio, M Moe, vol. 281 of *IAU Symposium*

Moll R, Raskin C, Kasen D, Woosley S. 2013. *ArXiv e-prints*

Nakar E, Sari R. 2010. *ApJ* 725:904–921

Nakar E, Sari R. 2012. *ApJ* 747:88

Napiwotzki R, Karl CA, Lisker T, Heber U, Christlieb N, et al. 2004. *Ap&SS* 291:321–328

Napiwotzki R, Karl CA, Nelemans G, Yungelson L, Christlieb N, et al. 2007. In *15th European Workshop on White Dwarfs*, eds. R Napiwotzki, MR Burleigh, vol. 372 of *Astronomical Society of the Pacific Conference Series*

Nelemans G, Napiwotzki R, Karl C, Marsh TR, Voss B, et al. 2005. *A&A* 440:1087–1095

Nelemans G, Toonen S, Bours M. 2013. In *IAU Symposium*, eds. R Di Stefano, M Orio, M Moe, vol. 281 of *IAU Symposium*

Nelemans G, Voss R, Roelofs G, Bassa C. 2008. *MNRAS* 388:487–494

Nelemans G, Yungelson LR, Portegies Zwart SF. 2001. *A&A* 375:890–898

Nelson T, Donato D, Mukai K, Sokoloski J, Chomiuk L. 2012. *ApJ* 748:43

Newsham G, Starrfield S, Timmes F. 2013. *ArXiv e-prints*

Nielsen MTB, Dominik C, Nelemans G, Voss R. 2013a. *A&A* 549:A32

Nielsen MTB, Nelemans G, Voss R, Toonen S. 2013b. *ArXiv e-prints*

Nielsen MTB, Voss R, Nelemans G. 2012. *MNRAS* 426:2668–2676

Nielsen MTB, Voss R, Nelemans G. 2013. *MNRAS* 435:187–193

Nomoto K. 1982. *ApJ* 253:798–810

Nomoto K, Iben Jr. I. 1985. *ApJ* 297:531–537

Nomoto K, Kobayashi C, Tominaga N. 2013. *ARA&A* 51:457–509

Nomoto K, Saio H, Kato M, Hachisu I. 2007. *ApJ* 663:1269–1276

Nomoto K, Thielemann FK, Yokoi K. 1984. *ApJ* 286:644–658

Nordhaus J, Wellons S, Spiegel DS, Metzger BD, Blackman EG. 2011. *Proceedings of the National Academy of Science* 108:3135–3140

Nugent PE, Sullivan M, Cenko SB, Thomas RC, Kasen D, et al. 2011. *Nature* 480:344–347

Orio M, Nelson T, Bianchini A, Di Mille F, Harbeck D. 2010. *ApJ* 717:739–765

Pakmor R, Kromer M, Taubenberger S, Sim SA, Röpke FK, Hillebrandt W. 2012. *ApJL* 747:L10

Pakmor R, Kromer M, Taubenberger S, Springel V. 2013. *ApJL* 770:L8

Pan KC, Ricker PM, Taam RE. 2013. *ApJ* 773:49

Pan YC, Sullivan M, Maguire K, Hook IM, Nugent PE, et al. 2013. *ArXiv e-prints*

Panagia N, Van Dyk SD, Weiler KW, Sramek RA, Stockdale CJ, Murata KP. 2006. *ApJ* 646:369–377

Parikh A, José J, Seitenzahl IR, Röpke FK. 2013. *A&A* 557:A3

Parrent JT, Howell DA, Friesen B, Thomas RC, Fesen RA, et al. 2012. *ApJL* 752:L26

Parrent JT, Thomas RC, Fesen RA, Marion GH, Challis P, et al. 2011. *ApJ* 732:30

Patat F. 2005. *MNRAS* 357:1161–1177

Patat F, Baade D, Höflich P, Maund JR, Wang L, Wheeler JC. 2009. *A&A* 508:229–246

Patat F, Benetti S, Cappellaro E, Turatto M. 2006. *MNRAS* 369:1949–1960

Patat F, Chandra P, Chevalier R, Justham S, Podsiadlowski P, et al. 2007. *Science* 317:924–

Patat F, Chugai NN, Podsiadlowski P, Mason E, Melo C, Pasquini L. 2011. *A&A* 530:A63

Patat F, Cordiner MA, Cox NLJ, Anderson RI, Harutyunyan A, et al. 2013. *A&A* 549:A62

Patat F, Höflich P, Baade D, Maund JR, Wang L, Wheeler JC. 2012. *A&A* 545:A7

Patnaude DJ, Badenes C, Park S, Laming JM. 2012. *ApJ* 756:6

Patterson J, Oksanen A, Monard B, Rea R, Hambsch FJ, et al. 2013. *ArXiv e-prints*

Perlmutter S, Aldering G, Goldhaber G, Knop RA, Nugent P, et al. 1999. *ApJ* 517:565–586

Perrett K, Sullivan M, Conley A, González-Gaitán S, Carlberg R, et al. 2012. *AJ* 144:59

Phillips MM. 1993. *ApJL* 413:L105–L108

Phillips MM, Simon JD, Morrell N, Burns CR, Cox NLJ, et al. 2013. *ApJ* 779:38

Piersanti L, Cassisi S, Iben Jr. I, Tornambé A. 2000. *ApJ* 535:932–942

Piersanti L, Gagliardi S, Iben Jr. I, Tornambé A. 2003. *ApJ* 583:885–901

Pinto PA, Eastman RG. 2000. *ApJ* 530:757–776

Piro AL. 2008. *ApJ* 679:616–625

Piro AL, Bildsten L. 2008. *ApJ* 673:1009–1013

Piro AL, Chang P, Weinberg NN. 2010. *ApJ* 708:598–604

Piro AL, Kulkarni SR. 2013. *ApJL* 762:L17

Piro AL, Nakar E. 2012. *ArXiv e-prints*

Piro AL, Nakar E. 2013. *ApJ* 769:67

Piro AL, Thompson TA, Kochanek CS. 2013. *ArXiv e-prints*

Pols OR, Marinus M. 1994. *A&A* 288:475–501

Poznanski D, Maoz D, Yasuda N, Foley RJ, Doi M, et al. 2007. *MNRAS* 382:1169–1186

Prieto JL, Garnavich PM, Phillips MM, DePoy DL, Parrent J, et al. 2007. *ArXiv e-prints (0706.4088)*

Pritchet CJ, Howell DA, Sullivan M. 2008. *ApJL* 683:L25–L28

Prodan S, Murray N, Thompson TA. 2013. *ArXiv e-prints*

Quinn JL, Garnavich PM, Li W, Panagia N, Riess A, et al. 2006. *ApJ* 652:512–517

Rabinak I, Livne E, Waxman E. 2012. *ApJ* 757:35

Rabinak I, Waxman E. 2011. *ApJ* 728:63

Rajoelimanana AF, Charles PA, Meintjes PJ, Odendaal A, Udalski A. 2013. *MNRAS* 432:2886–2894

Rappaport S, Chiang E, Kallman T, Malina R. 1994. *ApJ* 431:237–246

Raskin C, Kasen D. 2013. *ApJ* 772:1

Raskin C, Kasen D, Moll R, Schwab J, Woosley S. 2013. *ArXiv e-prints*

Raskin C, Scannapieco E, Fryer C, Rockefeller G, Timmes FX. 2012. *ApJ* 746:62

Raskin C, Scannapieco E, Rhoads J, Della Valle M. 2009. *ApJ* 707:74–78

Raskin C, Scannapieco E, Rockefeller G, Fryer C, Diehl S, Timmes FX. 2010. *ApJ* 724:111–125

Raymond JC, Korreck KE, Sedlacek QC, Blair WP, Ghavamian P, Sankrit R. 2007. *ApJ* 659:1257–1264

Remillard RA, Rappaport S, Macri LM. 1995. *ApJ* 439:646–651

Rest A, Matheson T, Blondin S, Bergmann M, Welch DL, et al. 2008a. *ApJ* 680:1137–1148

Rest A, Sinnott B, Welch DL. 2012. *PASA* 29:466–481

Rest A, Suntzeff NB, Olsen K, Prieto JL, Smith RC, et al. 2005. *Nature* 438:1132–1134

Rest A, Welch DL, Suntzeff NB, Oaster L, Lanning H, et al. 2008b. *ApJL* 681:L81–L84

Rettura A, Mei S, Stanford SA, Raichoor A, Moran S, et al. 2011. *ApJ* 732:94

Reynolds SP, Borkowski KJ, Hwang U, Hughes JP, Badenes C, et al. 2007. *ApJL* 668:L135–L138

Riess AG, Filippenko AV, Challis P, Clocchiatti A, Diercks A, et al. 1998. *AJ* 116:1009–1038

Rigault M, Copin Y, Aldering G, Antilogus P, Aragon C, et al. 2013. *A&A* 560:A66

Rodney S, et al. 2013, *ApJ*, submitted

Rodríguez-Gil P, Santander-García M, Knigge C, Corradi RLM, Gänsicke BT, et al. 2010. *MNRAS* 407:L21–L25

Roelofs G, Bassa C, Voss R, Nelemans G. 2008. *MNRAS* 391:290–296

Röpke FK, Kromer M, Seitenzahl IR, Pakmor R, Sim SA, et al. 2012. *ApJL* 750:L19

Rosswog S, Kasen D, Guillochon J, Ramirez-Ruiz E. 2009. *ApJL* 705:L128–L132

Ruiter AJ, Belczynski K, Fryer C. 2009. *ApJ* 699:2026–2036

Ruiter AJ, Sim SA, Pakmor R, Kromer M, Seitenzahl IR, et al. 2013. *MNRAS* 429:1425–1436

Ruiz-Lapuente P. 1997. *Science* 276:1813–1814

Ruiz-Lapuente P, Canal R. 1998. *ApJL* 497:L57

Ruiz-Lapuente P, Comeron F, Méndez J, Canal R, Smartt SJ, et al. 2004. *Nature* 431:1069–1072

Rupen MP, Mioduszewski AJ, Sokoloski JL. 2008. *ApJ* 688:559–567

Russell BR, Immler S. 2012. *ApJL* 748:L29

Sadat R, Blanchard A, Guiderdoni B, Silk J. 1998. *A&A* 331:L69–L72

Sahman DI, Dhillon VS, Marsh TR, Moll S, Thoroughgood TD, et al. 2013. *MNRAS* 433:1588–1598

Saio H, Nomoto K. 1998. *ApJ* 500:388

Saio H, Nomoto K. 2004. *ApJ* 615:444–449

Sako M, Bassett B, Becker A, Cinabro D, DeJongh F, et al. 2008. *AJ* 135:348–373

Sand DJ, Graham ML, Bildfell C, Zaritsky D, Pritchet C, et al. 2012. *ApJ* 746:163

Sand DJ, Zaritsky D, Herbert-Fort S, Sivanandam S, Clowe D. 2008. *AJ* 135:1917–1933

Sarazin CL, Kundu A, Irwin JA, Sivakoff GR, Blanton EL, Randall SW. 2003. *ApJ* 595:743–759

Scalzo R, Aldering G, Antilogus P, Aragon C, Bailey S, et al. 2012. *ApJ* 757:12

Scalzo RA, Aldering G, Antilogus P, Aragon C, Bailey S, et al. 2010. *ApJ* 713:1073–1094

Scannapieco E, Bildsten L. 2005. *ApJL* 629:L85–L88

Schaefer BE. 2010. *ApJS* 187:275–373

Schaefer BE. 2013. In *American Astronomical Society Meeting Abstracts*, vol. 221 of *American Astronomical Society Meeting Abstracts*

Schaefer BE, Pagnotta A. 2012. *Nature* 481:164–166

Schaefer BE, Pagnotta A, Shara MM. 2010. *ApJ* 708:381–402

Schaefer BE, Pagnotta A, Xiao L, Darnley MJ, Bode MF, et al. 2010. *AJ* 140:925–932

Schawinski K. 2009. *MNRAS* 397:717–725

Schmidt BP, Kirshner RP, Leibundgut B, Wells LA, Porter AC, et al. 1994. *ApJL* 434:L19–L23

Schwab J, Shen KJ, Quataert E, Dan M, Rosswog S. 2012. *MNRAS* 427:190–203

Scolnic DM, Riess AG, Foley RJ, Rest A, Rodney SA, et al. 2014. *ApJ* 780:37

Seitenzahl IR, Cescutti G, Röpke FK, Ruiter AJ, Pakmor R. 2013a. *A&A* 559:L5

Seitenzahl IR, Ciaraldi-Schoolmann F, Röpke FK, Fink M, Hillebrandt W, et al. 2013b. *MNRAS* 429:1156–1172

Selvelli P, Cassatella A, Gilmozzi R, González-Riestra R. 2008. *A&A* 492:787–803

Shappee BJ, Kochanek CS, Stanek KZ. 2013. *ApJ* 765:150

Shappee BJ, Stanek KZ, Pogge RW, Garnavich PM. 2013. *ApJL* 762:L5

Shara MM, Bibby JL, Zurek D, Crowther PA, Moffat AFJ, Drissen L. 2013. *AJ* 146:162

Shara MM, Hurley JR. 2002. *ApJ* 571:830–842

Sharon K, Gal-Yam A, Maoz D, Filippenko AV, Guhathakurta P. 2007. *ApJ* 660:1165–1175

Shen KJ, Bildsten L. 2007. *ApJ* 660:1444–1450

Shen KJ, Bildsten L. 2009. *ApJ* 699:1365–1373

Shen KJ, Bildsten L. 2013. *ArXiv e-prints*

Shen KJ, Bildsten L, Kasen D, Quataert E. 2012. *ApJ* 748:35

Shen KJ, Guillochon J, Foley RJ. 2013. *ApJL* 770:L35

Shore SN, Augusteijn T, Ederoclite A, Uthas H. 2011. *A&A* 533:L8

Silverman JM, Filippenko AV. 2012. *MNRAS* 425:1917–1933

Silverman JM, Ganeshalingam M, Filippenko AV. 2013. *MNRAS* 430:1030–1041

Silverman JM, Ganeshalingam M, Li W, Filippenko AV, Miller AA, Poznanski D. 2011. *MNRAS* 410:585–611

Silverman JM, Nugent PE, Gal-Yam A, Sullivan M, Howell DA, et al. 2013a. *ApJ* 772:125

Silverman JM, Nugent PE, Gal-Yam A, Sullivan M, Howell DA, et al. 2013b. *ApJS* 207:3

Simon JD, Gal-Yam A, Gnat O, Quimby RM, Ganeshalingam M, et al. 2009. *ApJ* 702:1157–1170

Smartt SJ. 2009. *ARA&A* 47:63–106

Smith M, Nichol RC, Dilday B, Marriner J, Kessler R, et al. 2012. *ApJ* 755:61

Smith PS, Williams GG, Smith N, Milne PA, Jannuzi BT, Green EM. 2011. *ArXiv e-prints (1111.6626)*

Soderberg AM, Margutti R, Zauderer BA, Krauss M, Katz B, et al. 2012. *ApJ* 752:78

Soker N. 2013. In *IAU Symposium*, eds. R Di Stefano, M Orio, M Moe, vol. 281 of *IAU Symposium*

Soker N, Garcia-Berro E, Althaus LG. 2013. *ArXiv e-prints*

Soker N, Kashi A, García-Berro E, Torres S, Camacho J. 2013. *MNRAS* 431:1541–1546

Sokoloski JL, Luna GJM, Mukai K, Kenyon SJ. 2006. *Nature* 442:276–278

Solheim JE. 2010. *PASP* 122:1133–1163

Sorokina EI, Blinnikov SI, Kosenko DI, Lundqvist P. 2004. *Astronomy Letters* 30:737–750

Sparks WB, Macchetto F, Panagia N, Boffi FR, Branch D, et al. 1999. *ApJ* 523:585–592

Spruit HC. 1998. *A&A* 333:603–612

Starrfield S, Sparks WM, Truran JW. 1985. *ApJ* 291:136–146

Starrfield S, Truran JW, Sparks WM, Kutter GS. 1972. *ApJ* 176:169

Stehle M, Mazzali PA, Benetti S, Hillebrandt W. 2005. *MNRAS* 360:1231–1243

Steiner JE, Diaz MP. 1998. *PASP* 110:276–282

Stephenson FR, Green DA. 2002. *Historical supernovae and their remnants, by F. Richard Stephenson and David A. Green. International series in astronomy and astrophysics, vol. 5. Oxford: Clarendon Press, 2002, ISBN 0198507666* 5

Sternberg A, Gal-Yam A, Simon D, Leonard DC, Quimby RM, et al. 2011. *Science* 333:856–859

Sternberg A, Gal Yam A, Simon JD, Patat F, Hillebrandt W, et al. 2013. *ArXiv e-prints*

Strolger LG, Dahlen T, Riess AG. 2010. *ApJ* 713:32–40

Strolger LG, Riess AG, Dahlen T, Livio M, Panagia N, et al. 2004. *ApJ* 613:200–223

Suh H, Yoon Sc, Jeong H, Yi SK. 2011. *ApJ* 730:110

Suijs MPL, Langer N, Poelarends AJ, Yoon SC, Heger A, Herwig F. 2008. *A&A* 481:L87–L90

Sullivan M, Le Borgne D, Pritchet CJ, Hodsman A, Neill JD, et al. 2006. *ApJ* 648:868–883

Summa A, Ulyanov A, Kromer M, Boyer S, Röpke FK, et al. 2013. *A&A* 554:A67

Taam RE. 1980. *ApJ* 237:142–147

Taddia F, Stritzinger MD, Phillips MM, Burns CR, Heinrich-Josties E, et al. 2012. *A&A* 545:L7

Tanaka M, Kawabata KS, Yamanaka M, Maeda K, Hattori T, et al. 2010. *ApJ* 714:1209–1216

Tanaka M, Mazzali PA, Stanishev V, Maurer I, Kerzendorf WE, Nomoto K. 2011. *MNRAS* 410:1725–1738

Taubenberger S, Benetti S, Childress M, Pakmor R, Hachinger S, et al. 2011. *MNRAS* 412:2735–2762

Taubenberger S, Kromer M, Hachinger S, Mazzali PA, Benetti S, et al. 2013a. *MNRAS* 432:3117–3130

Taubenberger S, Kromer M, Pakmor R, Pignata G, Maeda K, et al. 2013b. *ApJL* 775:L43

Thomas RC, Aldering G, Antilogus P, Aragon C, Bailey S, et al. 2011. *ApJ* 743:27

Thompson TA. 2011. *ApJ* 741:82

Thomson MG, Chary RR. 2011. *ApJ* 731:72

Thoroughgood TD, Dhillon VS, Littlefair SP, Marsh TR, Smith DA. 2001. *MNRAS* 327:1323–1333

Timmes FX, Brown EF, Truran JW. 2003. *ApJL* 590:L83–L86

Tinsley BM. 1979. *ApJ* 229:1046–1056

Tojeiro R, Wilkins S, Heavens AF, Panter B, Jimenez R. 2009. *ApJS* 185:1–19

Tominaga N, Morokuma T, Blinnikov SI, Baklanov P, Sorokina EI, Nomoto K. 2011. *ApJS* 193:20

Toonen S, Nelemans G, Portegies Zwart S. 2012. *A&A* 546:A70

Tornambé A, Piersanti L. 2013. *MNRAS* 431:1812–1822

Totani T, Morokuma T, Oda T, Doi M, Yasuda N. 2008. *PASJ* 60:1327–

Tout CA. 2005. In *The Astrophysics of Cataclysmic Variables and Related Objects*, eds. JM Hameury, JP Lasota, vol. 330 of *Astronomical Society of the Pacific Conference Series*

Tout CA, Wickramasinghe DT, Liebert J, Ferrario L, Pringle JE. 2008. *MNRAS* 387:897–901

Tovmassian G, Yungelson L, Rauch T, Suleimanov V, Napiwotzki R, et al. 2010. *ApJ* 714:178–193

Tremonti CA, Heckman TM, Kauffmann G, Brinchmann J, Charlot S, et al. 2004. *ApJ* 613:898–913

Trundle C, Kotak R, Vink JS, Meikle WPS. 2008. *A&A* 483:L47–L50

Truran JW, Livio M. 1986. *ApJ* 308:721–727

Tsujimoto T, Shigeyama T. 2012. *ApJL* 760:L38

Tucker BE. 2011. *Ap&SS* 335:223–230

Tutukov A, Yungelson L. 1996. *MNRAS* 280:1035–1045

Tutukov AV, Yungelson LR. 1981. *Nauchnye Informatsii* 49:3

Udalski A, Kubiak M, Szymanski M. 1997. *Acta Astron.* 47:319–344

Umeda H, Nomoto K, Kobayashi C, Hachisu I, Kato M. 1999. *ApJL* 522:L43–L47

Uthas H, Knigge C, Steeghs D. 2010. *MNRAS* 409:237–246

Šimon V. 2003. *A&A* 406:613–621

Valenti S, Pastorello A, Cappellaro E, Benetti S, Mazzali PA, et al. 2009. *Nature* 459:674–677

van den Heuvel EPJ, Bhattacharya D, Nomoto K, Rappaport SA. 1992. *A&A* 262:97–105

van Kerkwijk MH, Chang P, Justham S. 2010. *ApJL* 722:L157–L161

van Winckel H, Lloyd Evans T, Briquet M, De Cat P, Degroote P, et al. 2009. *A&A* 505:1221–1232

Vink J. 2008. *ApJ* 689:231–241

Vink J. 2012. *A&A Rev.* 20:49

Vink J, Bleeker J, van der Heyden K, Bykov A, Bamba A, Yamazaki R. 2006. *ApJL* 648:L33–L37

Vink J, Kaastra JS, Bleeker JAM. 1997. *A&A* 328:628–633

Vink J, Laming JM, Gu MF, Rasmussen A, Kaastra JS. 2003. *ApJL* 587:L31–L34

Voss R, Nelemans G. 2008. *Nature* 451:802–804

Voss R, Nelemans G. 2012. *A&A* 539:A77

Walker ES, Hachinger S, Mazzali PA, Ellis RS, Sullivan M, et al. 2012. *MNRAS* 427:103–113

Wang B, Han Z. 2012. *New A. Rev.* 56:122–141

Wang B, Li XD, Han ZW. 2010. *MNRAS* 401:2729–2738

Wang B, Meng X, Chen X, Han Z. 2009a. *MNRAS* 395:847–854

Wang L, Baade D, Höflich P, Wheeler JC, Kawabata K, et al. 2006. *ApJ* 653:490–502

Wang L, Baade D, Patat F. 2007. *Science* 315:212–

Wang L, Wheeler JC. 2008. *ARA&A* 46:433–474

Wang X, Filippenko AV, Ganeshalingam M, Li W, Silverman JM, et al. 2009b. *ApJL* 699:L139–L143

Wang X, Li W, Filippenko AV, Foley RJ, Smith N, Wang L. 2008. *ApJ* 677:1060–1068

Wang X, Wang L, Filippenko AV, Zhang T, Zhao X. 2013. *Science* 340:170–173

Warner B. 2003. *Cataclysmic Variable Stars*. Cambridge University Press

Washabaugh PC, Bregman JN. 2013. *ApJ* 762:1

Webbink RF. 1984. *ApJ* 277:355–360

Wheeler JC. 2012. *ApJ* 758:123

Wheeler JC, Pooley D. 2013. *ApJ* 762:75

Whelan J, Iben Jr. I. 1973. *ApJ* 186:1007–1014

Wiersma RPC, Schaye J, Theuns T. 2011. *MNRAS* 415:353–371

Williams BJ, Blair WP, Blondin JM, Borkowski KJ, Ghavamian P, et al. 2011. *ApJ* 741:96

Winkler PF, Long KS, Hamilton AJS, Fesen RA. 2005. *ApJ* 624:189–197

Wolf WM, Bildsten L, Brooks J, Paxton B. 2013. *ApJ* 777:136

Wood-Vasey WM, Sokoloski JL. 2006. *ApJL* 645:L53–L56

Woods TE, Gilfanov M. 2013a. *ArXiv e-prints*

Woods TE, Gilfanov M. 2013b. *MNRAS* 432:1640–1650

Woosley SE, Kasen D. 2011. *ApJ* 734:38

Woudt PA, Steeghs D, Karovska M, Warner B, Groot PJ, et al. 2009. *ApJ* 706:738–746

Wu CC, Crenshaw DM, Fesen RA, Hamilton AJS, Sarazin CL. 1993. *ApJ* 416:247

Xavier HS, Gupta RR, Sako M, D'Andrea CB, Frieman JA, et al. 2013. *MNRAS* 434:1443–1459

Yamaguchi H, Koyama K, Katsuda S, Nakajima H, Hughes JP, et al. 2008. *PASJ* 60:141

Yaron O, Prialnik D, Shara MM, Kovetz A. 2005. *ApJ* 623:398–410

Yoon SC, Langer N. 2004. *A&A* 419:623–644

Yoon SC, Langer N. 2005. *A&A* 435:967–985

Yungelson LR. 2005. In *White dwarfs: cosmological and galactic probes*, eds. EM Sion, S Vennes, HL Shipman, vol. 332 of *Astrophysics and Space Science Library*

Yungelson LR. 2008. *Astronomy Letters* 34:620–634

Yungelson LR. 2013. In *IAU Symposium*, eds. R Di Stefano, M Orio, M Moe, vol. 281 of *IAU Symposium*

Yungelson LR, Livio M. 2000. *ApJ* 528:108–117

Zelaya P, Quinn JR, Baade D, Clocchiatti A, Höflich P, et al. 2013. *AJ* 145:27

Zheng W, Silverman JM, Filippenko AV, Kasen D, Nugent PE, et al. 2013. *ApJL* 778:L15

Zhu C, Chang P, van Kerkwijk MH, Wadsley J. 2013. *ApJ* 767:164

Zhu G, Blanton MR, Moustakas J. 2010. *ApJ* 722:491–519

Zorotovic M, Schreiber MR, Gänsicke BT. 2011. *A&A* 536:A42